Cosmology with Baryon Acoustic Oscillations and with the Lyα forest

James Rich

SPP-IRFU
CEA-Saclay
91191 Gif-sur-Yvette

james.rich@cea.fr

DARKMOD, September , 2017

Outline

- BAO generalities
  - The physics: the sound horizon r_d
  - Results: $(D_M/r_d,\ D_H/r_d)$ vs. redshift
  - Cosmological constraints: with and without CMB and SNIa
- BAO with tracers (galaxies, quasars...)
  - Observations: 10^6 spectra
  - Data analysis
  - Redshift-space distortions
  - Reconstruction of real-space correlations
  - Relative-velocity bias
- The Lyα forest
  - Quasar spectra
  - BAO in the forest
  - Reconstructing the linear power spectrum
  - Constraints on neutrino masses

Propagation of a baryon-photon sound wave

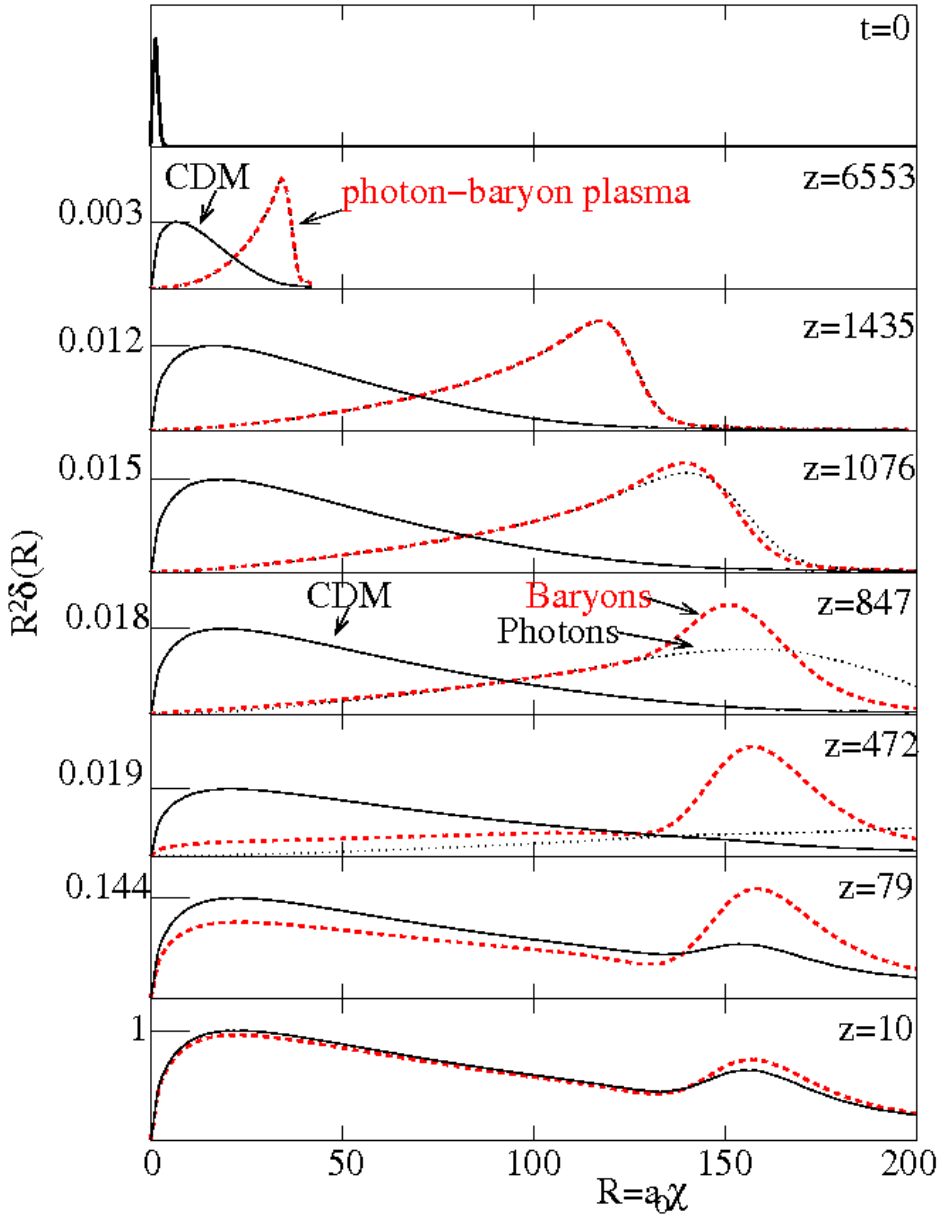

$t = 0$ (end of inflation)

$c_s \sim c/\sqrt(3)$
(γ,p,e plasma)

Wave stops at recombination
($r \sim 150\mathrm{kpc}$)

Today: Enhanced correlation at
$r_d = 147.5\mathrm{Mpc}$
"the sound horizon"

Calculation of the sound horizon

Same as "particle horizon" except $c_s < c$
$c_s = (c/\sqrt{3}) f(\rho_B/\rho_\gamma)$ (baryon inertia slows sound)

$$r_d = \int_{z_d}^{\infty} \frac{c_s(z)dz}{H(z)} = \sqrt{\frac{3}{8\pi G}} \int_{z_d}^{\infty} \frac{c_s(z)dz}{\sqrt{\rho_M + \rho_\gamma + \rho_\nu}}$$

Calculation of the sound horizon

Same as "particle horizon" except $c_s < c$
$c_s = (c/\sqrt{3}) f(\rho_B/\rho_\gamma)$ (baryon inertia slows sound)

$$r_d = \int_{z_d}^{\infty} \frac{c_s(z)dz}{H(z)} = \sqrt{\frac{3}{8\pi G}} \int_{z_d}^{\infty} \frac{c_s(z)dz}{\sqrt{\rho_M + \rho_\gamma + \rho_\nu}}$$

Normalize to the present photon density

$$r_d = \sqrt{\frac{3}{8\pi G \rho_\gamma(0)}} \int_{z_d}^{\infty} \frac{c_s(\rho_B/\rho_\gamma)dz}{(1+z)^2 \sqrt{\rho_M/\rho_\gamma + 1 + \rho_\nu/\rho_\gamma}}$$

COBE gives us $\rho_\gamma(0)$ and the CMB spectrum shape (Planck) gives us the density ratios ρ_M/ρ_γ, ρ_B/ρ_γ, ρ_ν/ρ_γ.

Harmonic spectrum of CMB, $C_\ell = \langle a_{\ell m} \rangle$

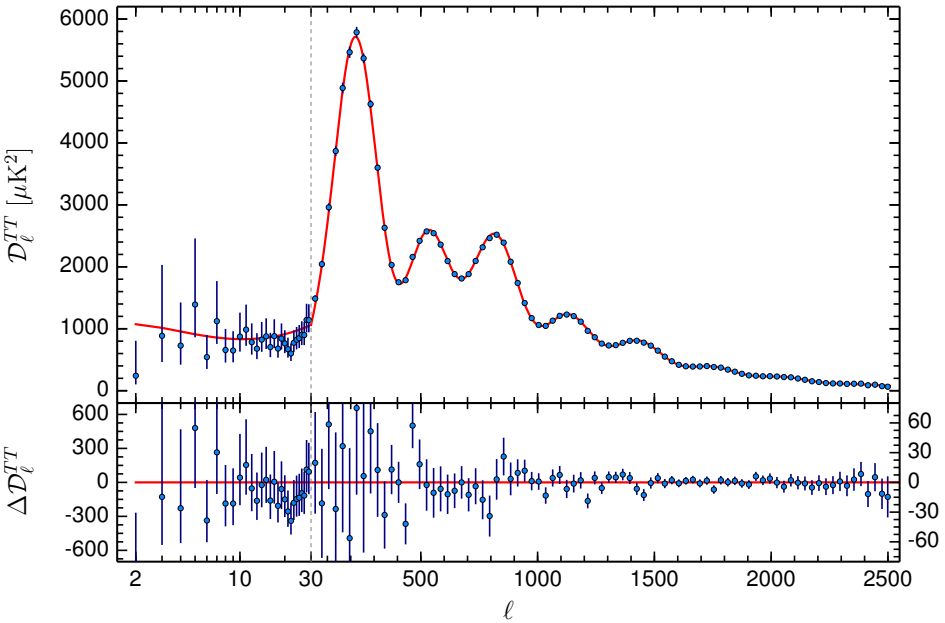

Peaks correspond to modes that were at an amplitude extrema at $z = 1070$; they have wavelengths that are harmonics of r_d.

$$\lambda \sim r_d/n$$

corresponding to

$$\ell \sim D(z = 1070)/\lambda$$

- Peak heights tell us about composition of the universe at $z = 1070 \Rightarrow (\Omega_M H_0^2, \Omega_b H_0^2) \rightarrow r_d$.
- Angular scale tells us how far the $z = 1070$ surface is from us. $D_M(z = 1070)$

r_d directly visible in TT correlation function

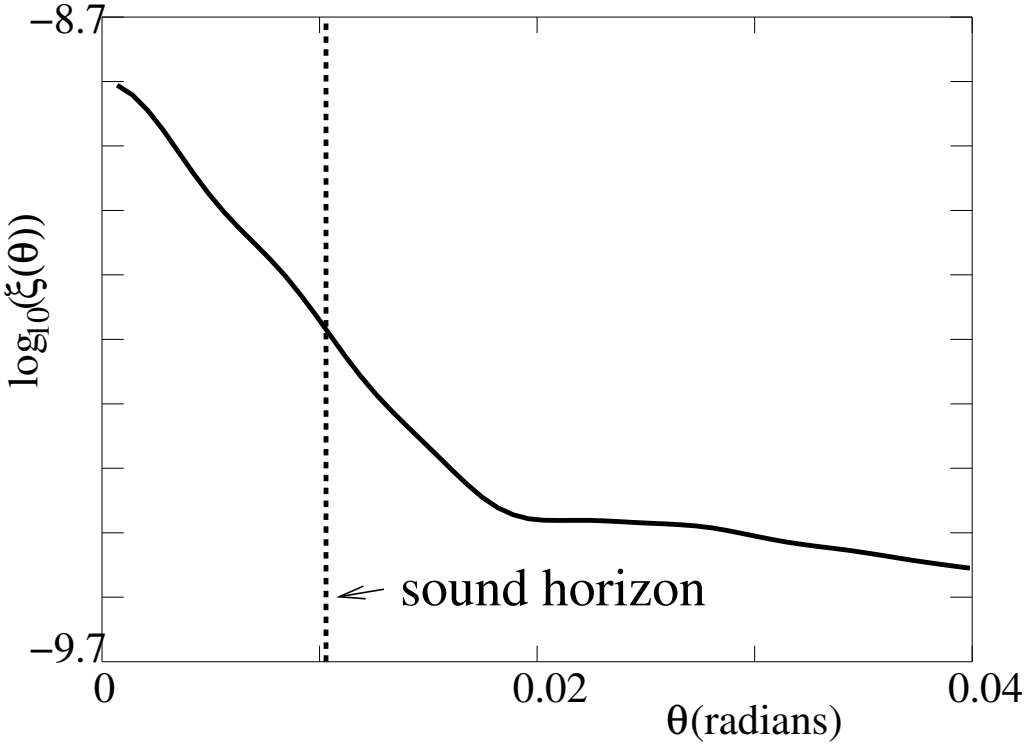

$$\frac{\langle (T(\vec{\theta}_1) - T_0)(T(\vec{\theta}_2) - T_0)\rangle}{T_0^2}$$

Large correlations for $\theta < 2r_d/D(z_{rec})$
Small (primordial) correlations for $\theta > 2r_d/D(z_{rec})$

r_d from COBE-Planck

$$r_d = \sqrt{\frac{3}{8\pi G \rho_\gamma(0)}} \int_{z_d}^{\infty} \frac{c_s(\rho_B/\rho_\gamma)dz}{(1+z)^2\sqrt{\rho_M/\rho_\gamma + 1 + \rho_\nu/\rho_\gamma}}$$

.

Imposing three neutrino families ($\rho_\nu = 0.23 N_\nu \rho_\gamma$) gives

$$r_d = (147.3 \pm 0.5)\mathrm{Mpc}$$

Fitting the CMB spectrum for N_ν gives $N_\nu = 2.99 \pm 0.2$ and

$$r_d = (147.4 \pm 1.5)\mathrm{Mpc}$$

Enhanced correlation at $r_d = 147.3$ Mpc

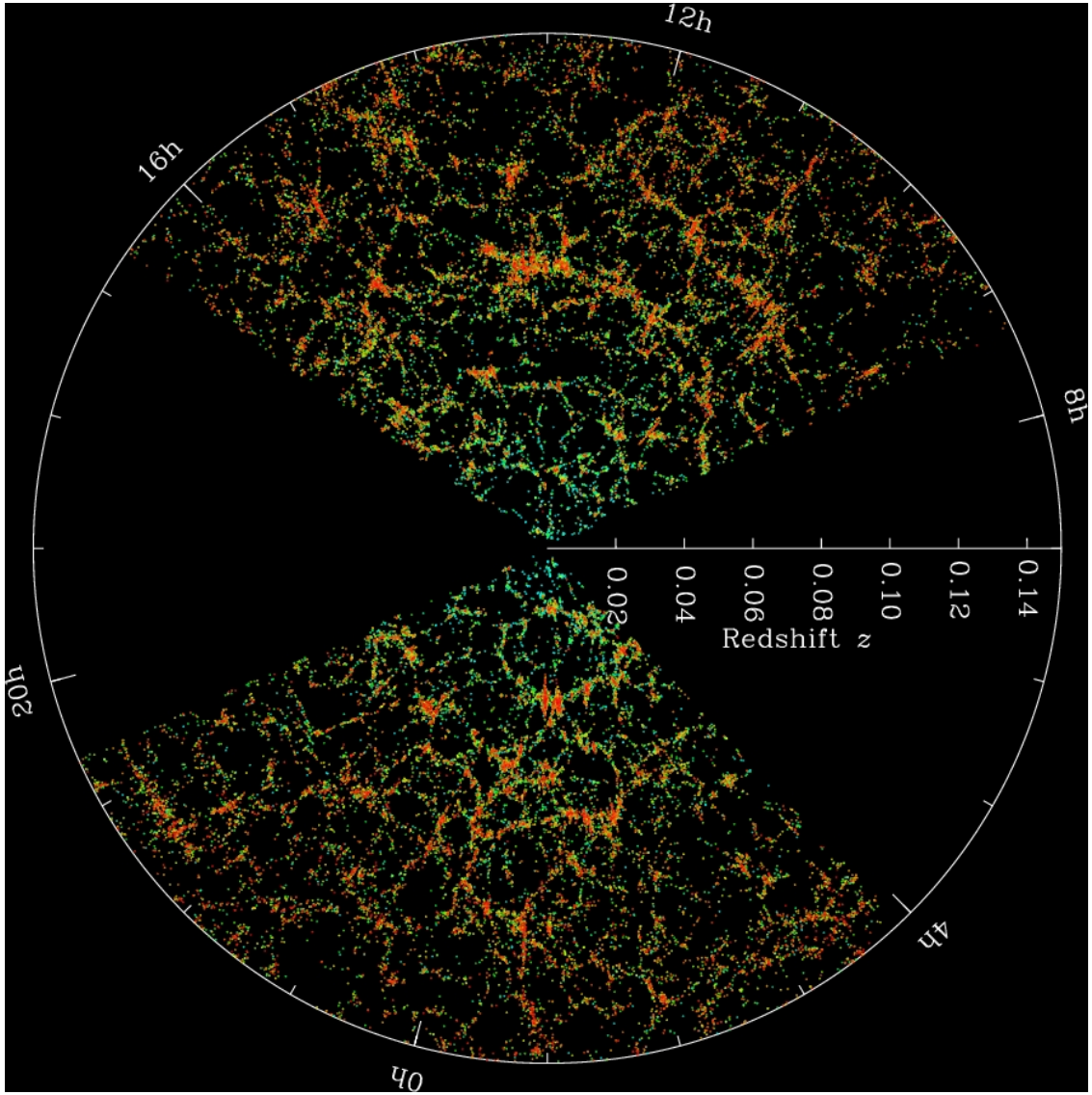

A slice of the nearby universe ($z < 0.14$) from the Sloan Digital Sky Survey (SDSS)

Much interesting structure on scales < 100Mpc.
But no obvious sign of a preferred length
$\Rightarrow$ statistical analysis

BAO Peak in galaxy correlation function

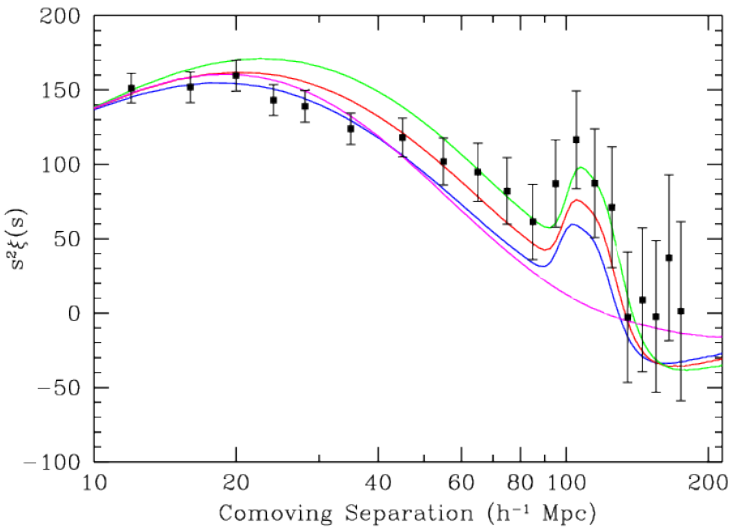

SDSS (2006): $z \sim 0.3$

SDSS-BOSS (2014): $z \sim 0.56$

Galaxies like to be separated by 105Mpc/h (147.5Mpc).

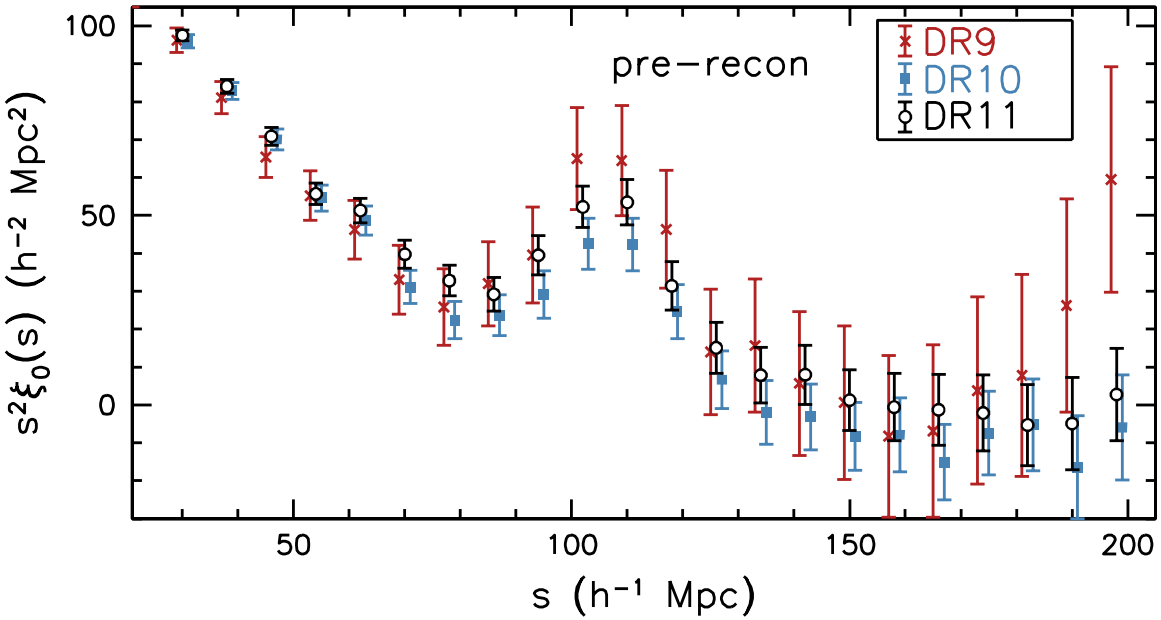

Final BOSS results

Power spectrum = Fourier transform of correlation function.

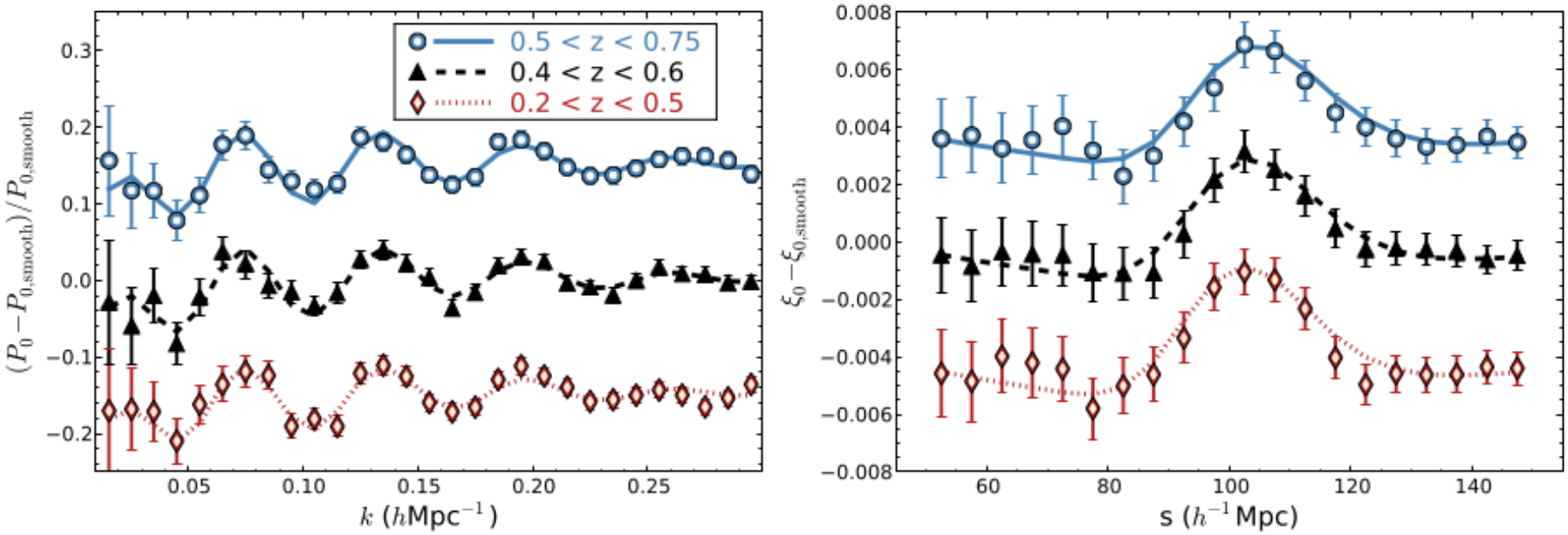

Alam et al. arXiv:1607.03155

"Fiducial cosmology": $(\Delta\theta, \Delta z) \rightarrow r$

Galaxies like to be separated by 105Mpc/h (147.5Mpc).

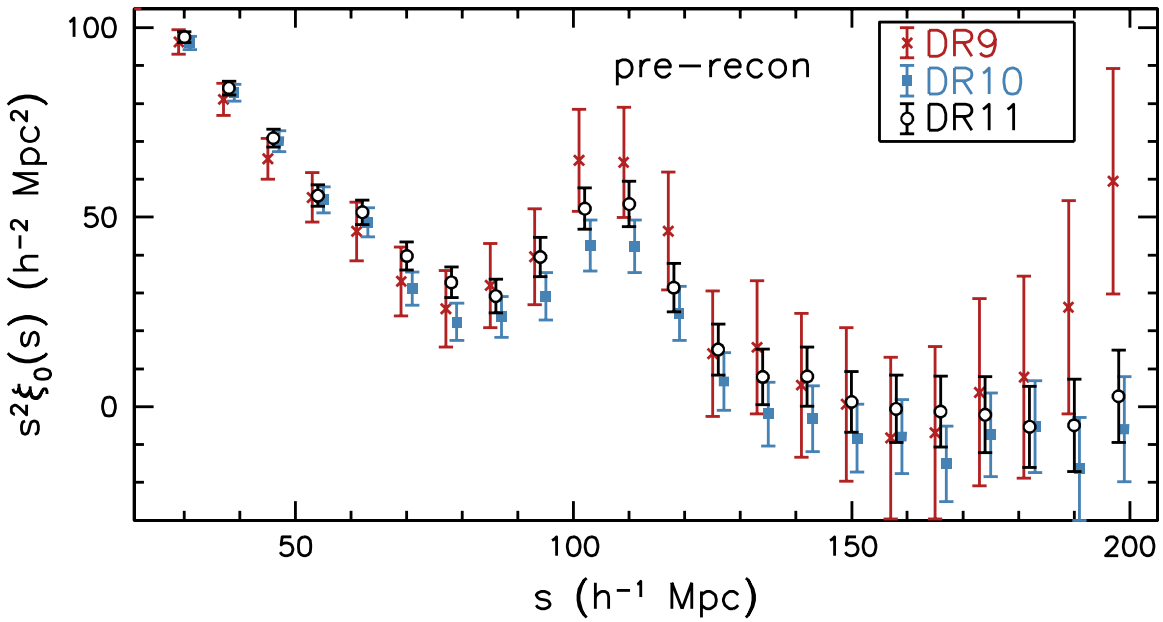

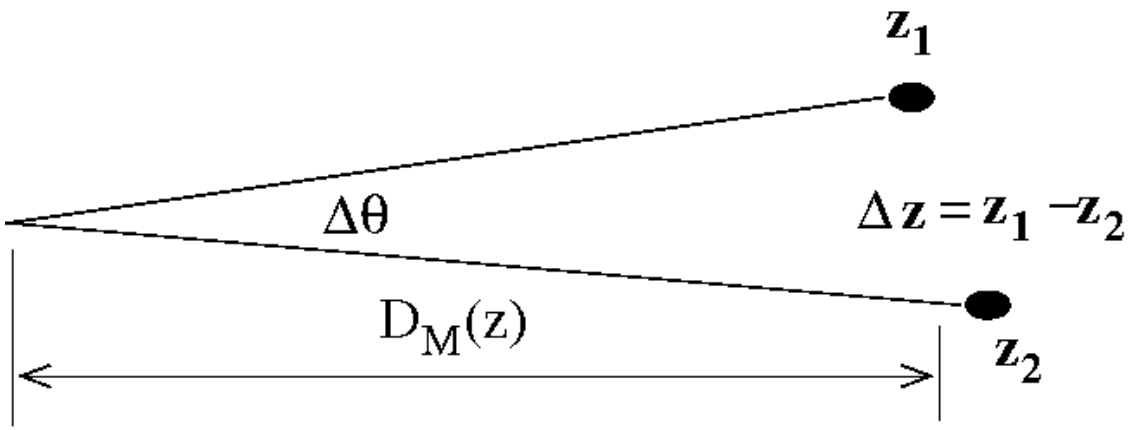

$$r^2 = r_\perp^2 + r_\parallel^2$$

$$r_\perp \sim D_M(z)\Delta\theta$$

$$r_\parallel \sim c\Delta z/H(z) = D_H(z)\Delta z$$

BAO ring in $\xi(r_\perp, r_\parallel)$ at $r_\perp^2 + r_\parallel^2 = r_d^2$

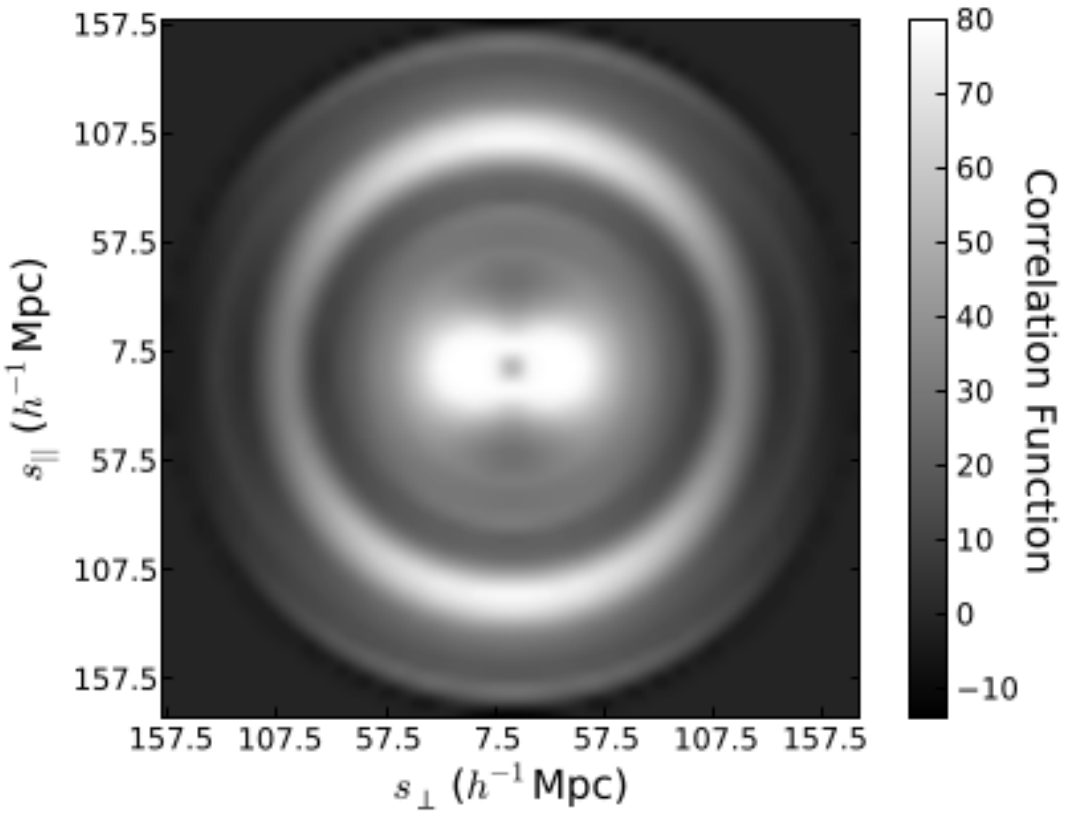

Measured radius is derived from angular separations and redshift differences.

A "fiducial cosmology" is used to transform $(\Delta\theta, \Delta z)$ to $(r_\perp, r_\parallel)$

$$transverse : r_d(measured) = r_d(true)\frac{D_M(fiducial)}{D_M(true)}$$

$$\Rightarrow \frac{D_M(fiducial)}{r_d(measured)} = \frac{D_M}{r_d}(true)$$

BAO ring in $\xi(r_\perp, r_\parallel)$ at $r_\perp^2 + r_\parallel^2 = r_d^2$

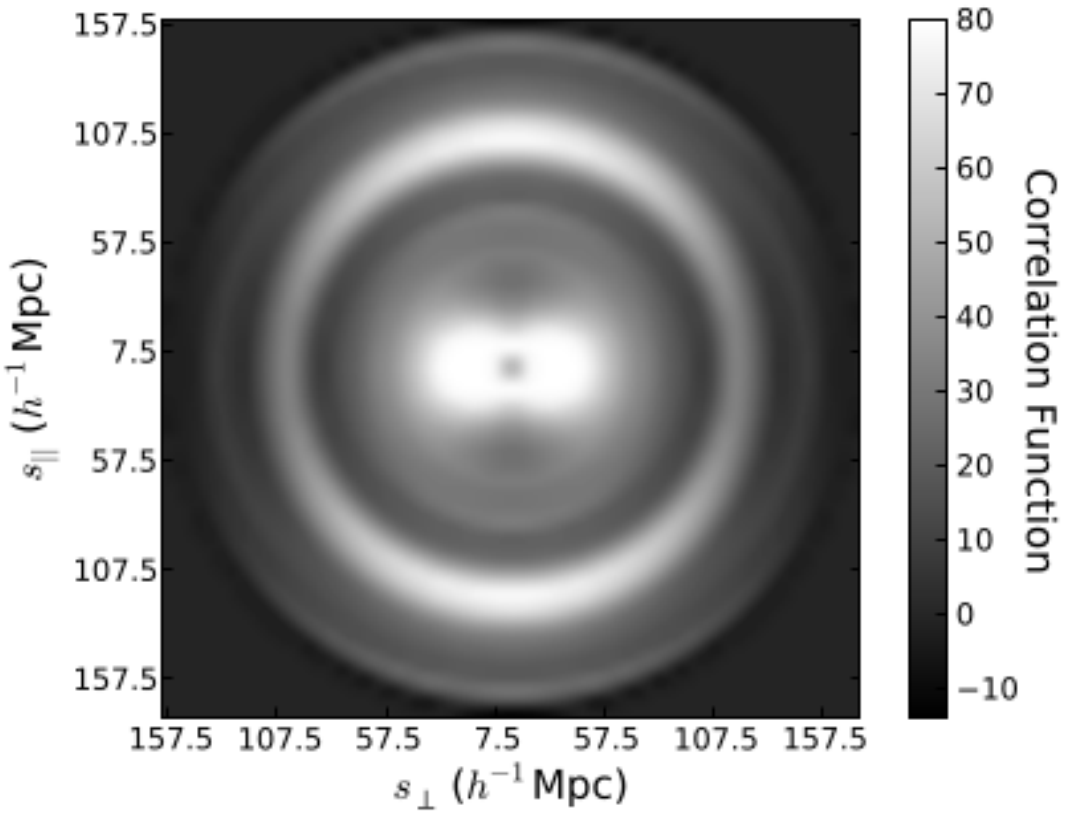

Measured radius is derived from angular separations and redshift differences.

A "fiducial cosmology" is used to transform $(\Delta\theta, \Delta z)$ to $(r_\perp, r_\parallel)$

$$radial : r_d(measured) = r_d(true)\frac{D_H(fiducial)}{D_H(true)}$$

$$\Rightarrow \frac{D_H(fiducial)}{r_d(measured)} = \frac{D_H}{r_d}(true) \qquad D_H(z) \equiv c/H(z)$$

BAO ring in $\xi(r_\perp, r_\parallel)$ at $r_\perp^2 + r_\parallel^2 = r_d^2$

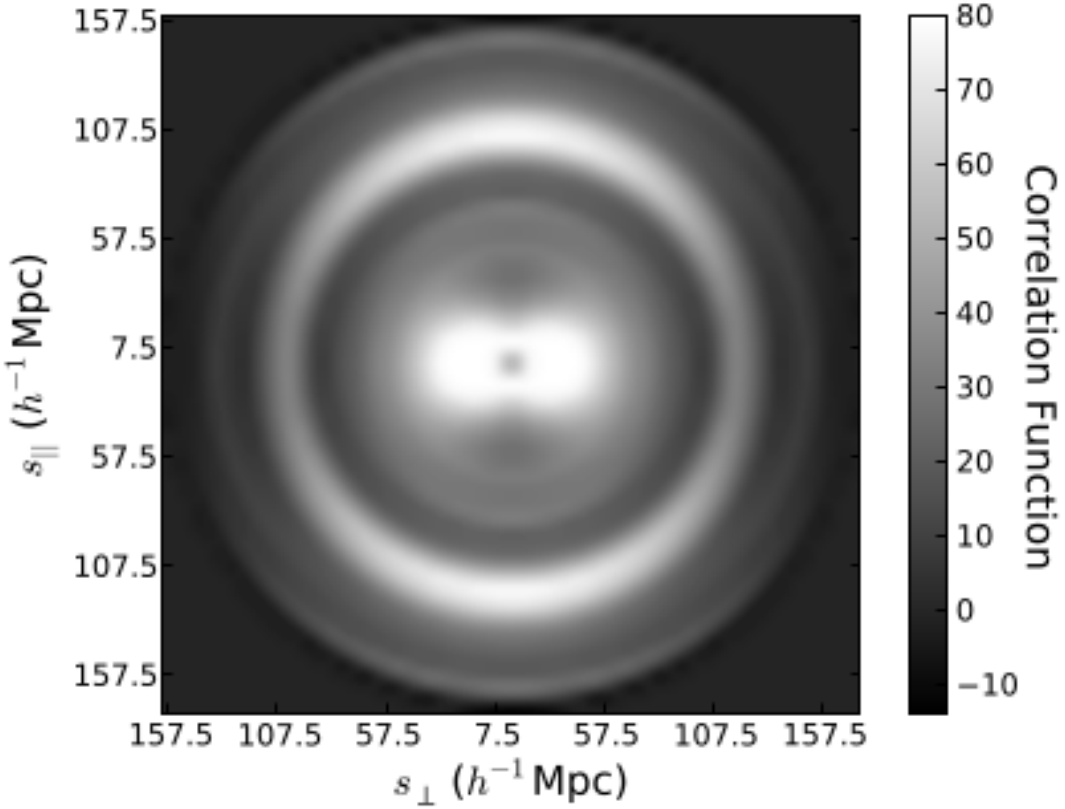

Measured radius is derived from angular separations and redshift differences.

A "fiducial cosmology" is used to transform $(\Delta\theta, \Delta z)$ to $(r_\perp, r_\parallel)$

Angled-averaged BAO measurements determine a "weighted geometric mean" of $D_M(z)/r_d$ and $D_H(z)/r_d$:

$$\textit{Galaxies}: \quad D_V(z)/r_d \equiv D_M^{2/3}(zD_H(z))^{1/3}/r_d$$

$$\mathrm{Ly}\alpha\ \textit{forest}: \quad D_H(z)^{0.7} D_M(z)^{0.3}/r_d$$

BAO Hubble diagrams: $D_M(z)/r_d$, $D_H(z)/r_d$

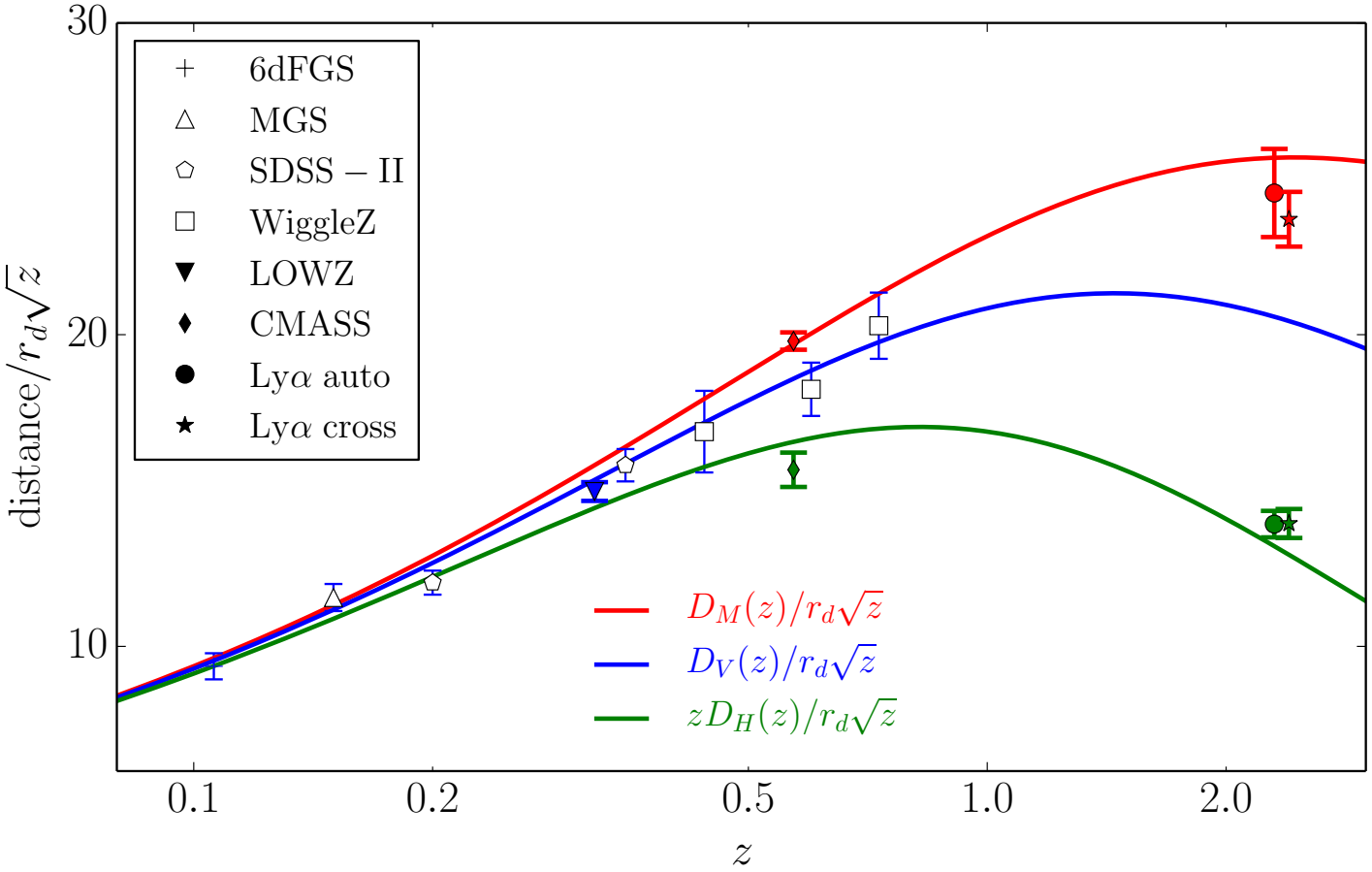

$D_M(z)/r_d$

$D_V(z)/r_d$

$D_H(z)/r_d = c/H(z)r_d$

Compare SNIa Hubble diagram: $D_M(z)/\sqrt{L_{SN}}$

SNIa Hubble diagram: $D_M(z)/\sqrt{L_{SN}}$

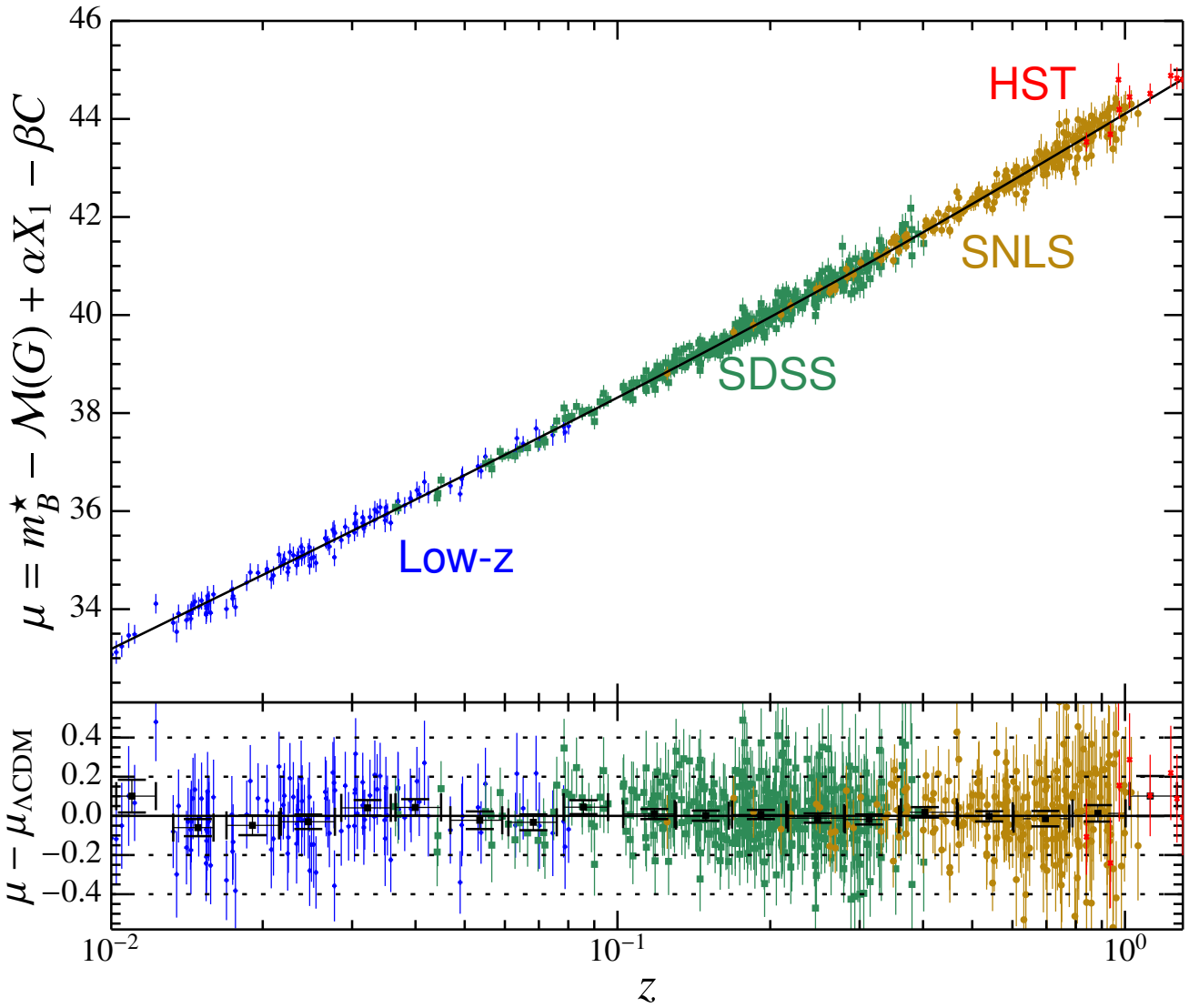

$D_M(z)/\sqrt{L_{SN}}$

Measurements for $z < 0.1 \Rightarrow$ SNIa necessary to measure H_0

Summary of BAO measurements of D/r_d

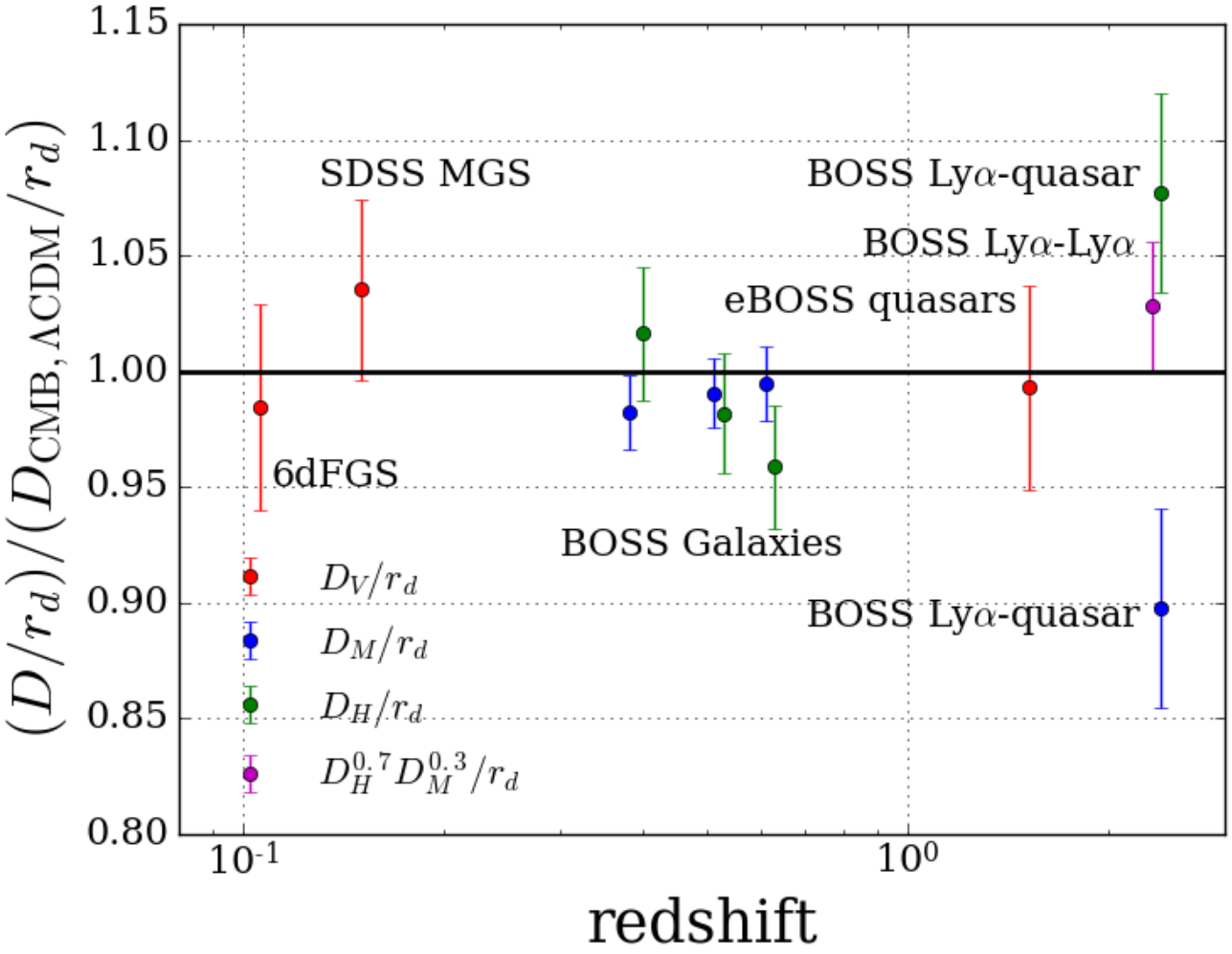

BAO and SNIa constraints on $(\Omega_\Lambda, \Omega_M)$

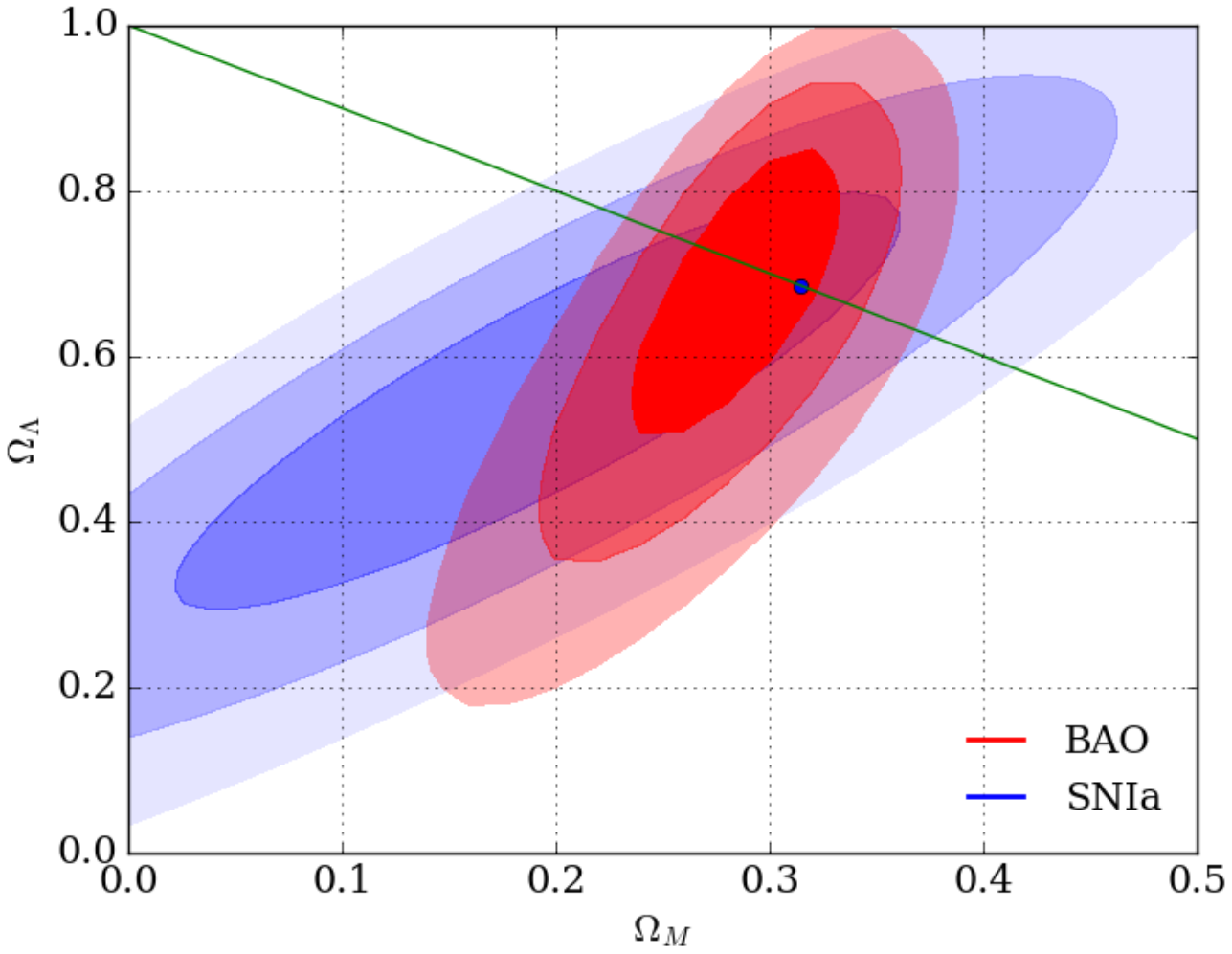

BAO $H(z) \Rightarrow$ deceleration$\rightarrow$acceleration

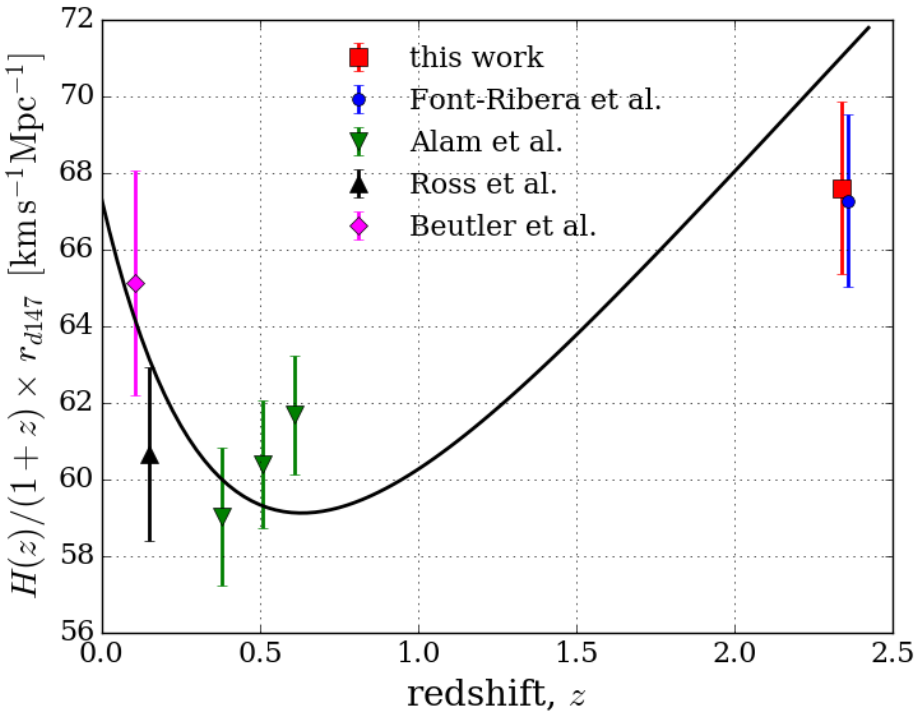

ΛCDM prediction

Data not precise enough (yet)

3 routes to $(\Omega_M, \Omega_\Lambda, \Omega_b, H_0)$

CMB (mostly):

- Peak heights (anisotropy spectrum) $\Rightarrow (\Omega_M H_0^2, \Omega_b H_0^2)$
- Peak positions $\Rightarrow D_M(z = 1090) \Rightarrow (H_0, \Omega_k)$ degeneracy
- CMB-lensing (or BAO) $\Rightarrow \Omega_k$ (assuming oΛCDM)

Low redshift only:

- BAO Hubble diagram $\Rightarrow (\Omega_M, \Omega_\Lambda)$
- Distance ladder calibration of $L_{SNIa} \Rightarrow H_0$
- Nucleosynthesis $\Rightarrow \Omega_b H_0^2$.

Low redshift + r_d from CMB:

- BAO Hubble diagram $\Rightarrow (\Omega_M, \Omega_\Lambda)$
- r_d calibration of $L_{SNIa} \Rightarrow H_0$
- Nucleosynthesis $\Rightarrow \Omega_b H_0^2$.

CMB geometric degeneracy

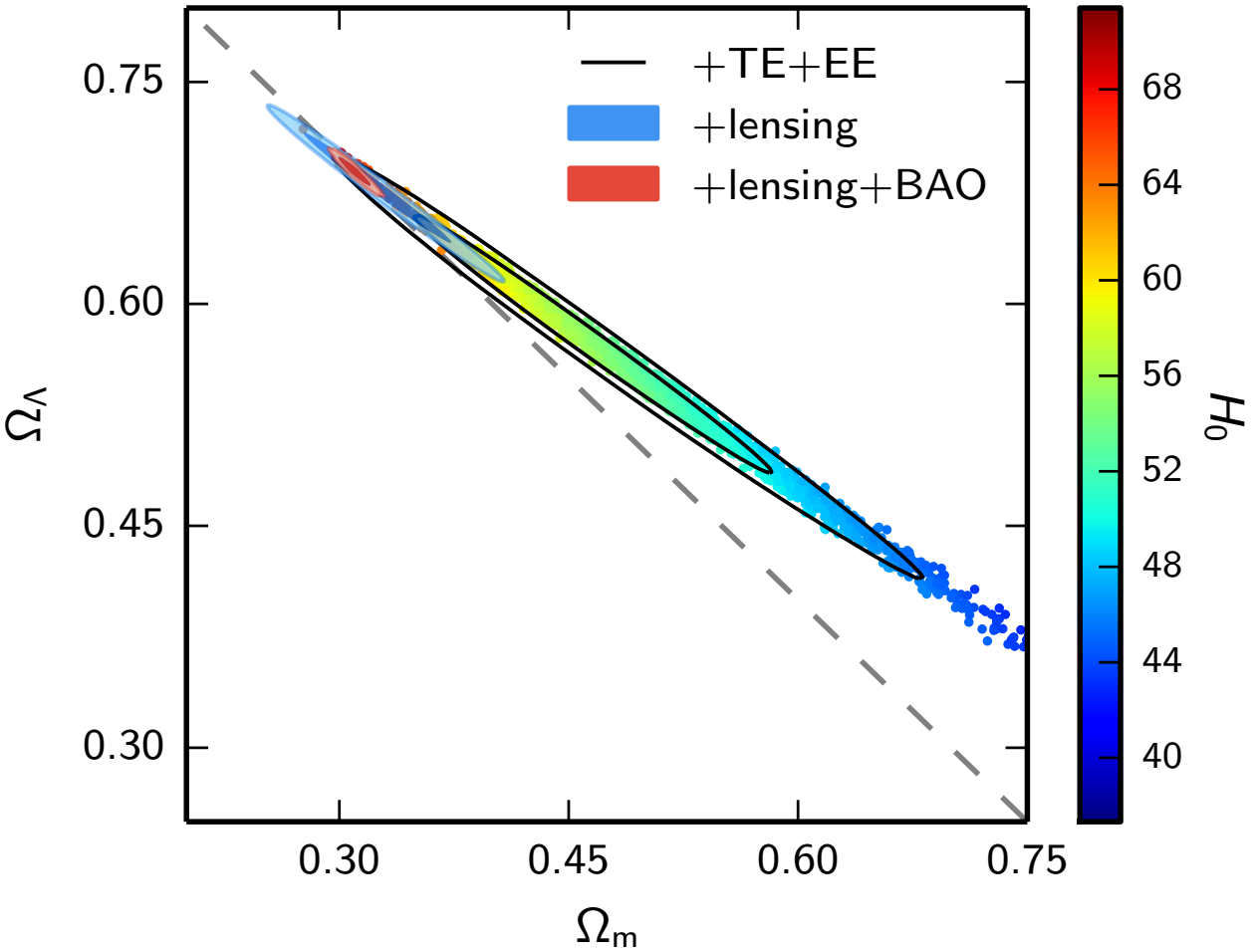

(TT,EE) contours give $(\Omega_M, \Omega_\Lambda, H_0)$ with nearly identical C_ℓ (spectrum shape and distance to LSS).

Adding low-redshift information (BAO or CMB-lensing) necessary to break degeneracy

Top-down: the BAO and SNIa Hubble diagram

Aubourg et al. arXiv:1411.1074

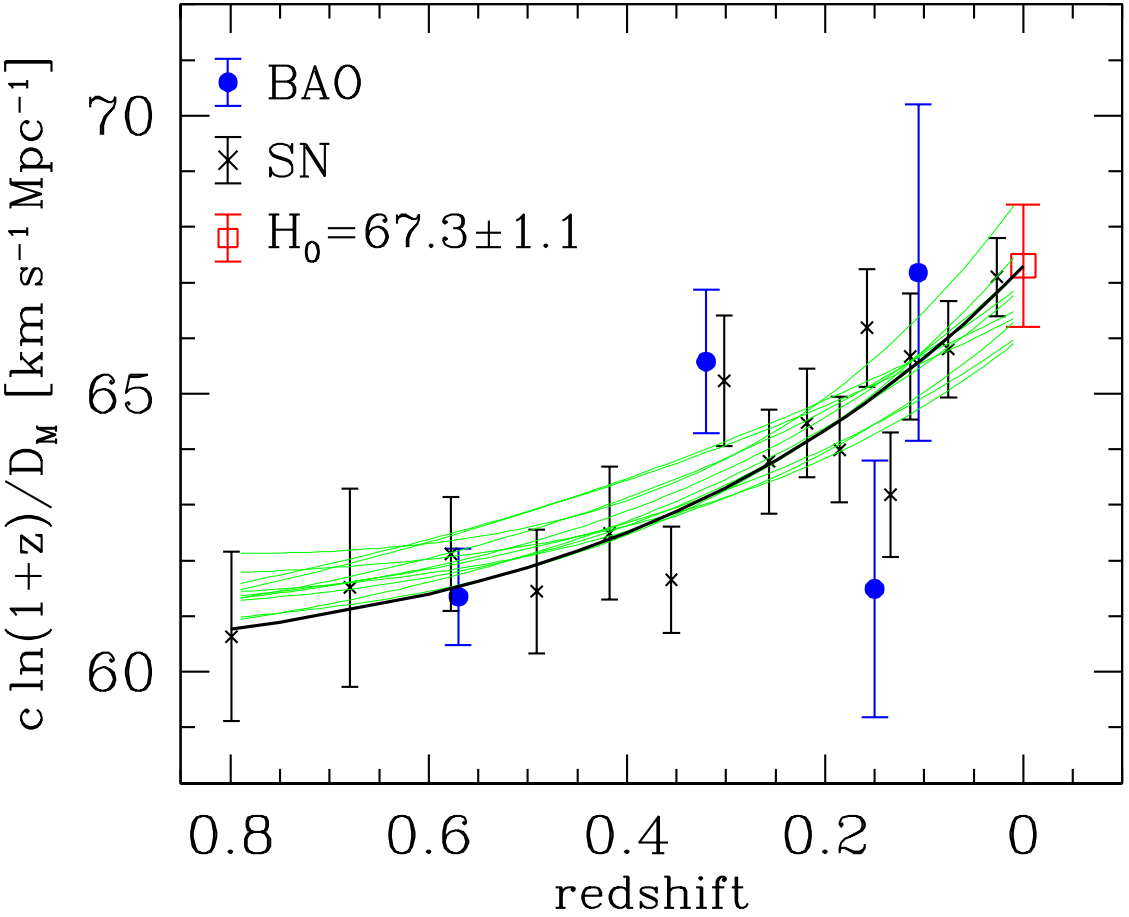

Calibrate SNIa luminosity by requiring $D_M(z = 0.57)$ from SNIa agree with $D_M(z = 0.57)$ from BAO

$\Rightarrow H_0 = 67.3 \pm 1.1$

Distance ladder: $H_0 = 73.24 \pm 1.74$, arXiv:1604.01424

Outline

- BAO generalities
  - The physics: the sound horizon r_d
  - Results: $(D_M/r_d,\ D_H/r_d)$ vs. redshift
  - Cosmological constraints: with and without CMB and SNIa
- BAO with tracers (galaxies, quasars...)
  - Observations: 10^6 spectra
  - Data analysis
  - Redshift-space distortions
  - Reconstruction of real-space correlations
  - Relative-velocity bias
- The Lyα forest
  - Quasar spectra
  - BAO in the forest
  - Reconstructing the linear power spectrum
  - Constraints on neutrino masses

BOSS: Baryon-Oscillation Spectroscopy Survey

2.5meter Sloan telescope
Apache Point, New Mexico

$7deg^2$ focal plane
connected to spectrograph
via 1000 optical fibers

BOSS Spectrograph

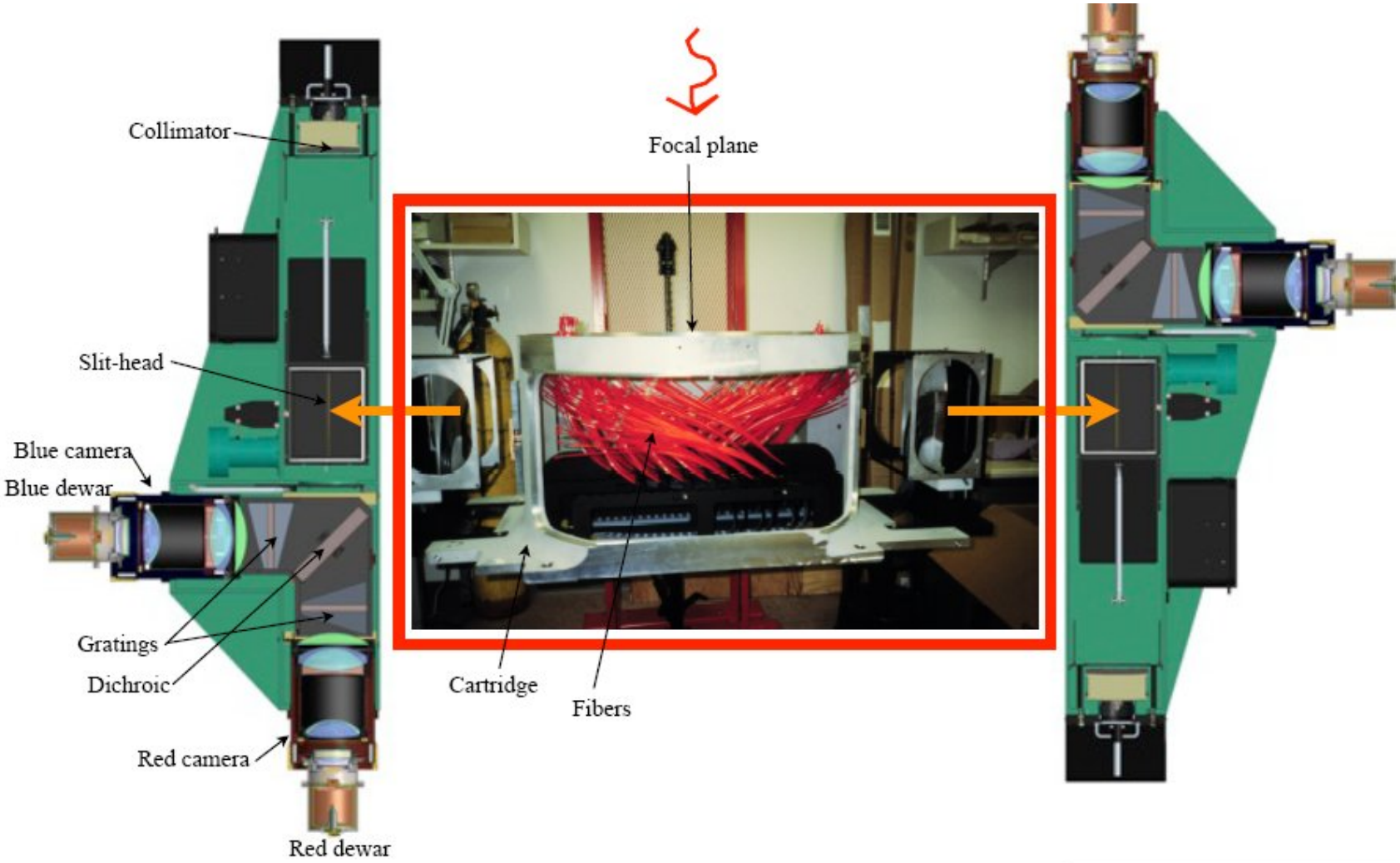

BOSS Spectrograph,CCD

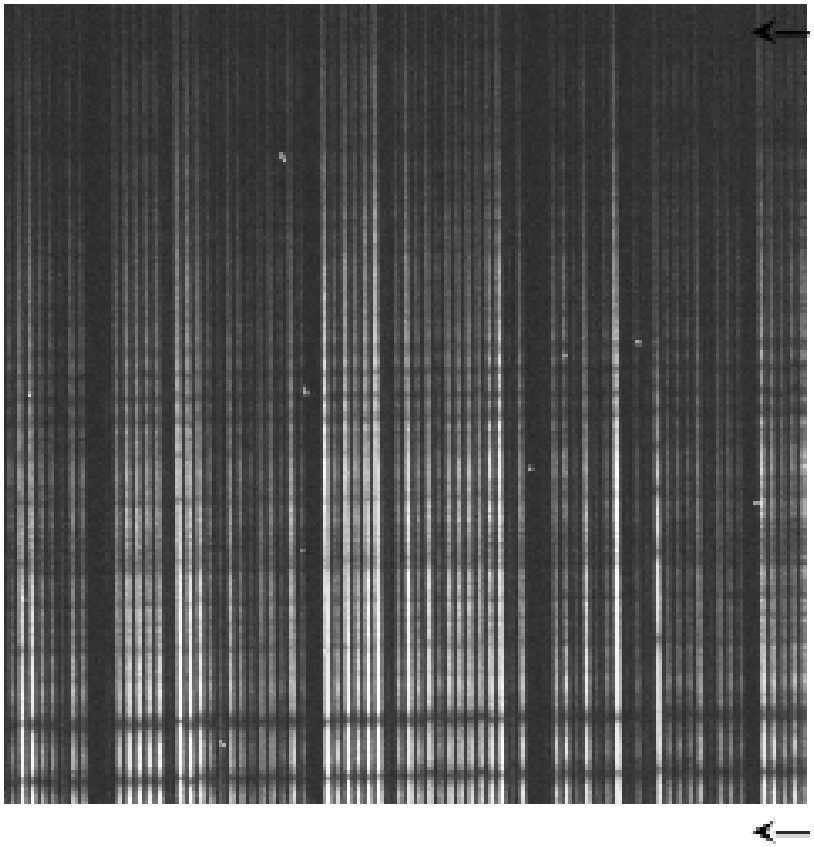

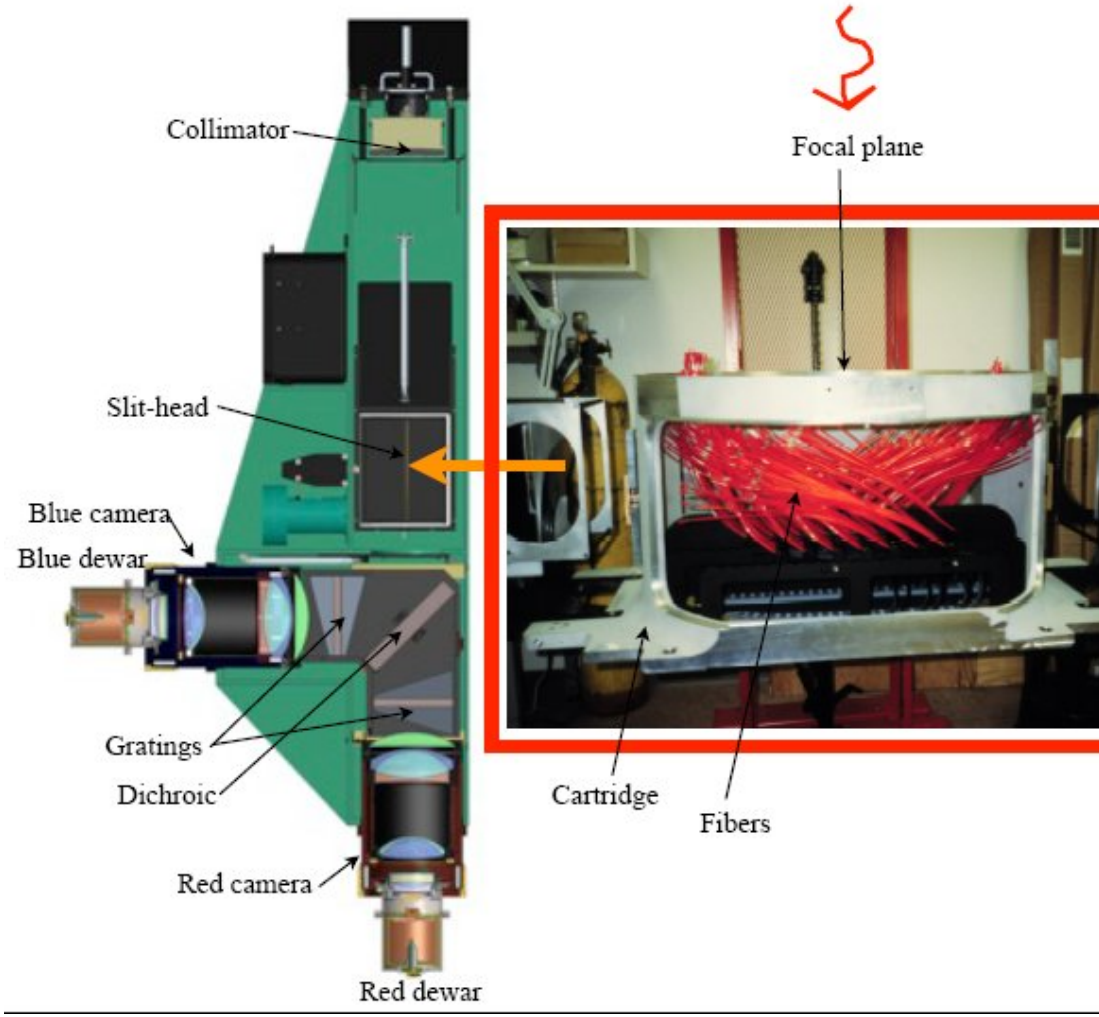

2 BOSS surveys ($10^4 deg^2$ 5 years)

- 6×10^5 Large Red Galaxies (LRG)
  $\sim$ 500 fibers per plate
  (candidates from SDSS-I photometry)
  $\langle z \rangle \sim 0.6$, $n \sim 10^{-4} Mpc^{-3}$
  BAO results: arXiv:1607.03155
- 1.6×10^5 quasars with Lyα absorption
  $\sim$ 280 fibers per plate
  (candidates from SDSS-I photometry)
  $\langle z \rangle \sim 2.4$
  BAO results: arXiv:1702.00176; 1708.02225

Statistics of galaxy-pairs in BOSS (simulation)

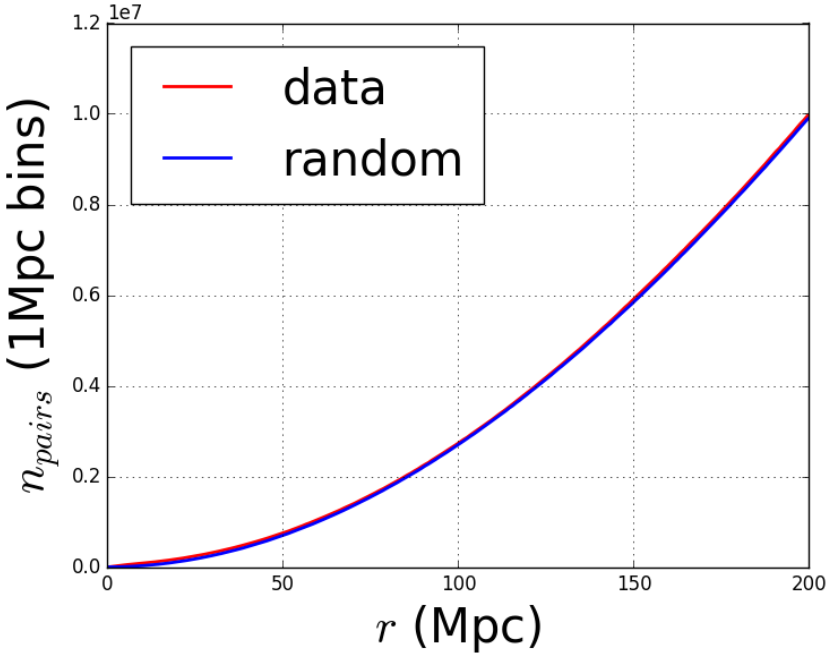

$$n_{pairs}(r) \sim r^2$$

(nearly random distribution)
$\sim 10^7$ pairs per 1Mpc bin

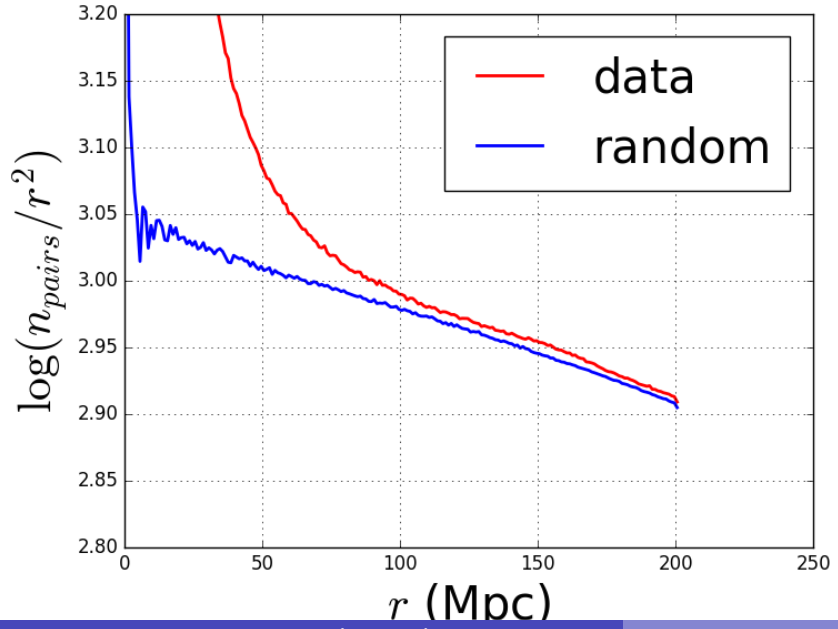

Compared to random distribution, data has:
Significant excess for $r < 50$Mpc (structure formation)
Tiny excess at $r \sim 150$Mpc (BAO peak)

(Unofficial) Correlation function (angle average)

Subtract n_{pairs}^{random} from n_{pairs}^{data} to derive correlation function:

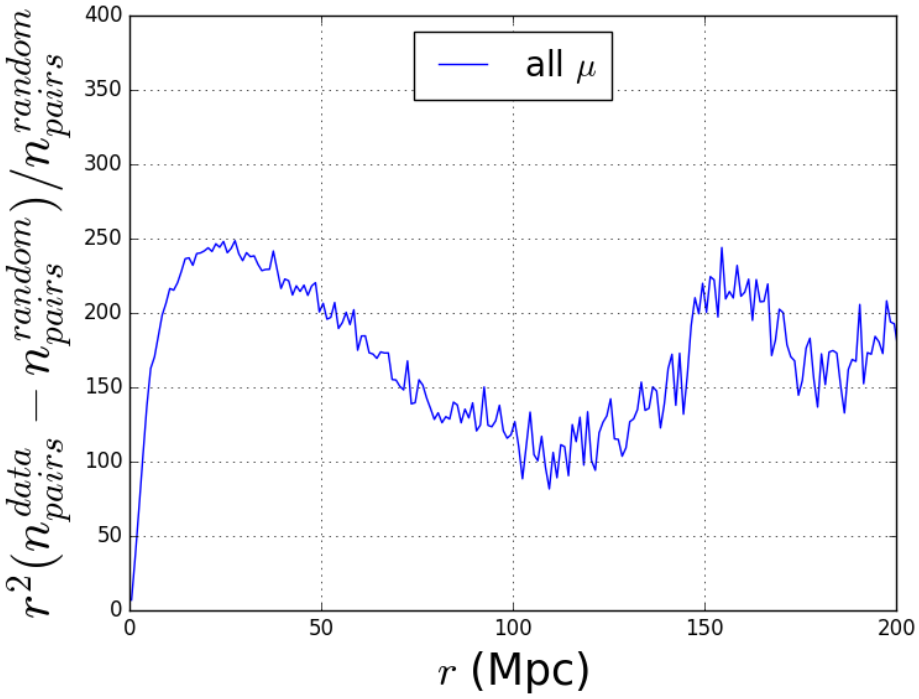

1. Importance of relative normalization (weights).
2. Fit to find $r_d(measured)$
   "related" to "peak position"
   Need to model full $P(\vec{k})$
3. Covariance matrix from simulations
4. Divide $r_d(measured)$ by $D_V(\bar{z})(fiducial)$ to find $D_V(\bar{z})/r_d$
5. Compare $D_V(\bar{z})/r_d$ with model prediction. $(\Omega_M, \Omega_\Lambda)$

Correlation function (radial and transverse)

Correlation function $\xi(r,\mu)$ in bins of $\mu = r_{\parallel}/\sqrt{r_{\parallel}^2 + r_{\perp}^2}$.

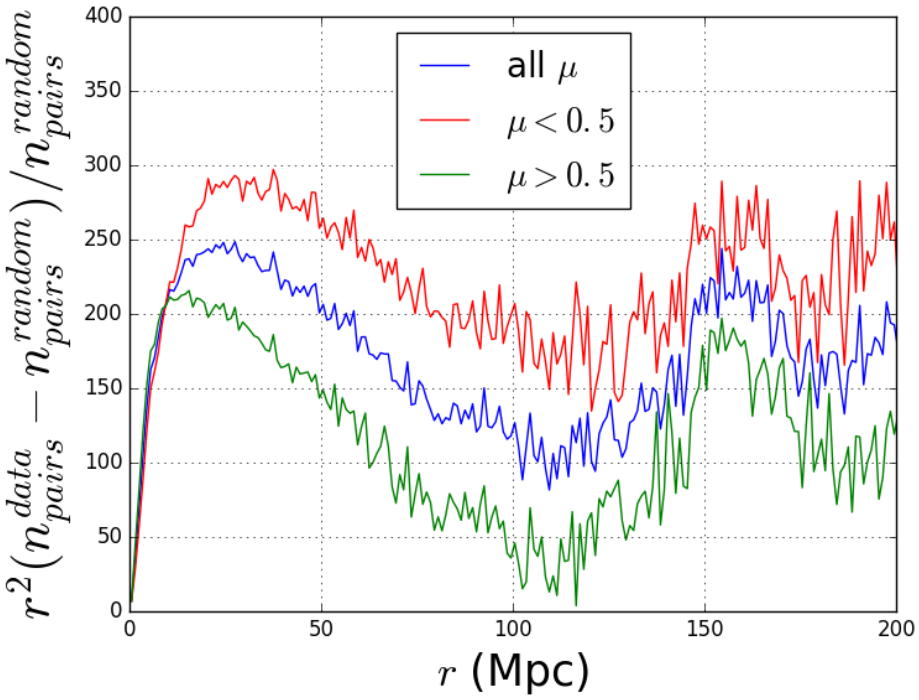

1. peak at $\mu \sim 0 \Rightarrow D_M(\bar{z})/r_d$
2. peak at $\mu \sim 1 \Rightarrow D_H(\bar{z})/r_d$
3. $\xi(r,\mu)$ depends on μ because of redshift-space distortions.

Redshift-space distortions (k-space)

A radial density-perturbation mode, $\delta_{\vec{k}} = (\rho - \bar{\rho})/\bar{\rho}$, and associated radial-peculiar velocity perturbation:

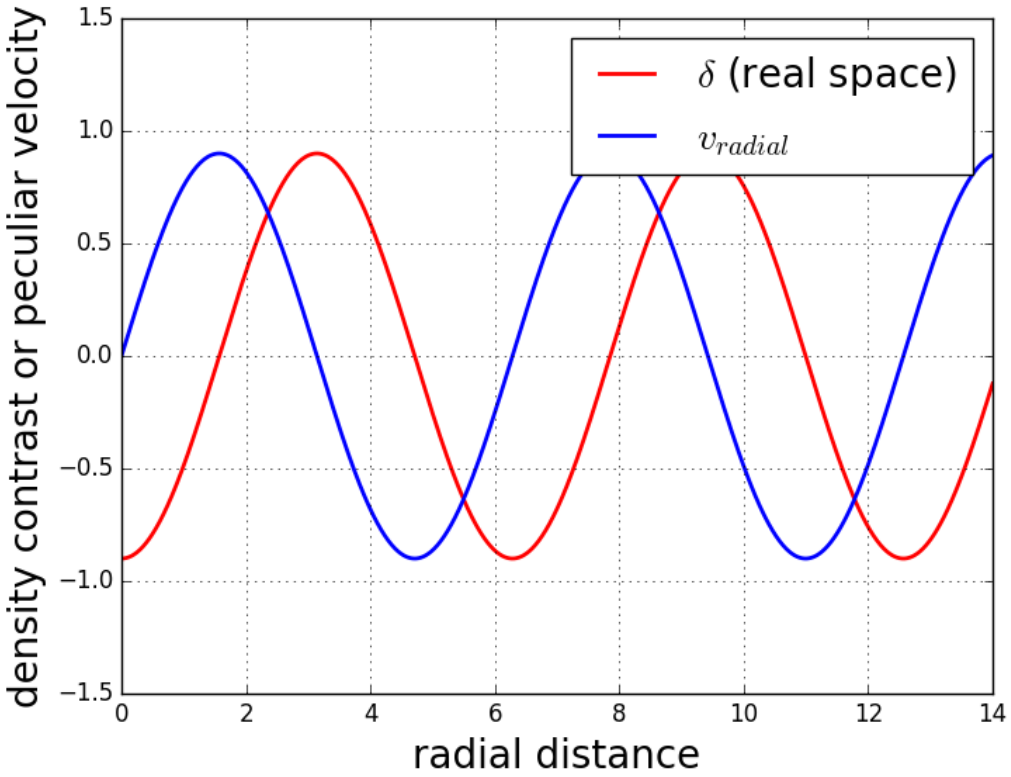

velocity mode shifted by $\pi/2$ from density mode

Adding radial-peculiar velocity to Hubble velocity shifts particles toward high-density peaks in redshift space. (just a coordinate transformation)

Redshift-space distortion

Amplitude of radial density perturbation is enhanced in redshift space:

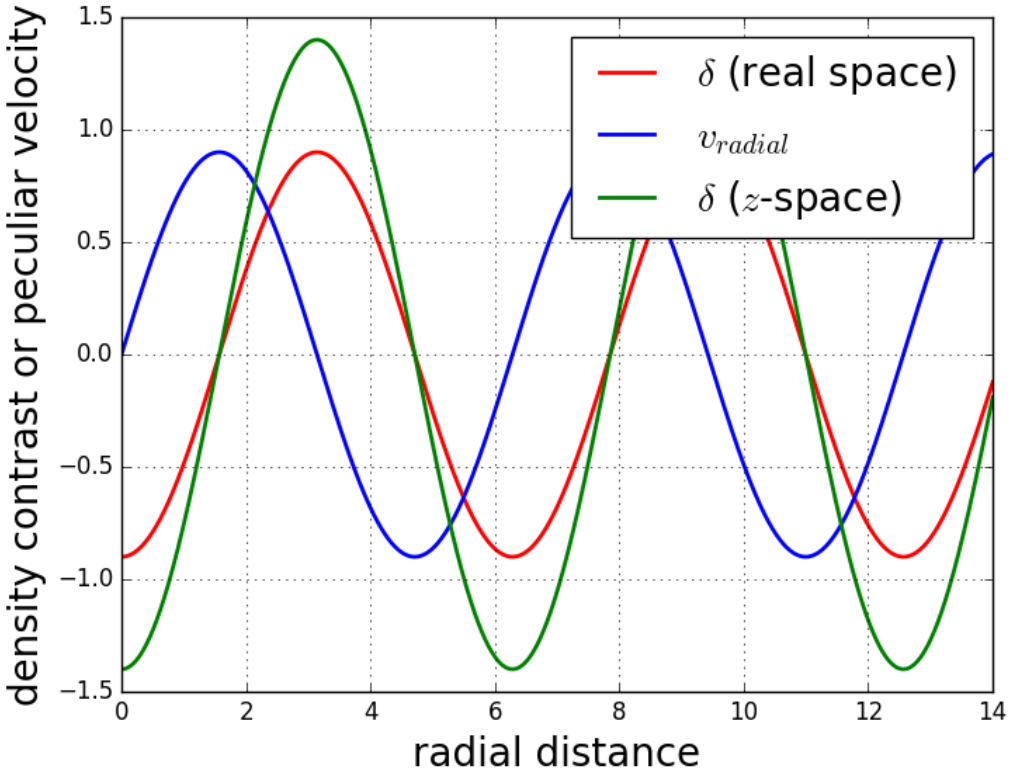

$|\delta_{\vec{k}}|^2 \rightarrow |\delta_{\vec{k}}|^2(1 + f\mu_{\vec{k}}^2)^2$ where $\mu_{\vec{k}} = k_{\parallel}/k$ (Kaiser, 1988)

$f = d\log\delta_k/d\log(1+z) \sim \Omega_M(z)^{0.6}$ ("growth rate of perturbations")

Linear redshift-space power spectra

$$Matter : P(k,\mu) = P_{Lin}(k)(1 + f\mu_{\vec{k}}^2)^2$$

$$Tracer\ i : \quad P(k,\mu) = P_{Lin}(k)(b_i + f\mu_{\vec{k}}^2)^2$$

$b_i =$ linear bias $= d\delta_k(tracer)/d\delta_k(matter)$

$b_{LRG} \sim 3$ (LRGs formed at density peaks)
$\sim$ independent of k for $k \to 0$ (local physics determines galaxy formation)

$f =$ linear growth rate

Measurement of $\sqrt{P(k,\mu}$ determines $b_i\sigma_8$ and $f\sigma_8$
(σ_8^2 is normalization of $P(k)$ for $k \sim 2\pi(8h^{-1}\mathrm{Mpc})^{-1}$)

$f\sigma_8$ from RSD measurements

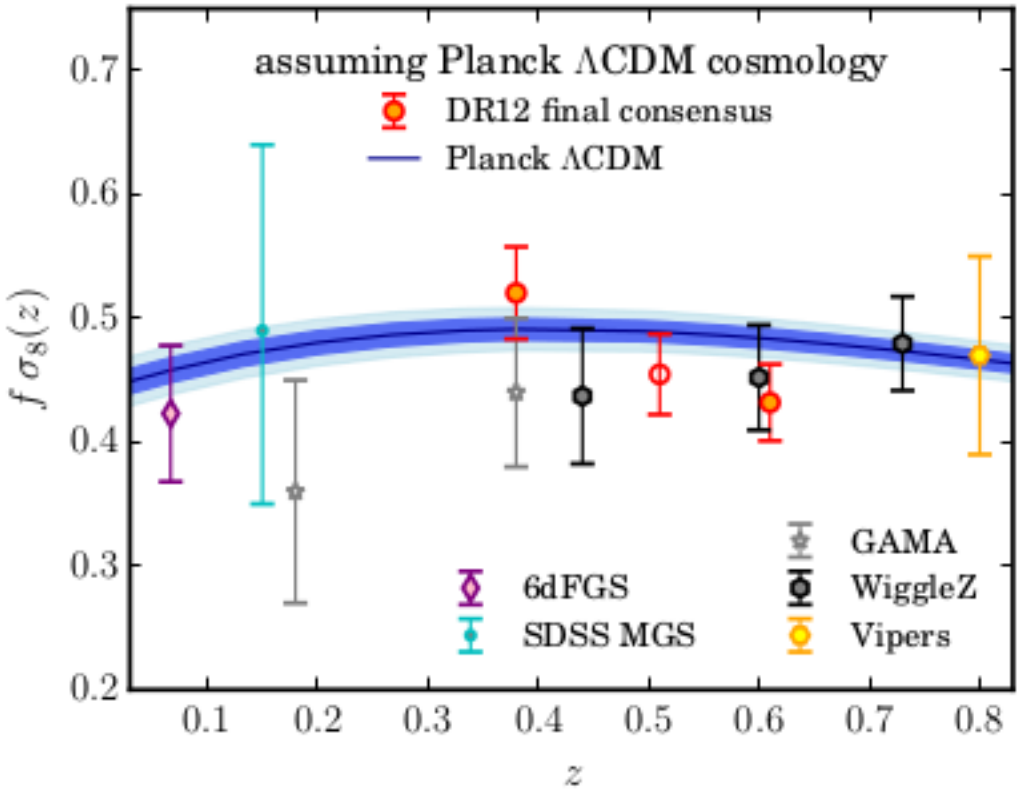

Note: can derive f and σ_8 separately from 3-point functions. (Gil-Marín et al. arXiv:1606.00439

Other sources of $f\sigma_8$: weak-lensing, cluster abundances
σ_8 from Lyα forest.
σ_8 from CMB modulo effects of m_ν.
$f = ?\Omega_M(z)^{0.6} \Rightarrow$ test of gravity

Reconstruction of real-space correlations

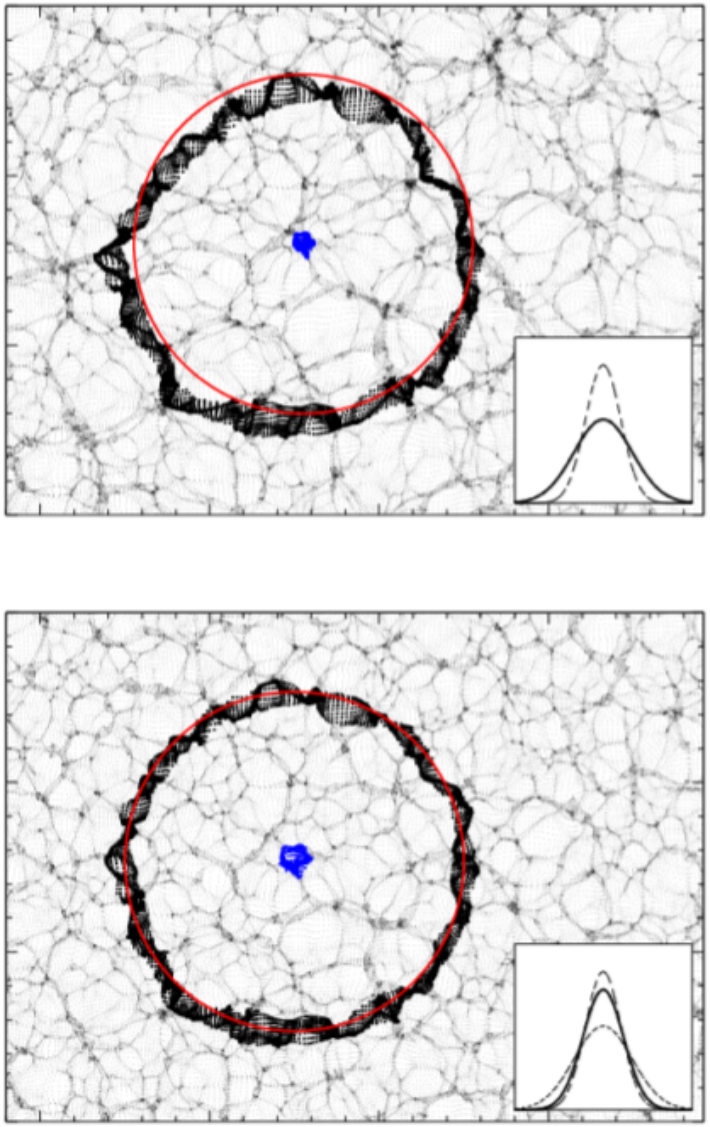

Galaxies originally on BAO ring displaced by peculiar velocities due to acceleration toward mass concentrations.

Use observed density map to move galaxies back to their original comoving position.

$\Rightarrow$ improved resolution on BAO peak position

Padmanabhan et al. arXiv:1202.0090

Relative-velocity bias

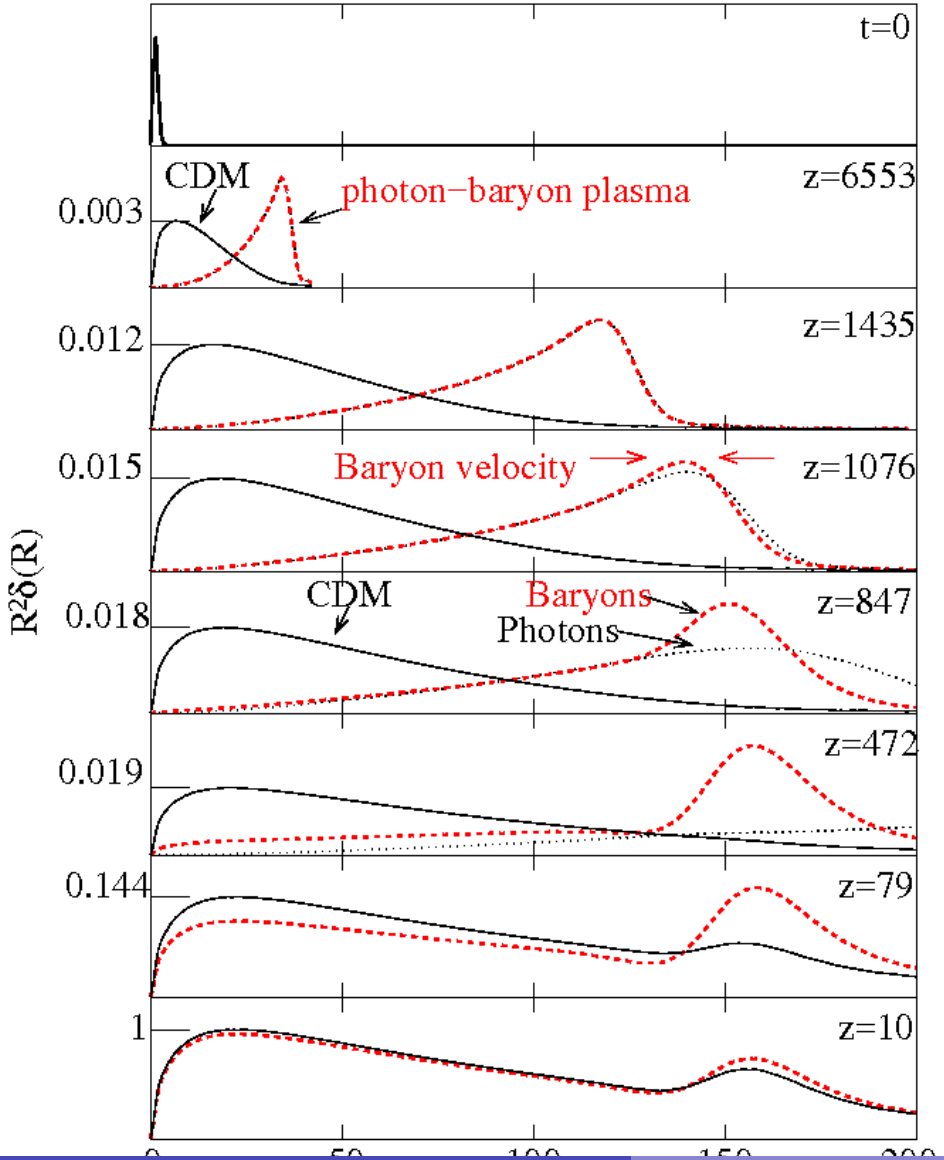

At BAO peak, v_{baryon} changes sign whereas v_{cdm} always points to origin.

$\Rightarrow$ may favor galaxy formation on one side of BAO peak?

Relative-velocity bias

Unknown parameter, b_v gives excess probability to form a galaxy with initial $v_{cdm} - v_b \neq 0$.

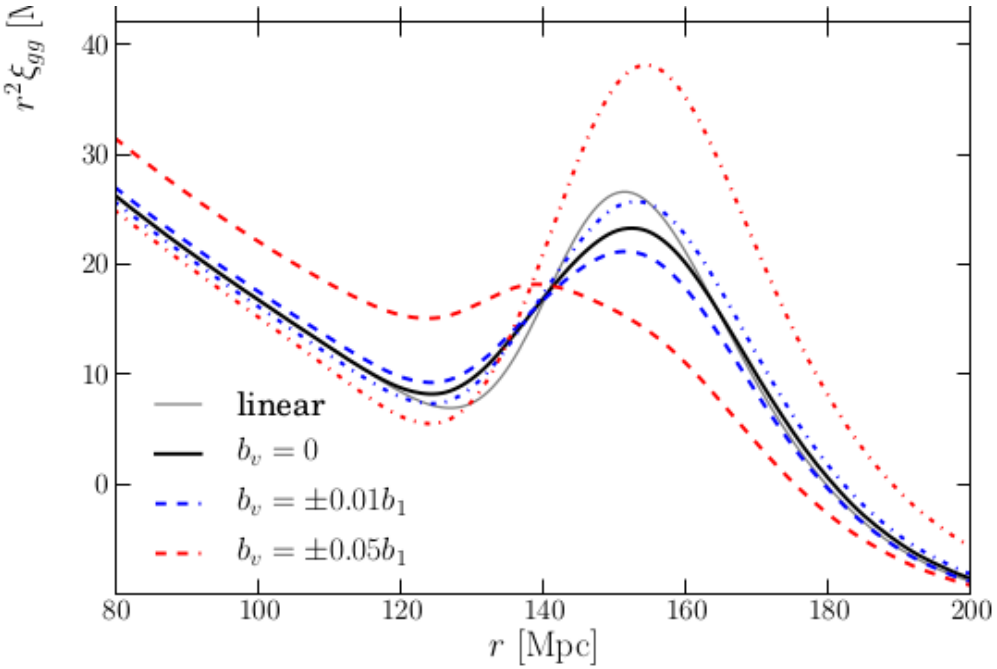

Peak shift and shape deformation depends on value of b_v.
Blazek, McEwen, Hirata arXiv:1510.03554

Fortunately, effect is not degenerate with a simple shift in $(D_M/r_d, D_H/r_d)$.

Beutler,Seljak,Vlah arXiv:1612.04720: $<$ 0.5σ effect on present measurements.
May be a limiting factor in next generation of measurements (0.1% precision).

Outline

- BAO generalities
  - The physics: the round horizon r_d
  - Results: $(D_M/r_d,\ D_H/r_d)$ vs. redshift
  - Cosmological constraints: with and without CMB and SNIa
- BAO with tracers (galaxies, quasars...)
  - Observations: 10^6 spectra
  - Reconstruction
  - Redshift-space distortions
  - Relative-velocity bias
- The Lyα forest
  - Quasar spectra
  - BAO in the forest
  - Reconstructing the linear power spectrum
  - Constraints on neutrino masses

Quasar = Black hole accreting hot gas

Spectrum: power-law + emission lines

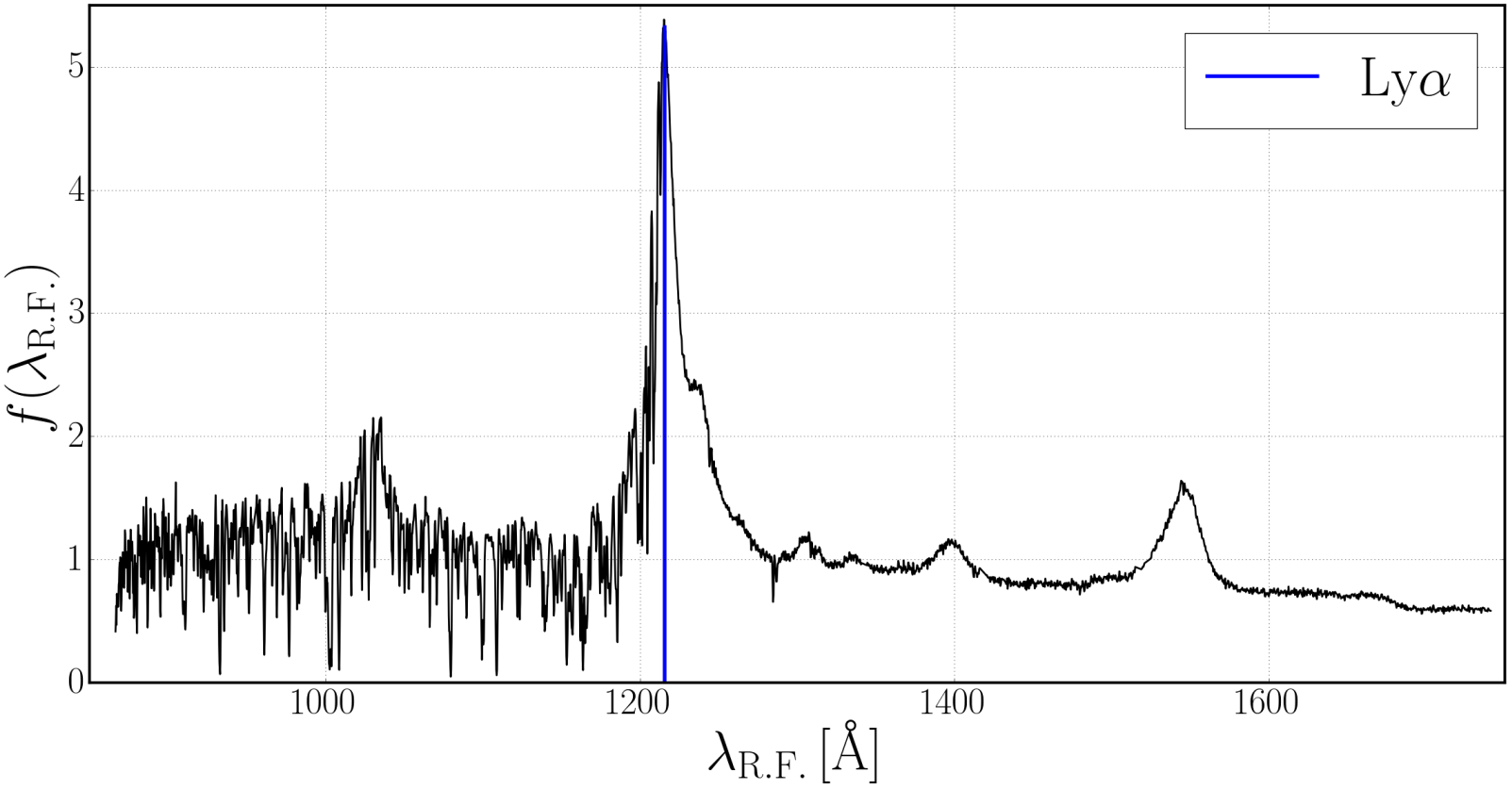

Quasar = Black hole accreting hot gas

Absorption by atomic hydrogen (HI) blueward of Lyα emission

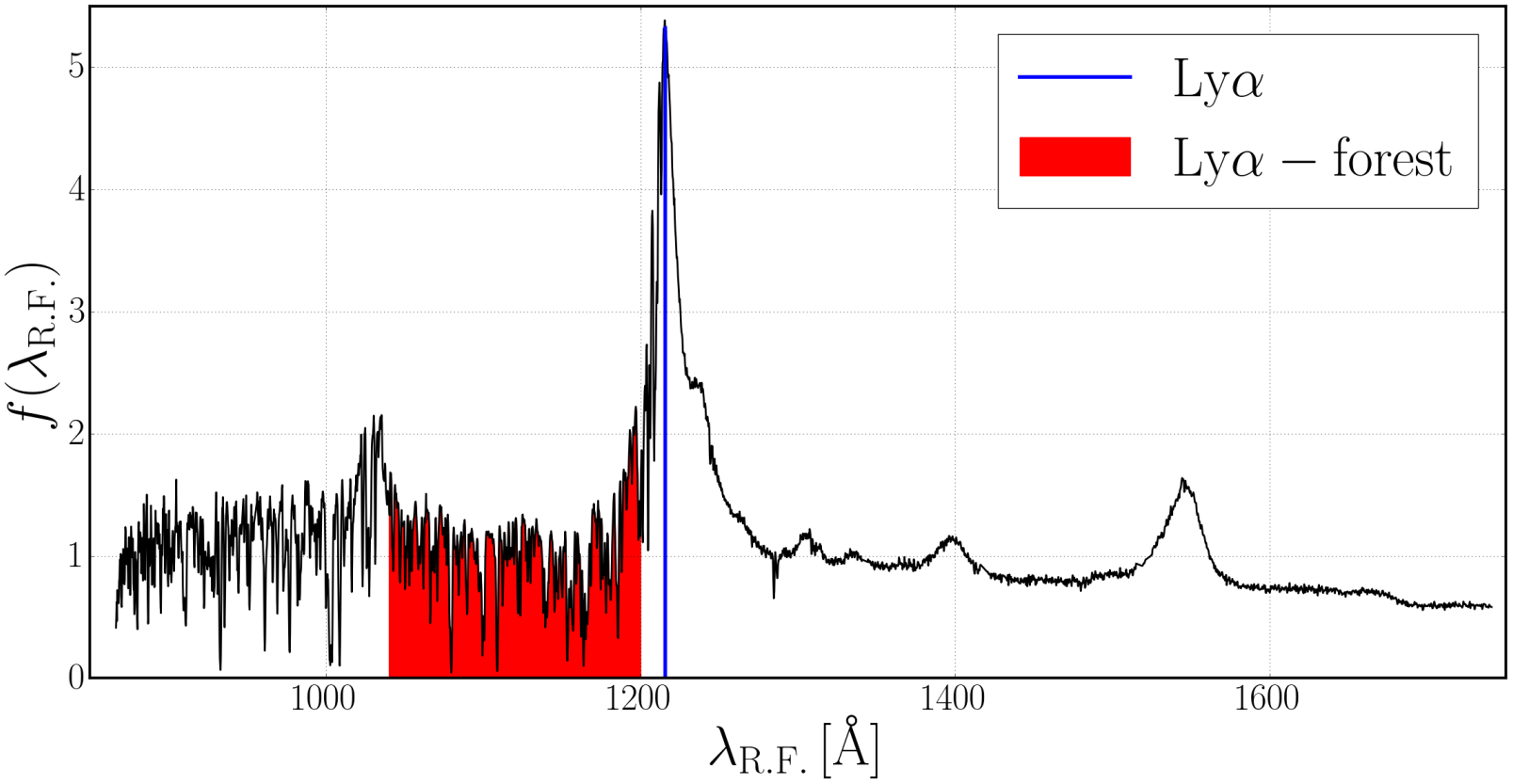

Absorption at $\lambda_{observed}$ depends on n_{HI} at $z + 1 = \lambda_{obs}/1215$.

Model forest spectrum to find $\delta_q(\lambda)$

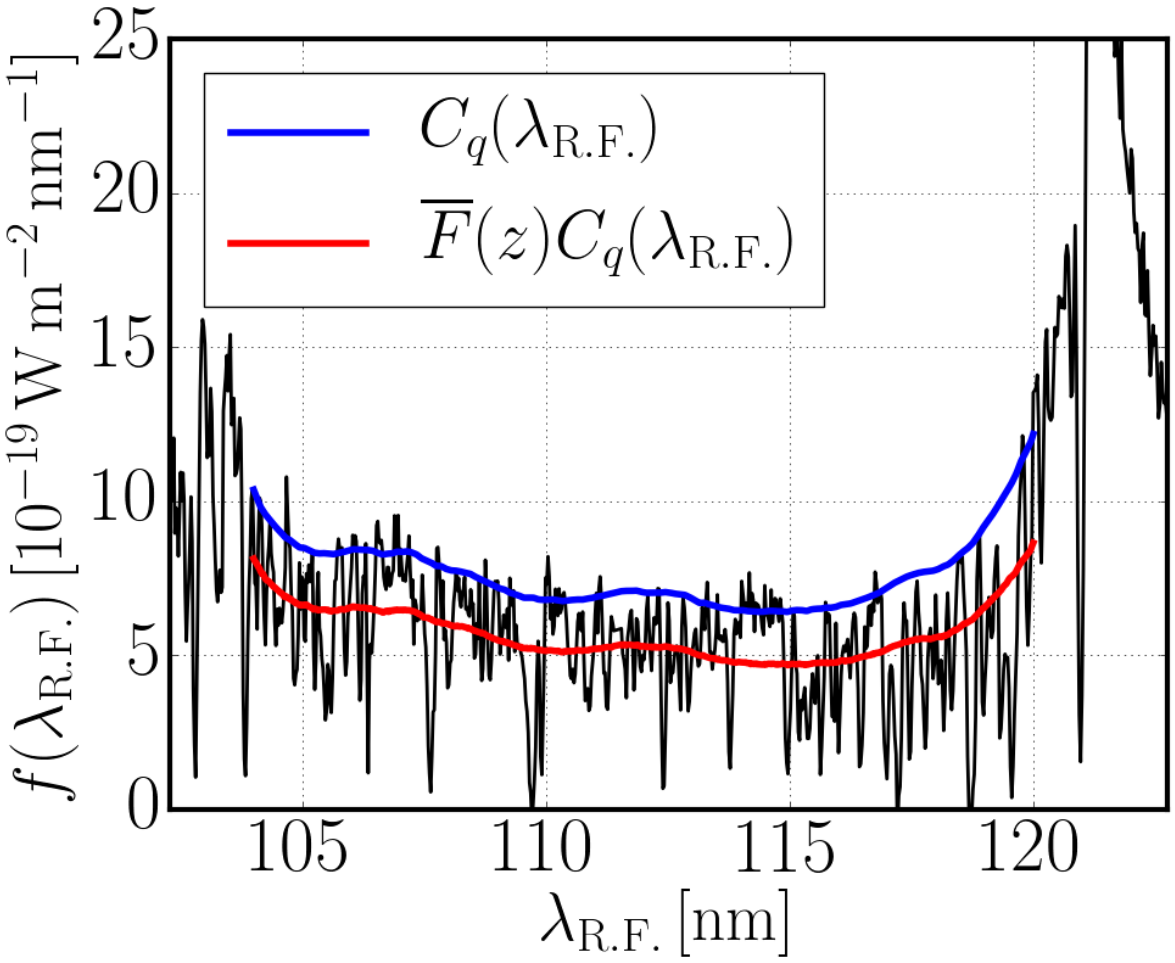

$$\delta_q(\lambda) = \frac{f_q(\lambda)}{\bar{F}(z)C_q(\lambda)} - 1 \qquad \delta_q < 0\ (> 0) \Rightarrow n_{HI} >\ (<)\bar{n}_{HI}$$

Correlate forests to find $\xi(r_\perp, r_\parallel)$

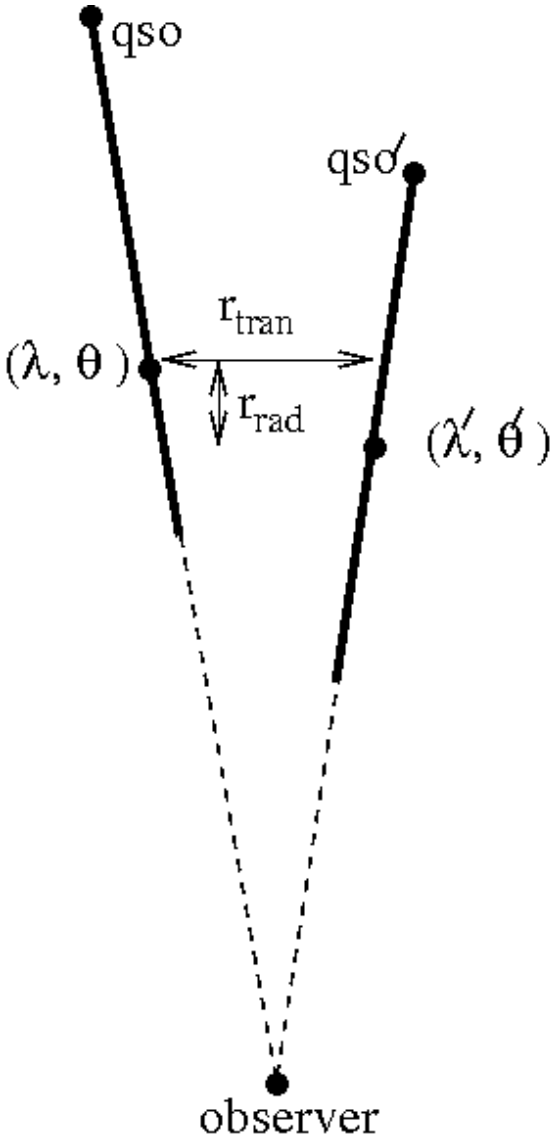

$$\xi(r_\perp, r_\parallel) = \frac{\sum w_i w_j \delta_i \delta_j}{\sum w_i w_j}$$

Sums over pixel pairs (i, j) separated by $(r_\perp, r_\parallel)$
w_i is weight chosen to minimize variance of ξ.

Note: no random catalog is necessary.

BOSS results: Bautista et al. (2017)

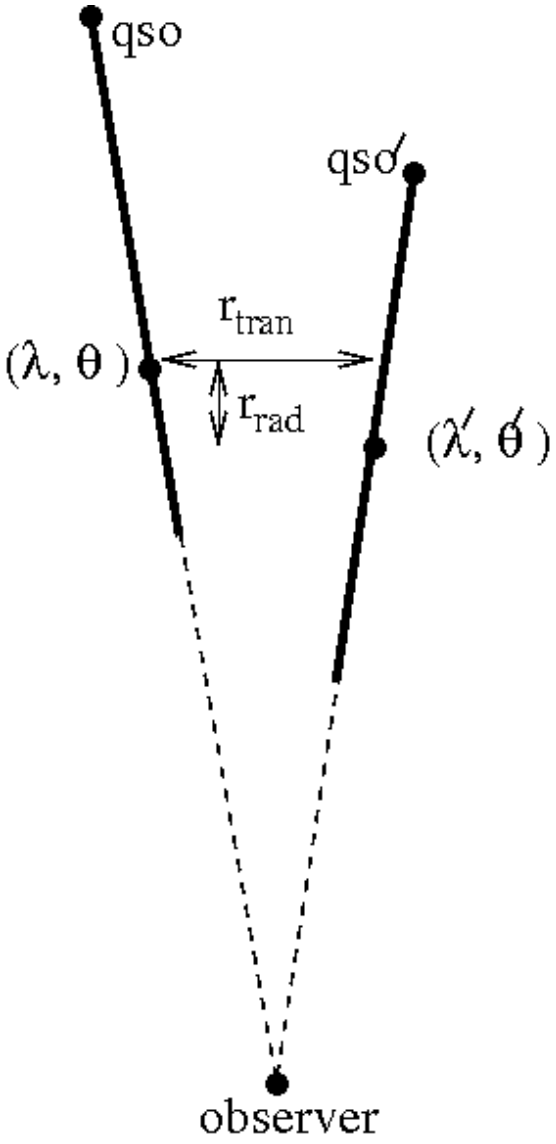

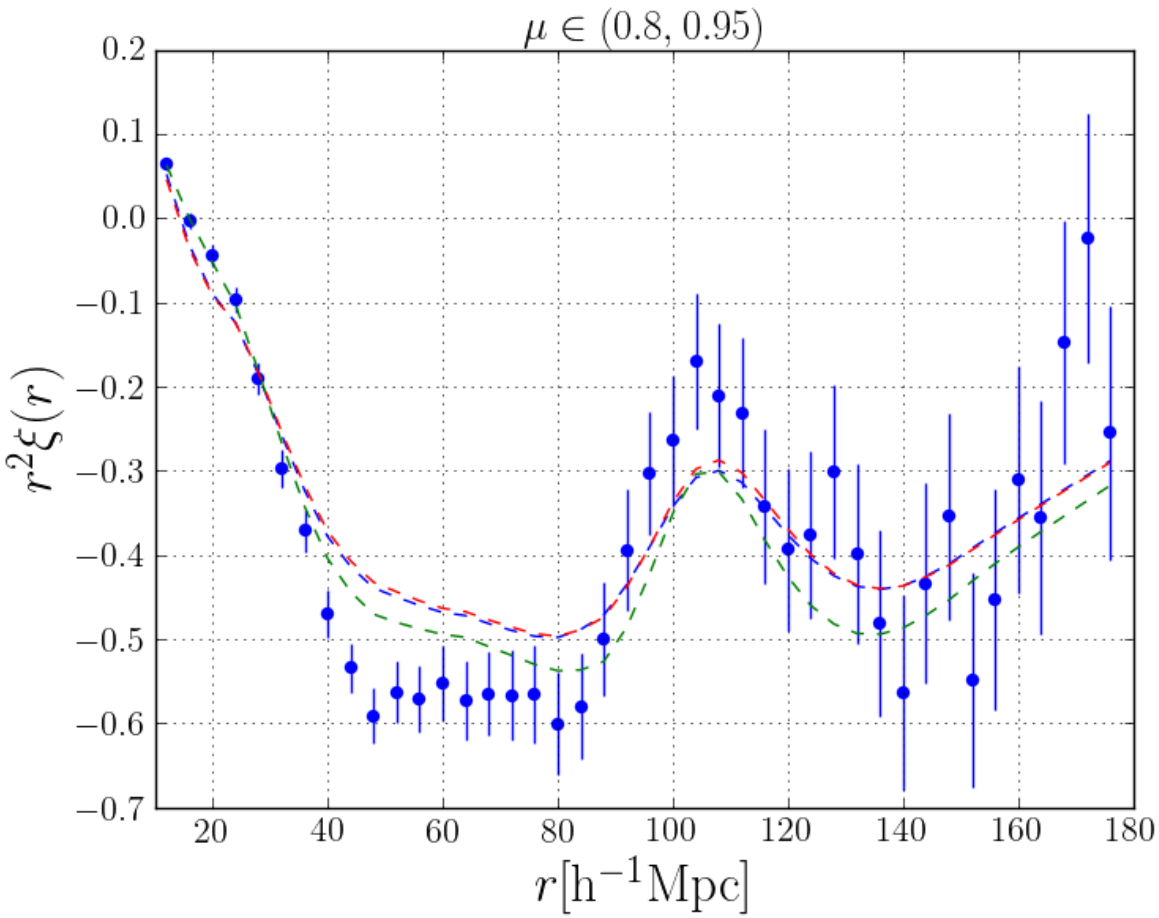

Most of BAO signal at large μ
(low bias of forest)

Correlate forests and quasars

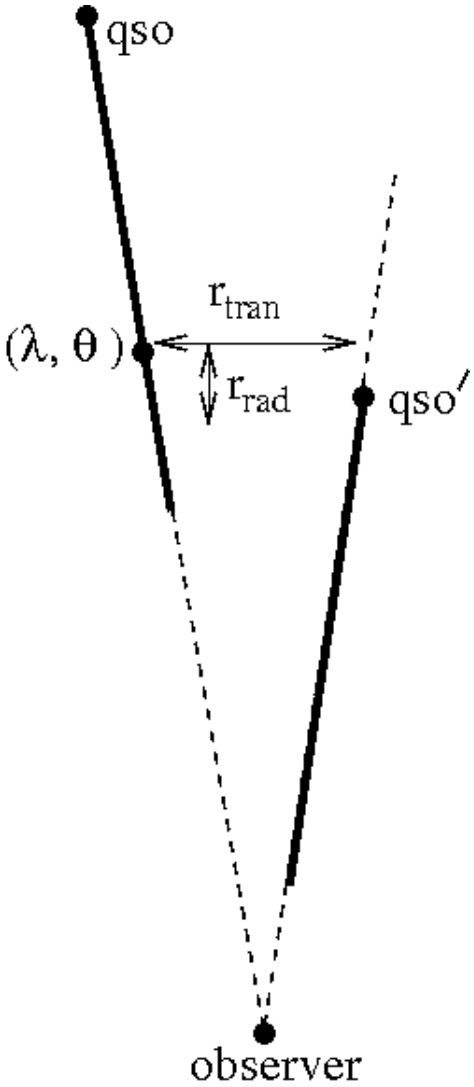

$$\xi(r_\perp, r_\parallel) = \frac{\sum w_i \delta_i}{\sum w_i}$$

Sums over pixel-quasar pairs (i, q) separated by $(r_\perp, r_\parallel)$
w_i is weight chosen to minimize variance of ξ.

Note: no random catalog is necessary.

BOSS: du Mas des Bourboux et al. (2017)

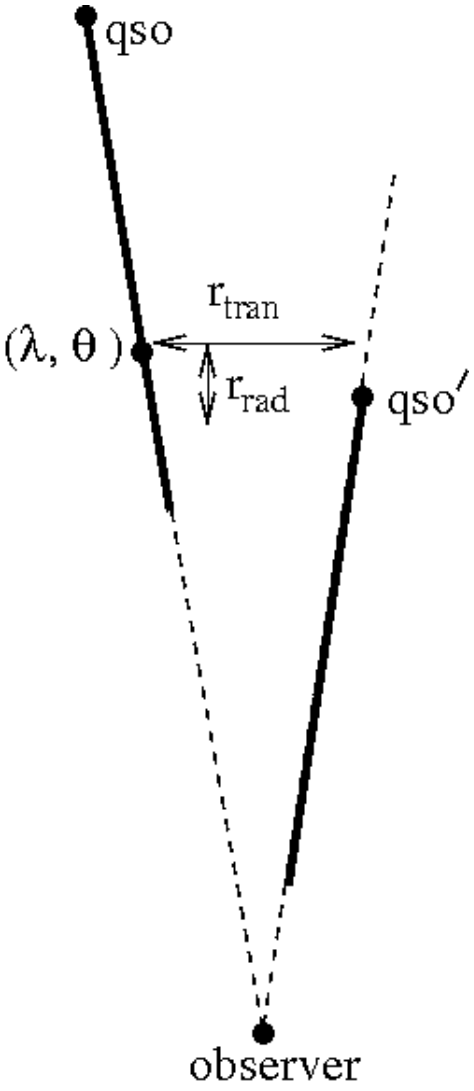

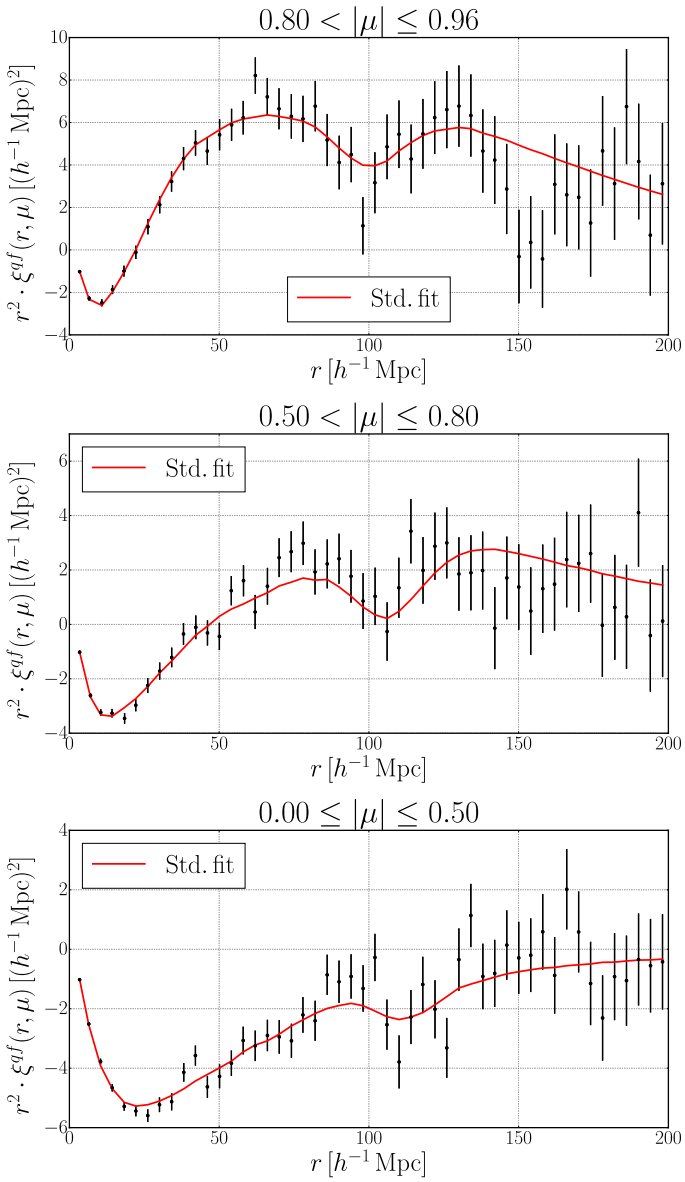

radial

transverse

Constraints on $(D_M/r_d, D_H/r_d)$ at $z = 2.4$

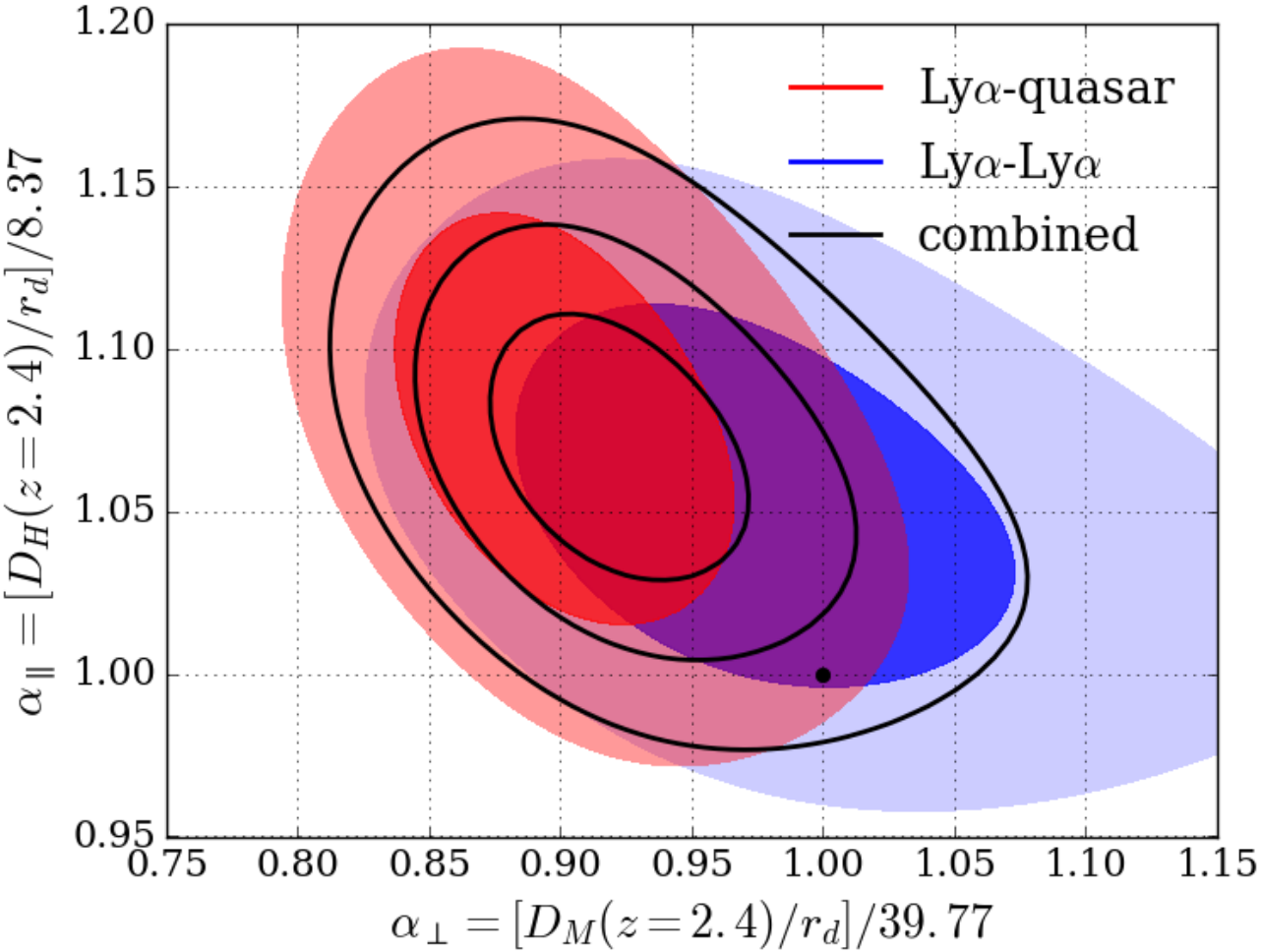

Lyα-Lyα 1σ from Planck flat-ΛCDM
Lyα-quasar 1.8σ from Planck flat-ΛCDM
Combined 2.3σ from Planck flat-ΛCDM

Summary of BAO measurements of D/r_d

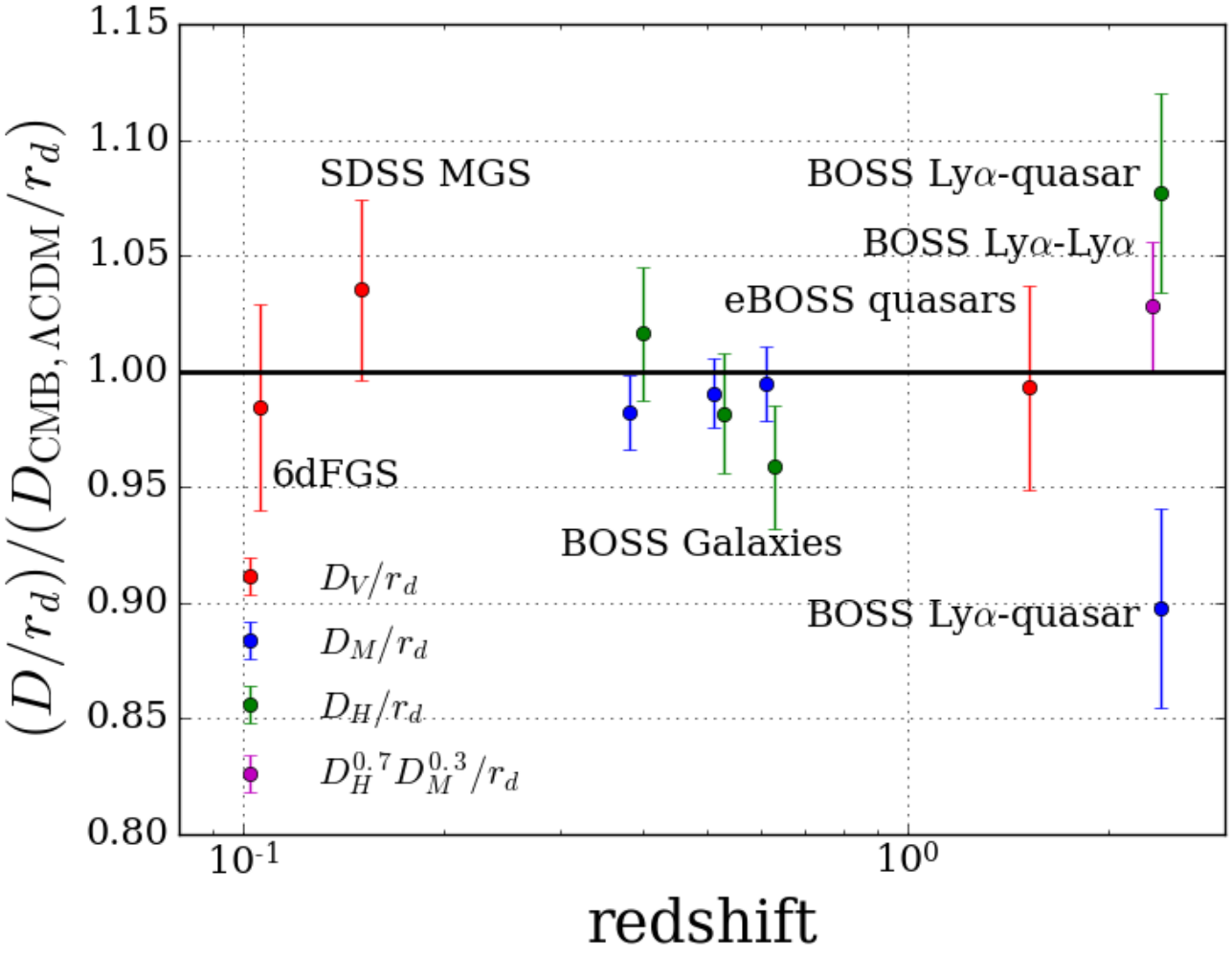

Lyα flux transmission power spectrum

$$P_F(\vec{k}) = P_{lin}(k) b_F^2 (1 + \beta \mu_{\vec{k}}^2) F_{NL}(\vec{k})$$

Bias parameters (b_f, β).

$F_{NL}(\vec{k})$ describes "non-linear" effects.

Galaxy power spectrum depends on unknown astrophysics of galaxy and star formation.

Lyα power spectrum depends on complicated but mostly understood hydrodynamics of the inter-galactic medium.

$\Rightarrow$Use simulations of IGM to find $(b_F, \beta, F_{NL}(\vec{k}))$ to derive $P_{lin}(k)$ from measured $P_F(\vec{k})$

The Lyα forest: structure smoothed at $\sim$ 100kpc

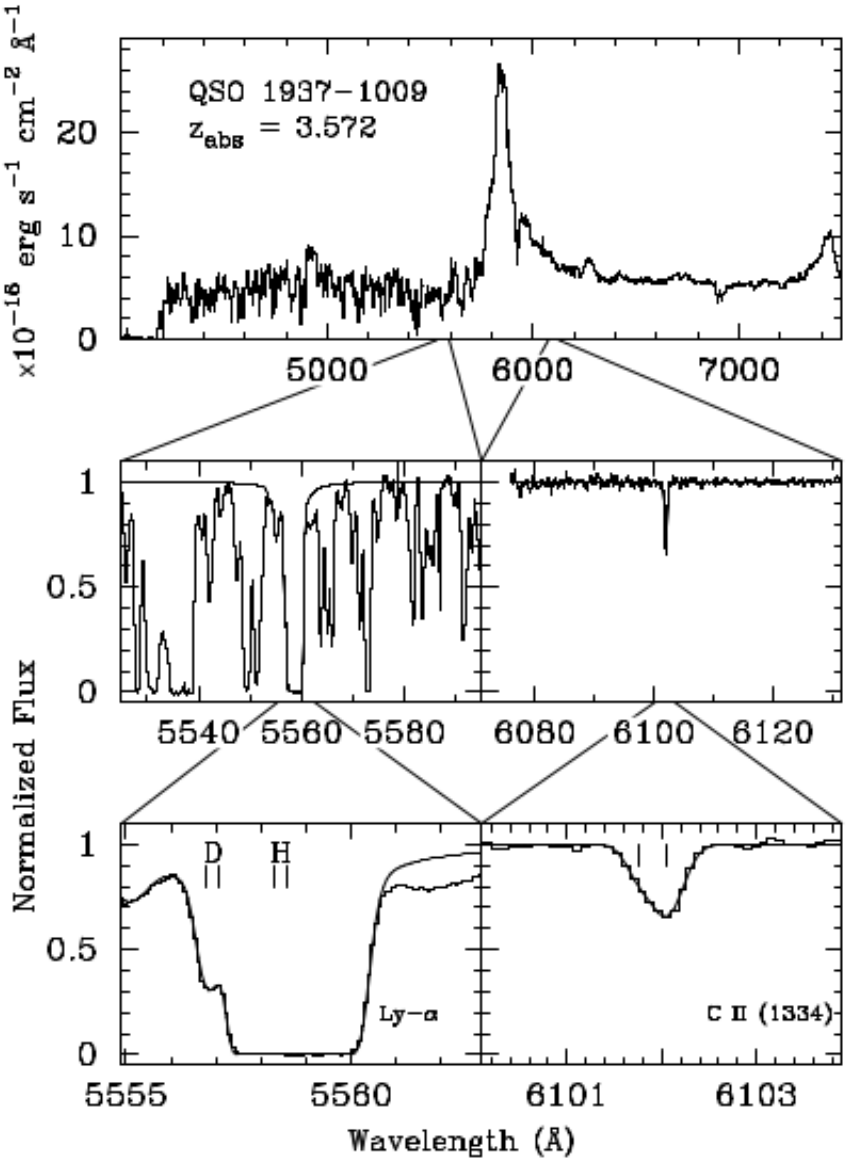

Simulations must resolve Jeans-length of IGM ($\sim$ 100kpc).

High-resolution spectrum (Keck).

How can the power spectrum of such a non-linear field be proportional to the linear dark-matter power?

Bias: reaction to long-wavelength mode

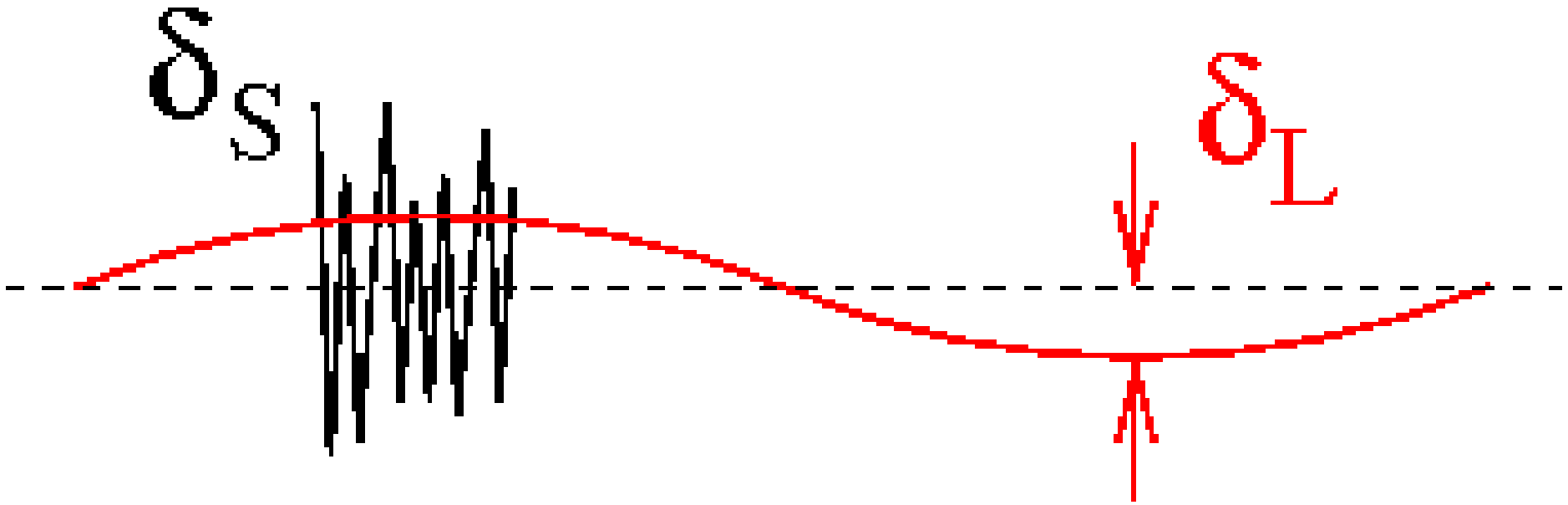

Bias determined by how transmitted flux fraction, F, depends on δ_L

$$F \equiv e^{-\tau(\delta)} \qquad b_\delta \equiv \frac{1}{\overline{F}}\frac{d\overline{F}}{d\delta_L}(\delta_L = 0)$$

$$\text{FGP approximation}: \quad \tau = A(1+\delta_S+\delta_L)^\alpha \quad \alpha \sim 1.6 \quad \text{and(!)}\ \eta = 0$$

Linear growth: δ_S independent of δ_L

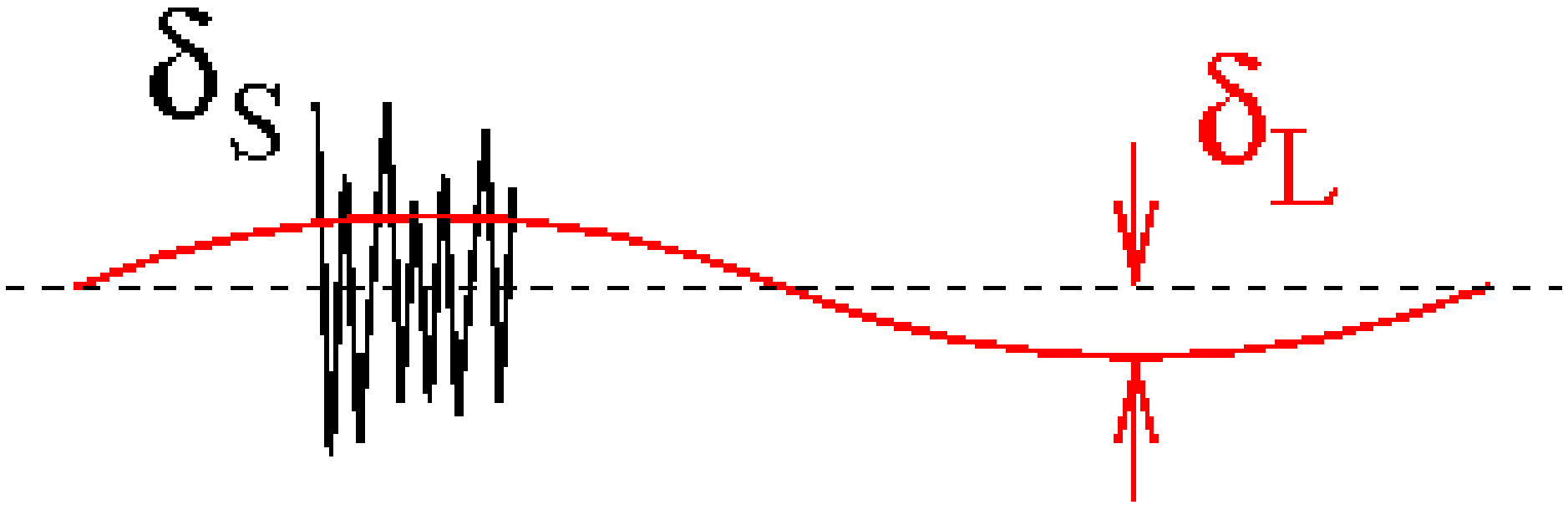

$$b_\delta \equiv \frac{1}{\overline{F}}\frac{d\overline{F}}{d\delta_L}(\delta_L = 0) = \frac{\alpha}{\overline{F}}\left\langle \frac{F \ln F}{(\ln F/A)^{1/\alpha}} \right\rangle$$

Interesting limits: $\alpha = 0 \Rightarrow b_\delta = 0$;
$\alpha = 1 \Rightarrow b_\delta = A$.

Non-Linear growth: δ_S depends on δ_L

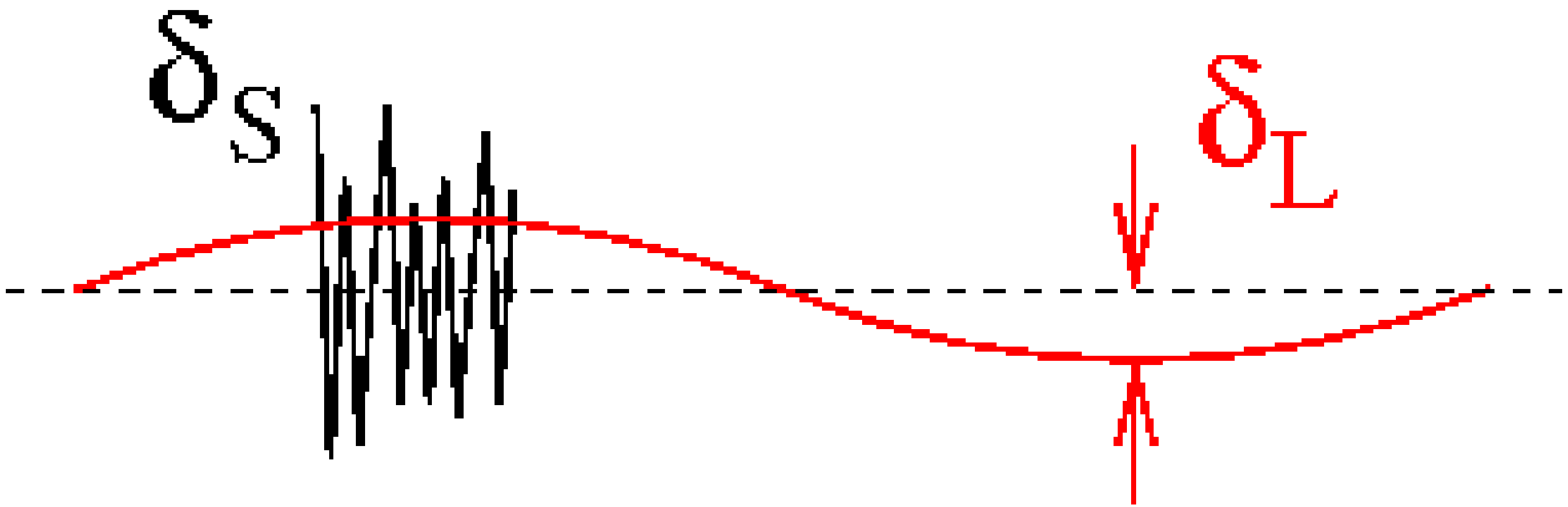

$\delta_S^{(2)} = (1 + \nu_2 \delta_L)\delta_S^{(1)}$ where $\nu_2 = 34/21$ (second order pert. kernel).

$$b_\delta = \frac{\alpha}{\overline{F}} \left\langle \frac{F \ln F}{(\ln F/A)^{1/\alpha}} \left[1 + \nu_2 \left(\left[\frac{\ln F}{A} \right]^{1/\alpha} - 1 \right) \right] \right\rangle$$

Interesting limit: $\ln F/A - 1$ averages to zero for symmetric δ_S distribution $\Rightarrow \nu_2$ term $\rightarrow 0$

Non-Linear growth: origin of $\nu_2 = 34/21$

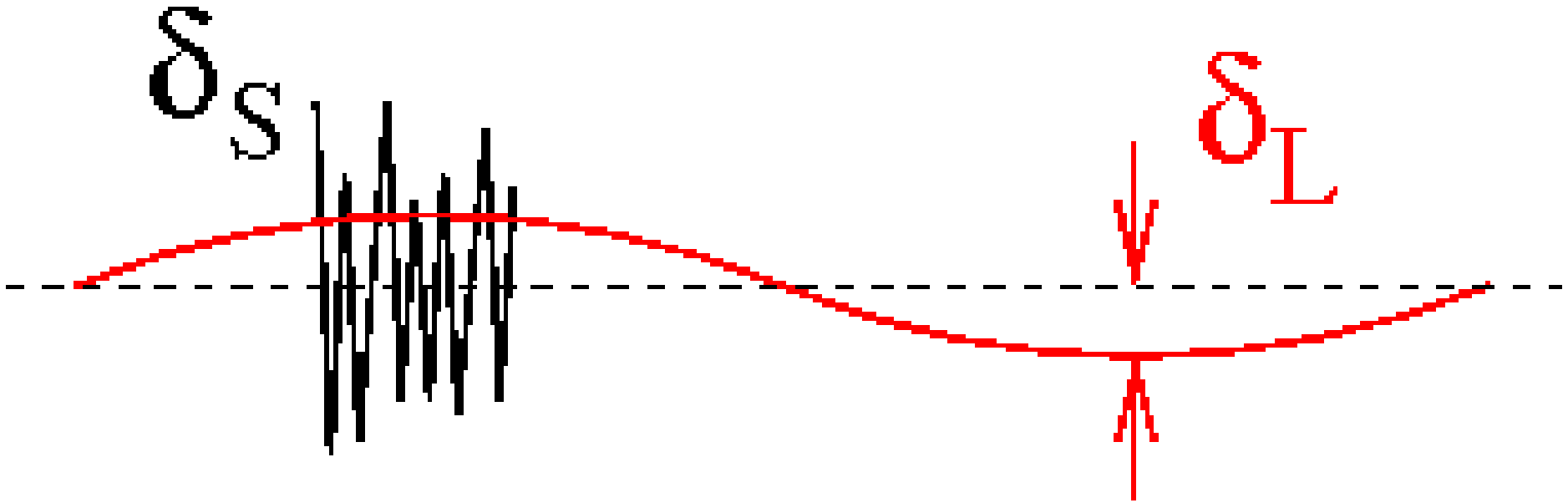

The short-wavelength modes think that they are in a universe with different cosmological parameters (higher or lower density).

See Seljak arXiv:1201.0594 for an elementary derivation of 34/21

Directly seen in CMB-lensing-$\langle\delta^2\rangle$ correlation (Doux et al. 1607.03625)

CMB-lensing-Lyα bispectrum

Doux et al. 1607.03625:

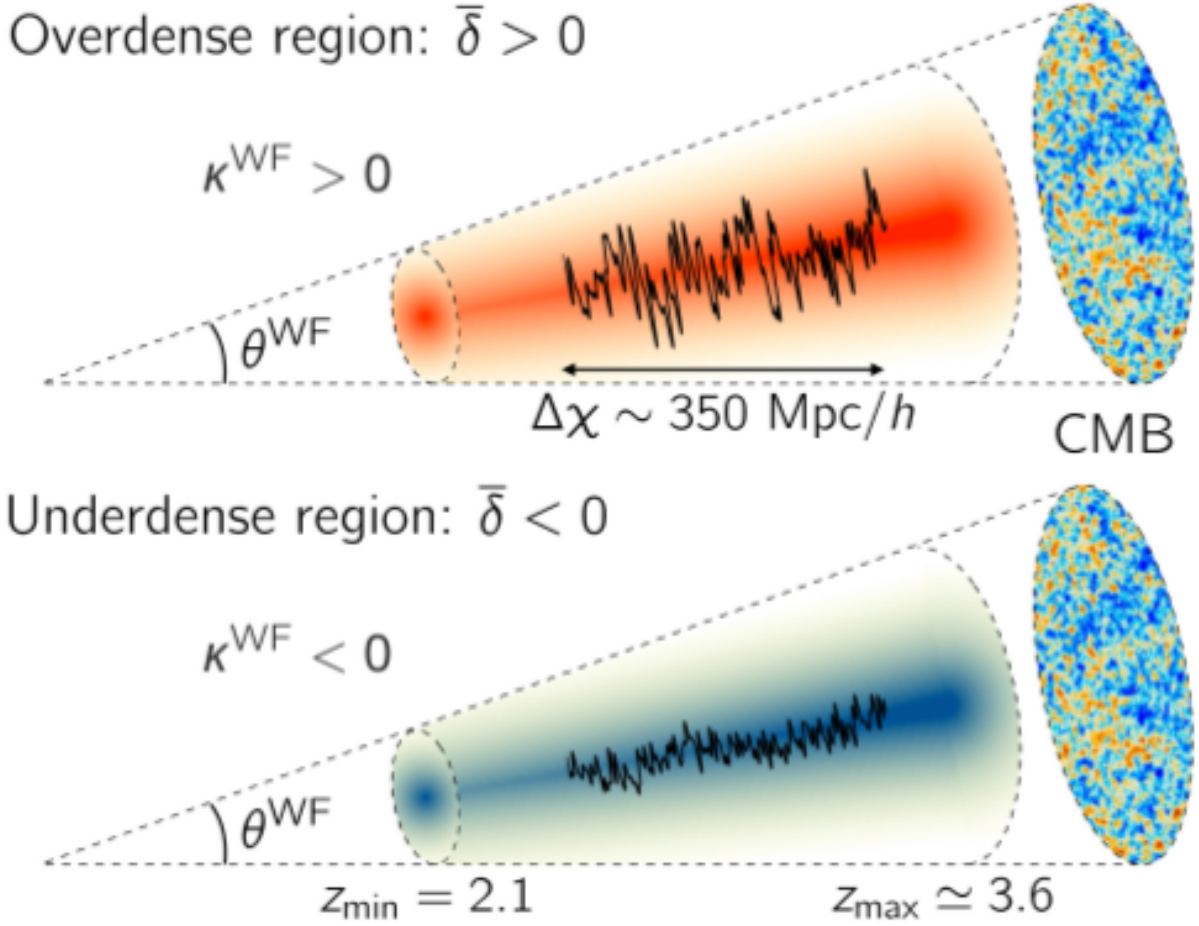

Non-Linear growth: δ_S depends on δ_L

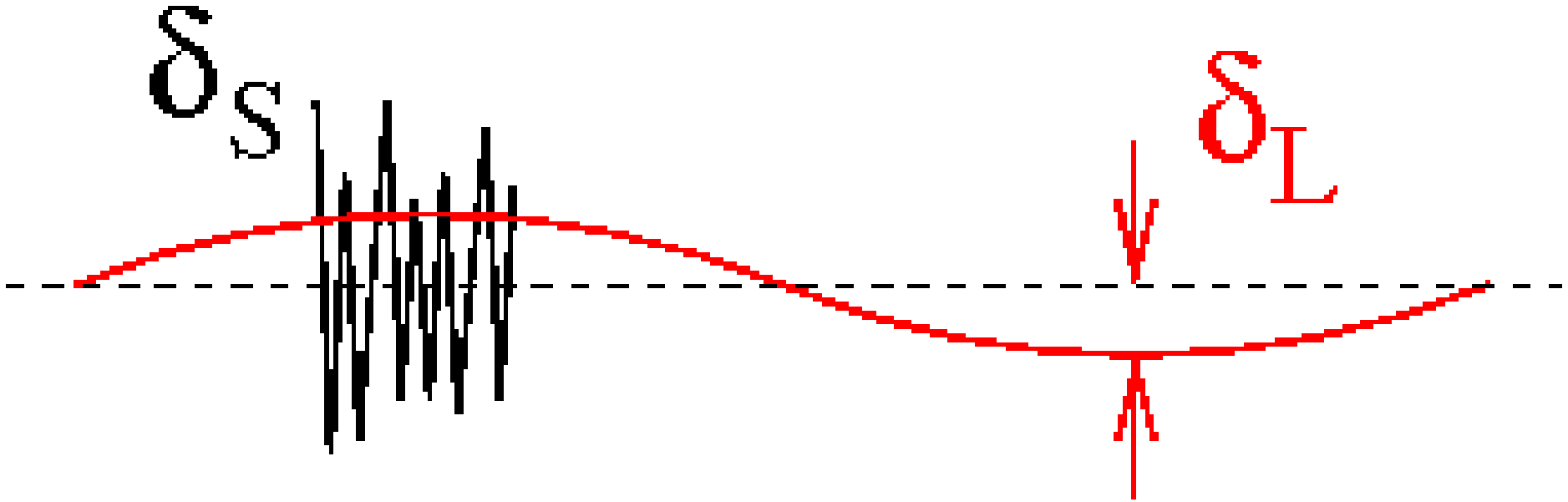

$\delta_S^{(2)} = (1 + \nu_2 \delta_L)\delta_S^{(1)}$ where $\nu_2 = 34/21$ (second order pert. kernel).

$$b_\delta = \frac{\alpha}{\overline{F}} \left\langle \frac{F \ln F}{(\ln F/A)^{1/\alpha}} \left[1 + \nu_2 \left(\left[\frac{\ln F}{A} \right]^{1/\alpha} - 1 \right) \right] \right\rangle$$

Formula works within only factor ~ 2: ignores effects of peculiar velocities and thermal broadening.
$\Rightarrow$ need simulations.

Simple calculation ⇒ key elements of simulations

A photon of wavelength λ traverses a medium containing neutral hydrogen (number density n_{HI}), velocity gradient v'.

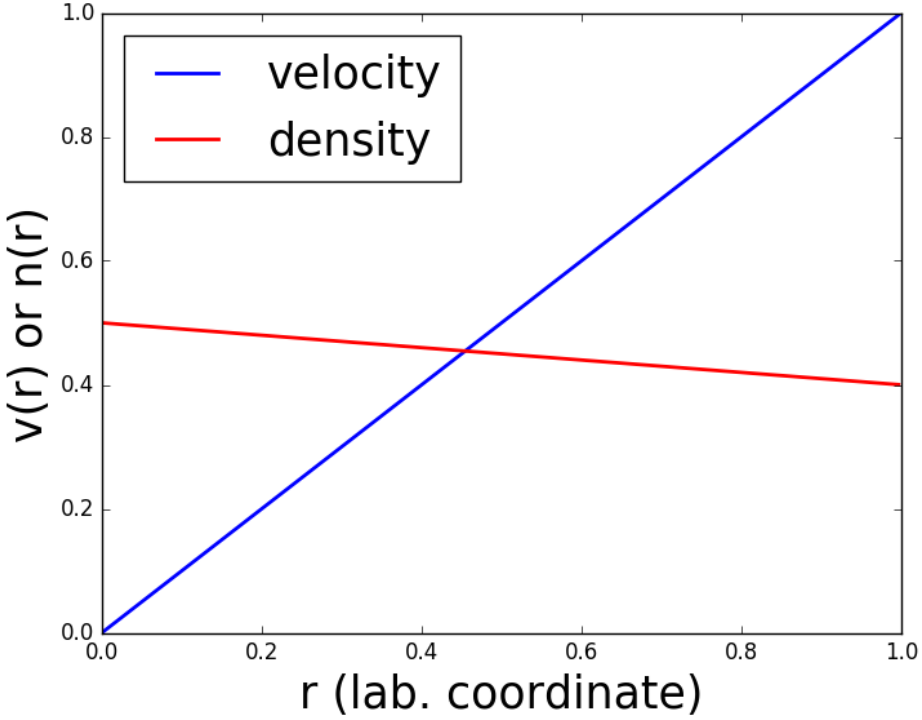

Resonant absorption when

$$\lambda(1 + v(r)/c) = \lambda_\alpha$$

Absorption probability:

$$\tau = 0.416 \frac{\sigma_{Thom}}{\alpha^3} \frac{n_{HI}}{v'/c}$$

The velocity gradient has a cosmological component $H(z)$ and a fluctuating (peculiar velocity, v'_p) component.
The formula for τ assumes a well-defined velocity at each point (perfect fluid) with no thermal fluctuations

How many baryons for a given n_{HI}?

hydrogen atoms, electrons, and protons irradiated by non-thermal photons ($E > 13.6eV$) from quasars
If photoionization rate = recombination rate and $n_{HI} \ll n_H$:

$$n_\gamma n_{HI} \langle \sigma_{ioniz} c \rangle = n_p n_e \langle \sigma_{rec} v \rangle_T$$

$$\Rightarrow n_{HI} = n_b^2 \frac{\langle \sigma_{rec} v \rangle_T}{n_\gamma \langle \sigma_{ioniz} c \rangle} \qquad \langle \sigma_{rec} v \rangle_T \propto T^{-0.7}$$

$$\Rightarrow n_{HI} \propto \frac{(1+z)^6 \, \Omega_b^2 \, (1+\delta)^2 \, T^{-0.7}}{\text{ionizing photon flux}} \qquad \delta = \Delta\rho_b/\rho_b$$

Temperature fluctuations tied to density fluctuations:
$T = \bar{T}(z)(1+\delta)^{\gamma(z)-1}$, $\gamma(z \sim 3) \sim 1.6$
Photon flux fluctuations from quasar number density fluctuations.....

Optical depth, τ, at redshift z

$$\tau(z) \propto \Omega_b^2 \frac{(1+z)^6\,\bar{T}(z)^{-0.7}}{H(z)J_\gamma(z)}\,\frac{(1+\delta(z))^\beta}{(1+\eta(z))^1} \qquad \eta \equiv \frac{v_p'(z)}{H(z)}$$

where $\beta = 2 - 0.7(\gamma(z) - 1) \sim 1.6$.
Formula assumes well defined $v_p(z)$ (no thermal broadening or trajectory crossings!).
Fluctuations of density, δ, and velocity gradient, η, $\Rightarrow \tau$ fluctuations

Power spectrum of $F = e^{-\tau}$ depends on

- $\Omega_b^2\,\bar{T}/J_\gamma \rightarrow \bar{F}$
- $P_L(k) \Rightarrow$ statistics of δ and η
- $(\bar{T}, \gamma) \Rightarrow$ thermal broadening
- Non-linear astrophysics: Supernovae, shock-heating.....

Strategy to measure $P_L(k)$ (McDonald, 2003)

Simulate the hydrodynamics of the IGM to predict $P_{F1d}(k_{\|})$ as a function of.

- $\Omega_b^2 \bar{T}/J_\gamma \rightarrow \bar{F}$
- $(\bar{T}, \gamma)$
- $P_L(k)$ parameterized by

$$\Delta_L^2(k_p, z_p) \equiv k^3 P_L(k_p, z_p)/2\pi^2, \qquad n_{eff}(k_p, z_p) = \frac{dlogP_L}{dlogk}(k_p, z_p)$$

$$k_p = 0.009(km/sec)^{-1} \sim 1(h^{-1}\mathrm{Mpc})^{-1} \qquad z_p = 3$$

In ΛCDM, $\Delta_L^2(k_p, z_p)$,$n_{eff}(k_p, z_p)$ determined by $(A_s, n_s, \Omega_c, \Omega_k, h)$

Hopefully, the poorly known astrophysics $(\bar{F}, T, \gamma, SN, shocks....)$ will not spoil the $P_{F1d} - P_L$ connection.

Predicted $P_{F3d}(\vec{k})/P_L(k)$ (McDonald,2003)

radial

transverse

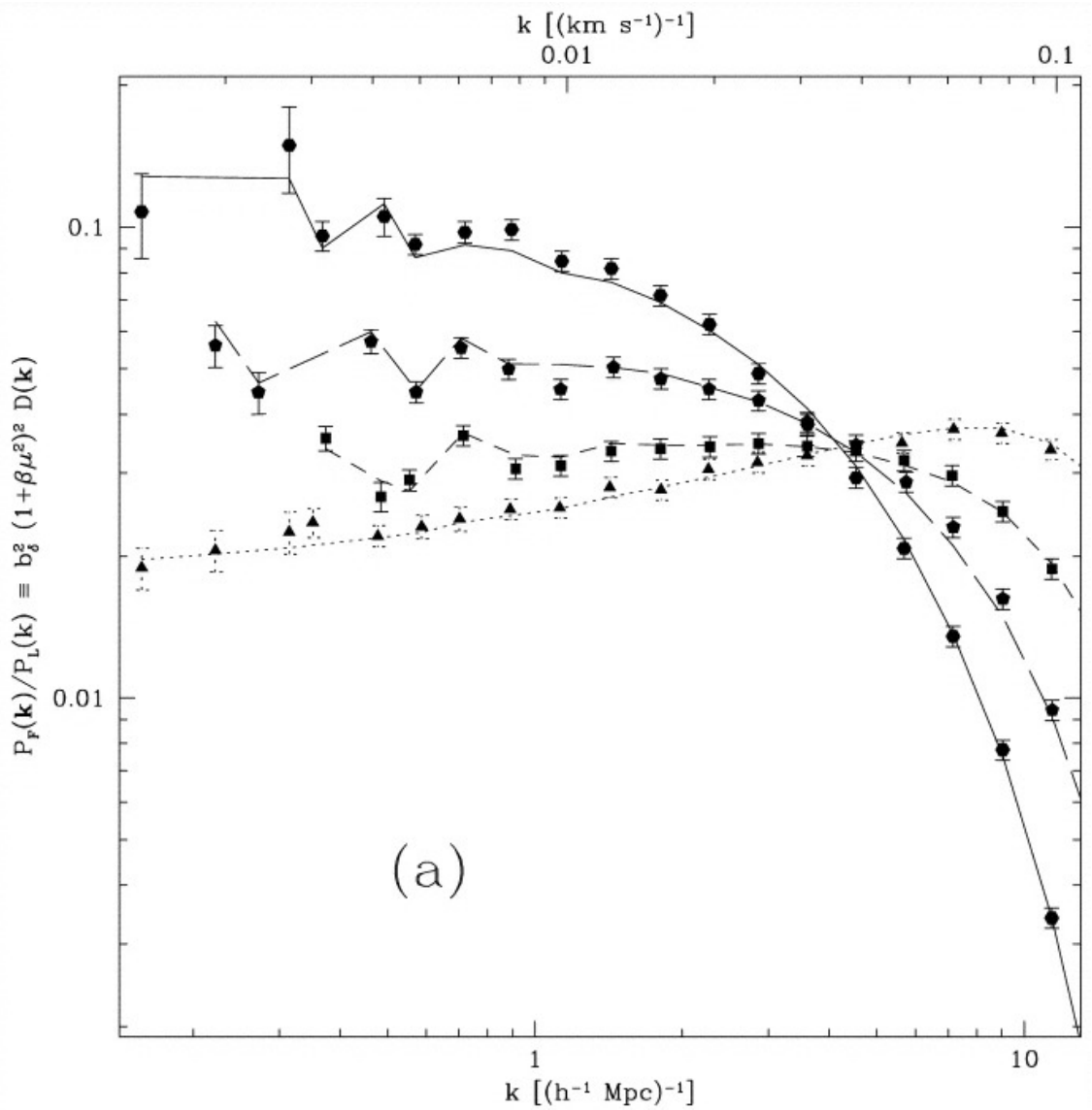

In radial direction, peculiar velocity fluctuations:

enhance power (Kaiser factor) at small k;

suppress power at large k. (like FOG for galaxies)

Predicted $P_{F3d}(\vec{k})/P_L(k)$ (Arinyo et al.,2016)

radial

transverse

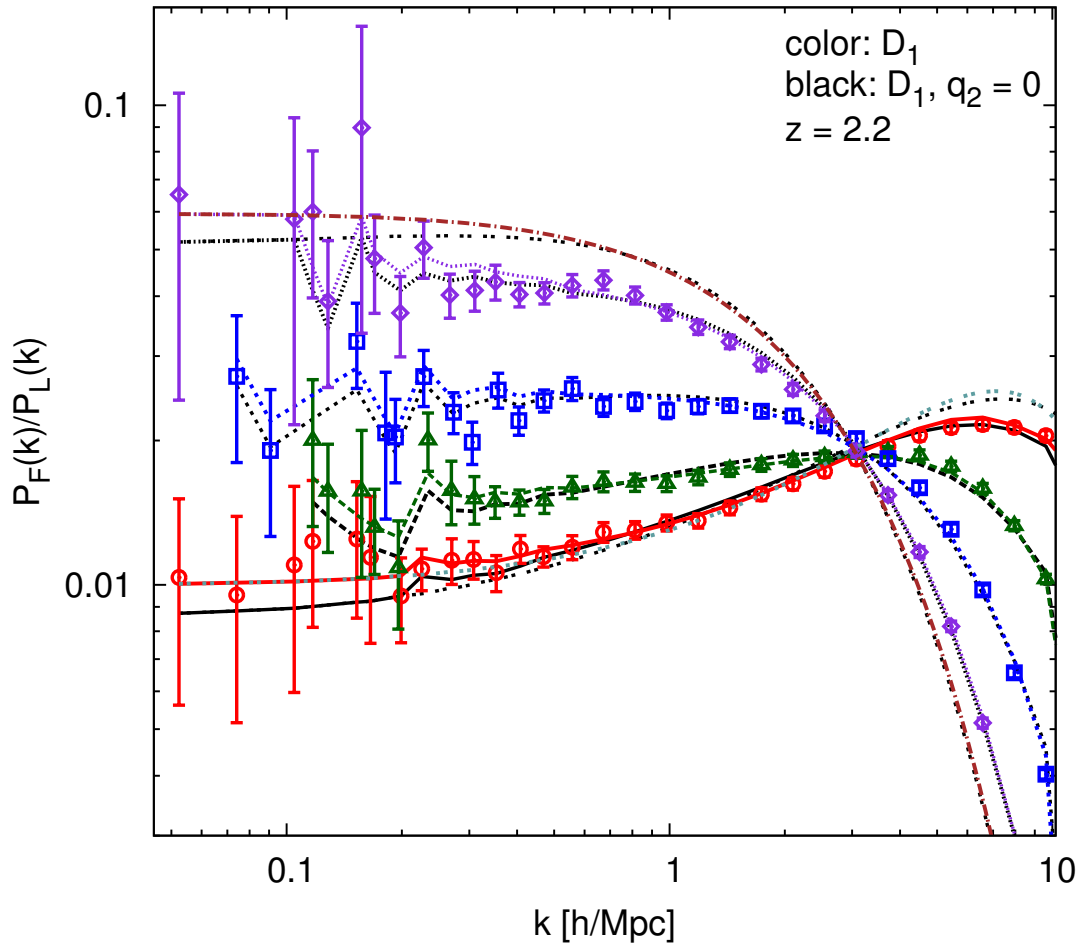

In radial direction, peculiar velocity fluctuations:

enhance power (Kaiser factor) at small k;

suppress power at large k. (like FOG for galaxies)

Predicted $P_{F3d}(\vec{k})/P_L(k)$ (Arinyo et al.,2016)

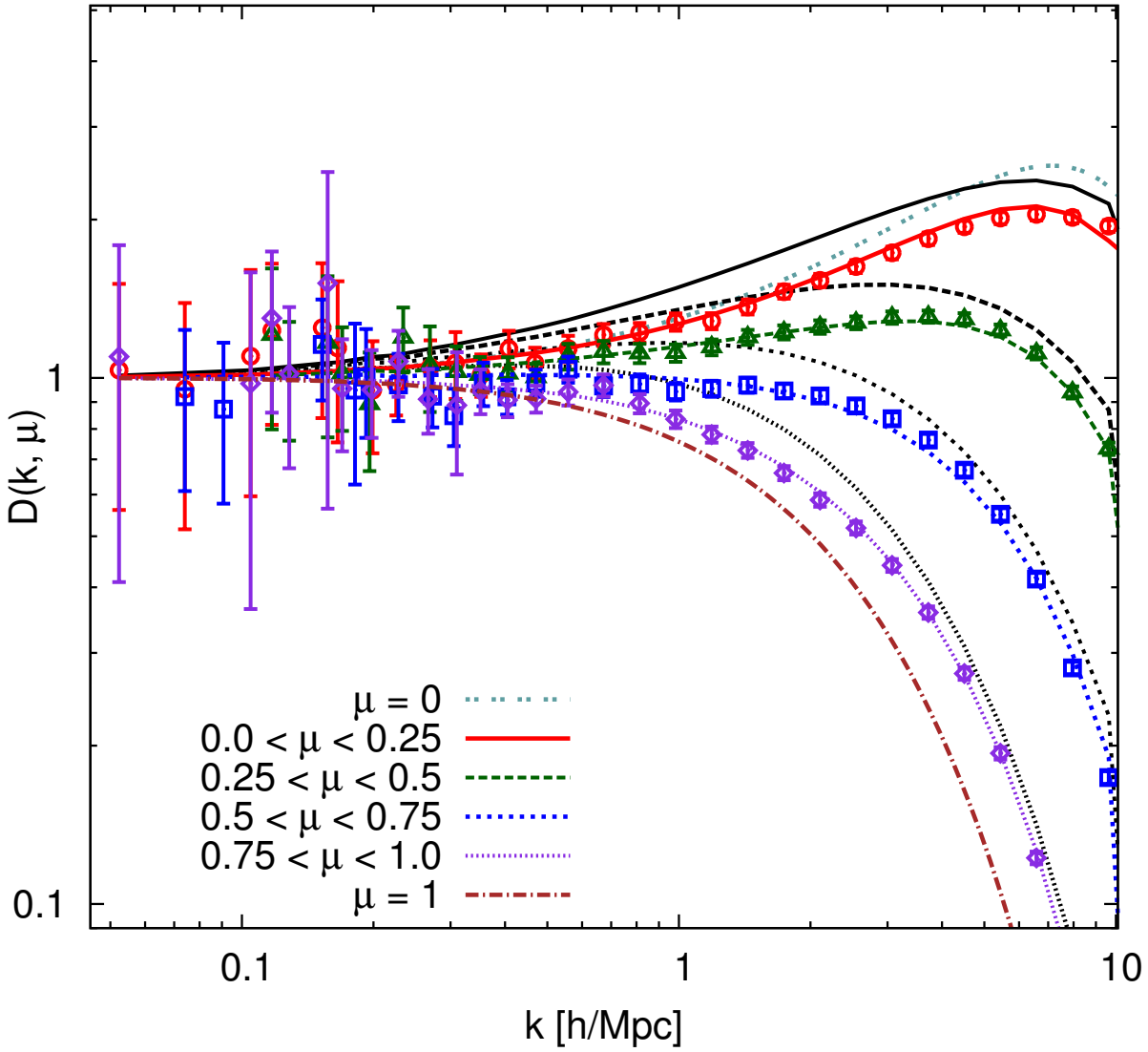

In radial direction, peculiar velocity fluctuations:

enhance power (Kaiser factor) at small k;

suppress power at large k. (like FOG for galaxies)

Suppression of small scale radial power

- velocity spread at one point in real-space (thermal or trajectory crossing) $\Rightarrow$ high density regions contribute to many redshifts

and/or

- More than one real-space point at same velocity $\Rightarrow$ more than one density contributes to one redshift.

Effect of increasing $P_L(k_0)$ or n_{eff} on P_{F3d}

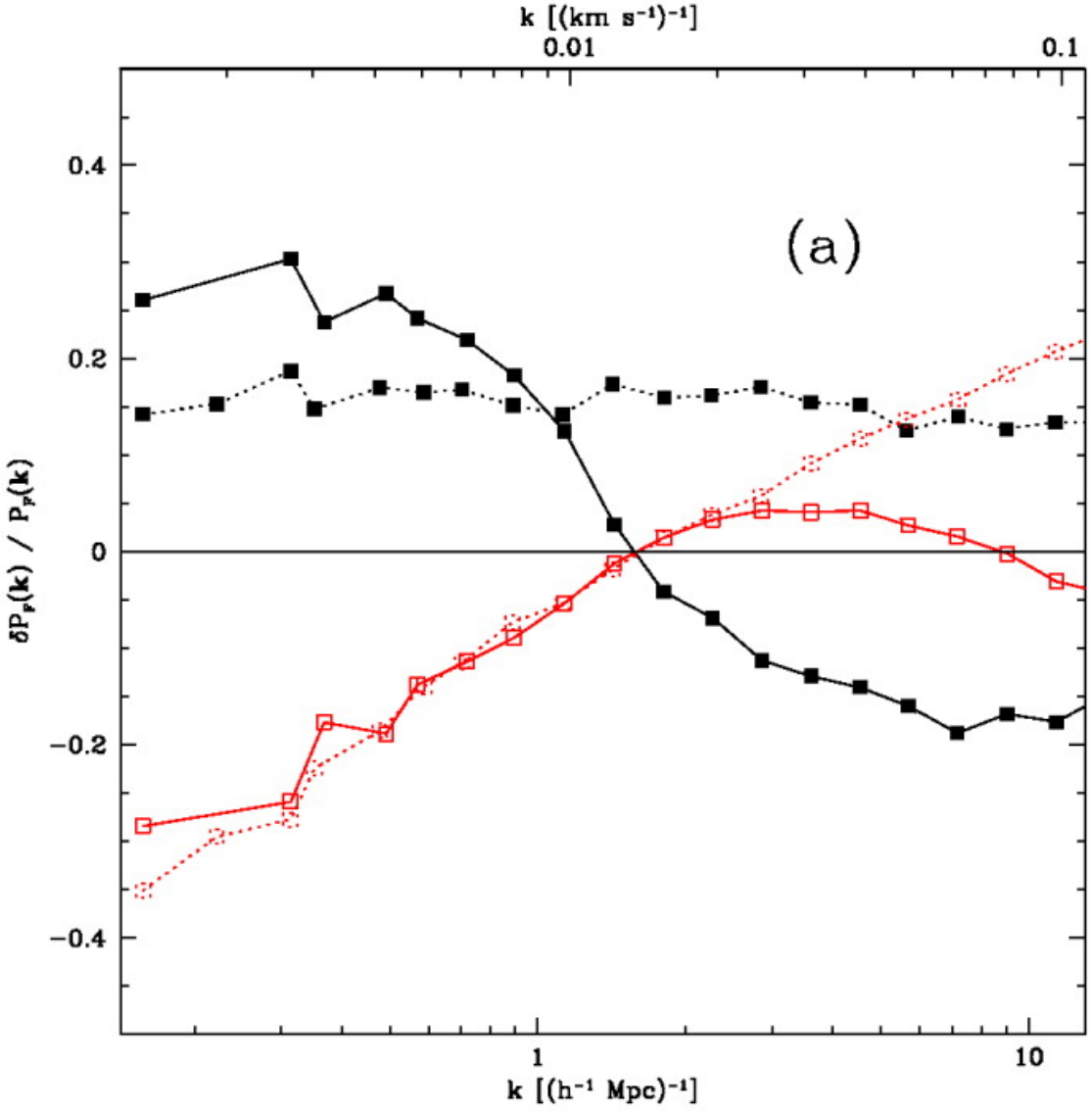

Solid lines: radial direction
dotted lines: transverse

"For $k > 1(h^{-1}\mathrm{Mpc})^{-1}$, it is interesting to note that increasing the mass power actually decreases the flux power along the line of sight, presumably by increasing the power suppression by nonlinear peculiar velocities." (McDonald, 2003)

Effect of increasing $\bar{T}$ or γ on P_{F3d}

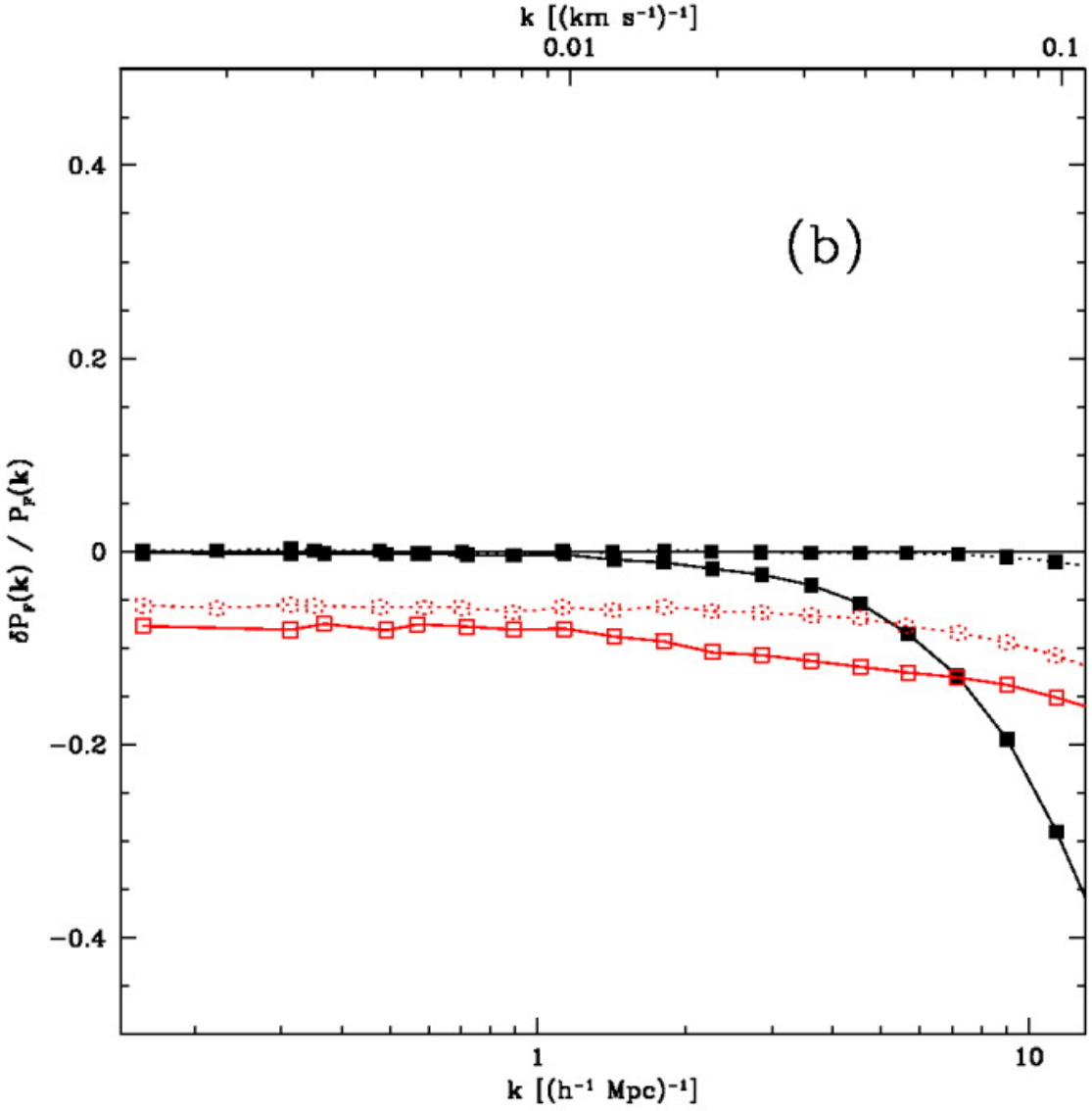

Solid lines: radial direction
dotted lines: transverse

Effect of increasing $\bar{z}$ or $\bar{F}$ on P_{F3d}

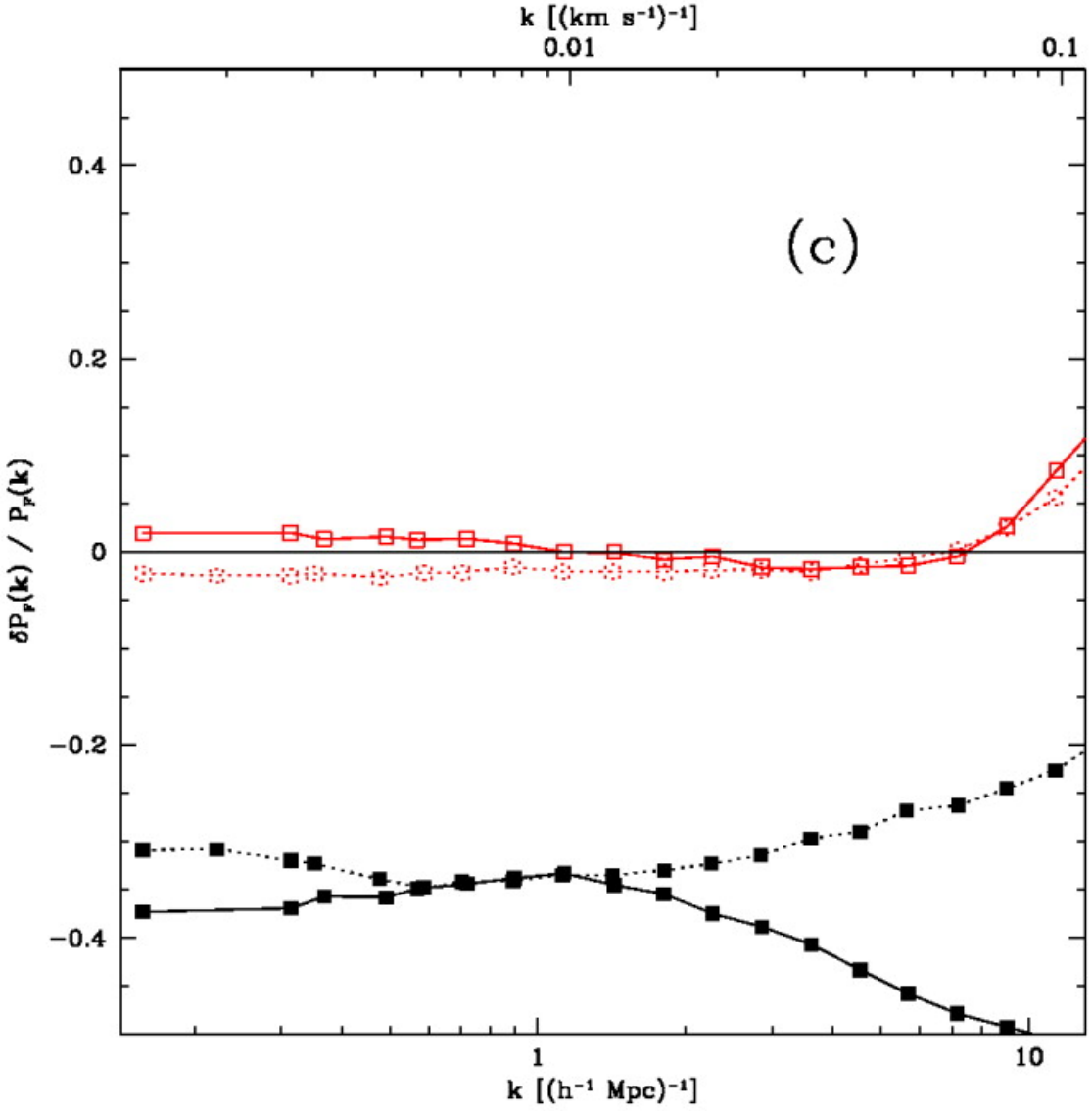

Solid lines: radial direction
dotted lines: transverse

Predicted $P_{F1d}(k_{\|})$ (McDonald et al., 2005)

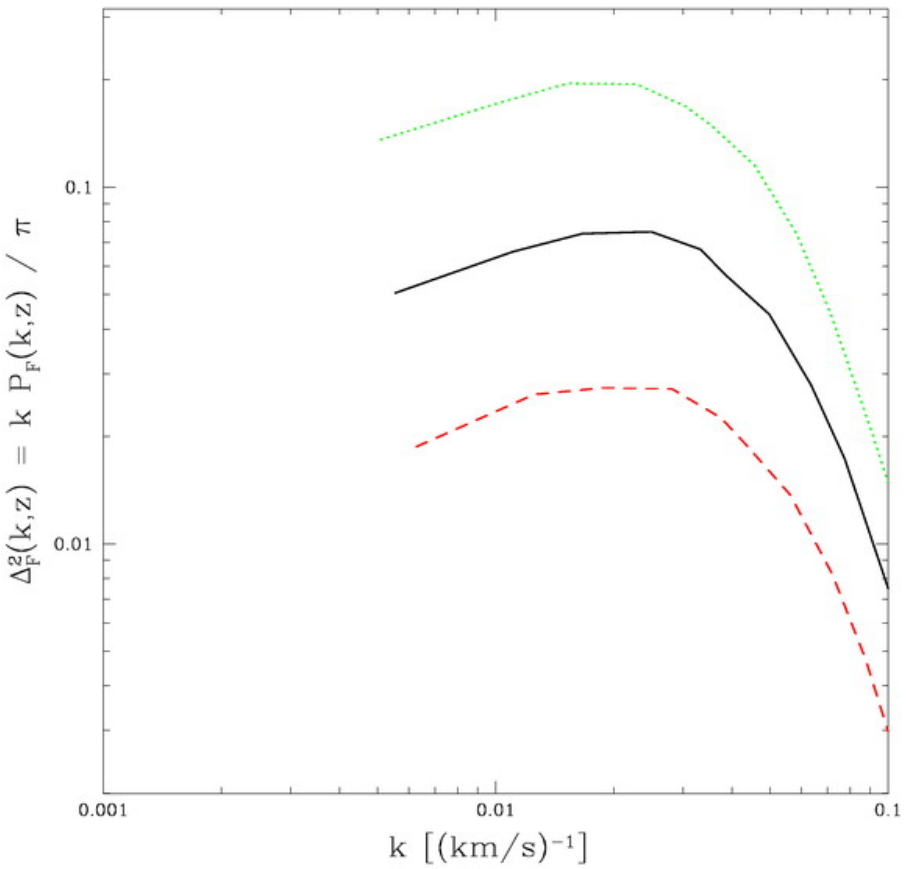

$$\Delta^2_{F1d}(k_\perp) \equiv kP_{F1d}(k_{\|})/\pi$$

$$P_{F1d}(k_{\|}) \sim \int_0^\infty k_\perp dk_\perp P_{F3d}(k_\perp, k_{\|})$$

Effect of increasing P_L or $\bar{F}$ on $P_{F1d}(k, z = 2.12)$

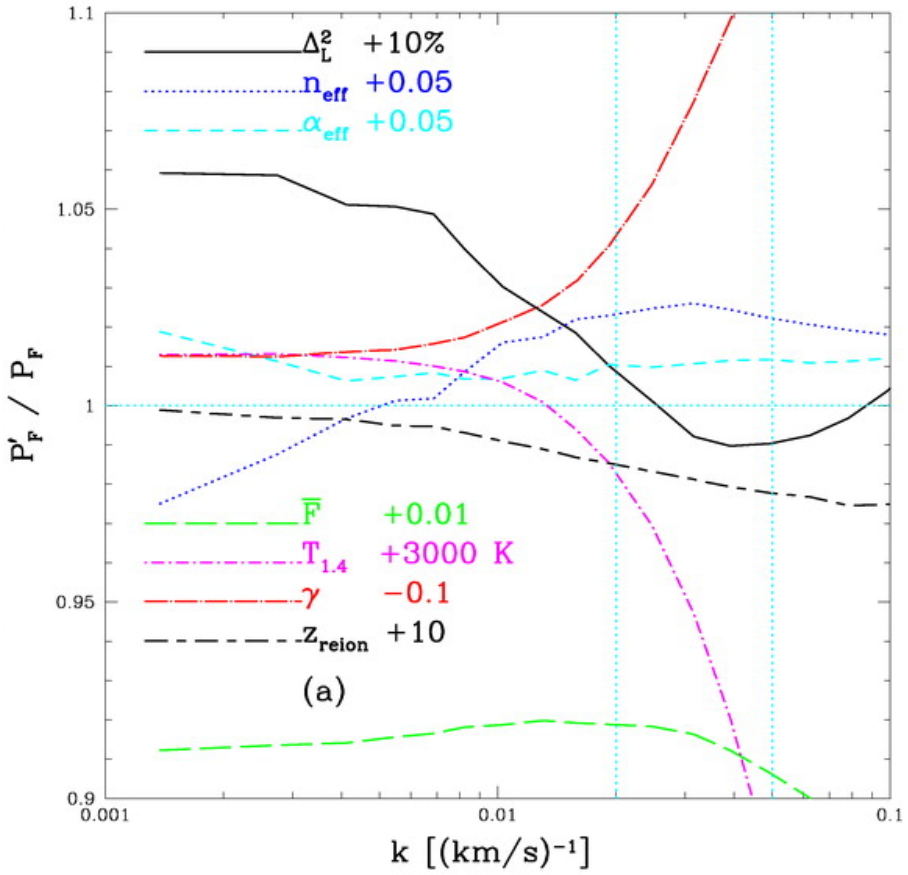

"Increasing $\Delta_L^2(k_p, z_p)$ enhances the power on large scales put actually suppresses the power on small scales"

"(Increasing) $\bar{F}$ produces a relatively flat, large change, which is commonly assumed to be degenerate with Δ_L, although we see that the shapes are not the same, nor are the relative effects at different redshifts:" (McDonald et al., 2005)

Effect of increasing P_L or $\bar{F}$ on $P_{F1d}(k, z = 3.17)$

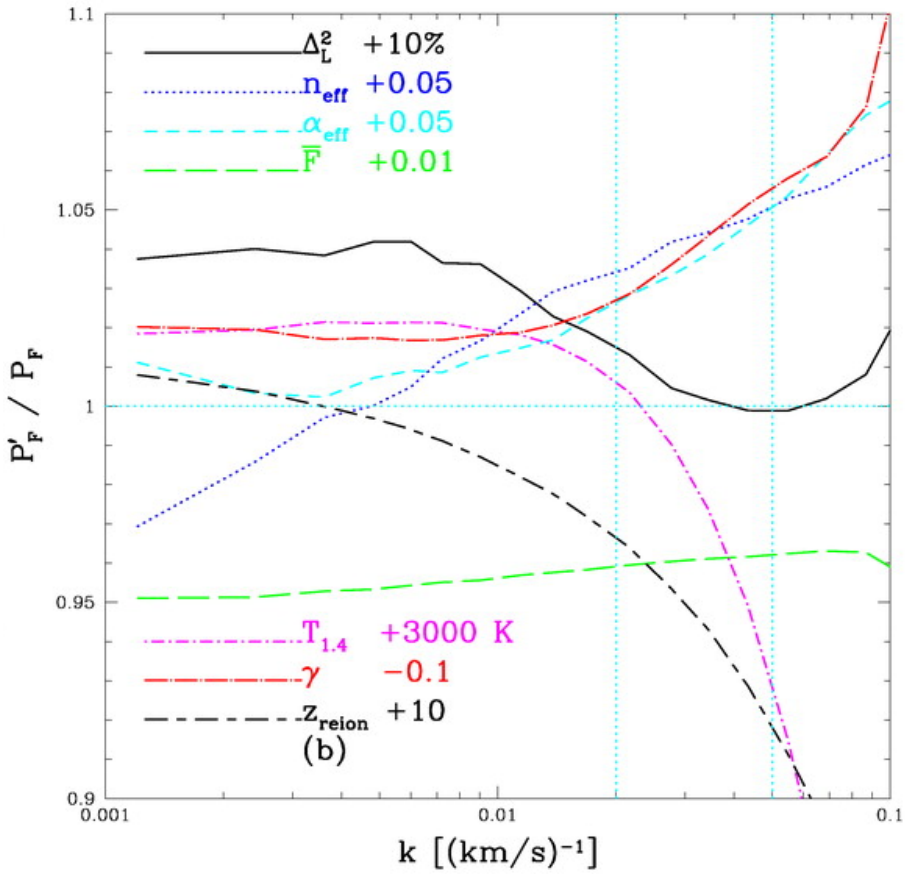

Effect of increasing P_L or $\bar{F}$ on $P_{F1d}(k, z = 4)$

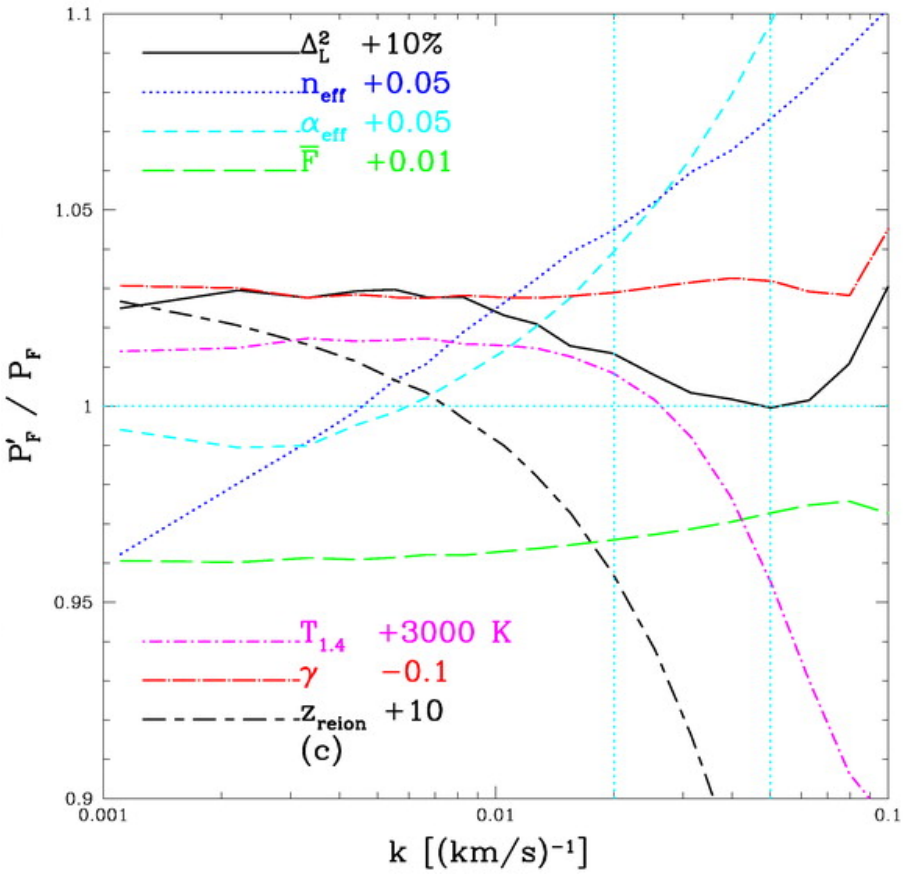

Observed 1d flux power spectrum

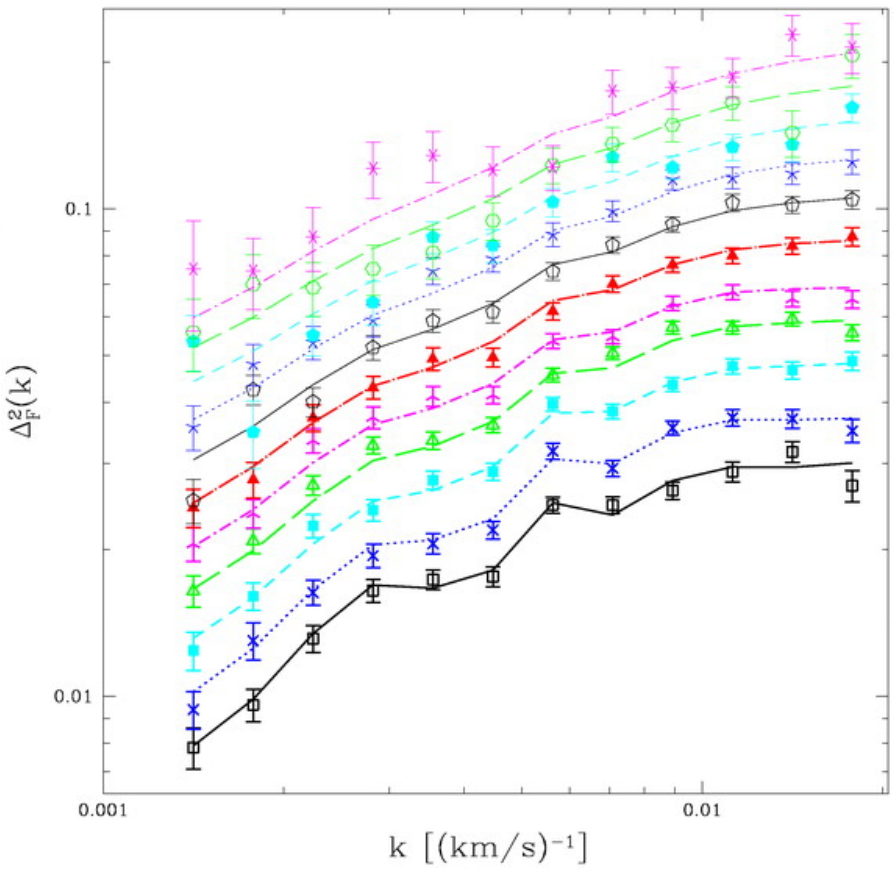

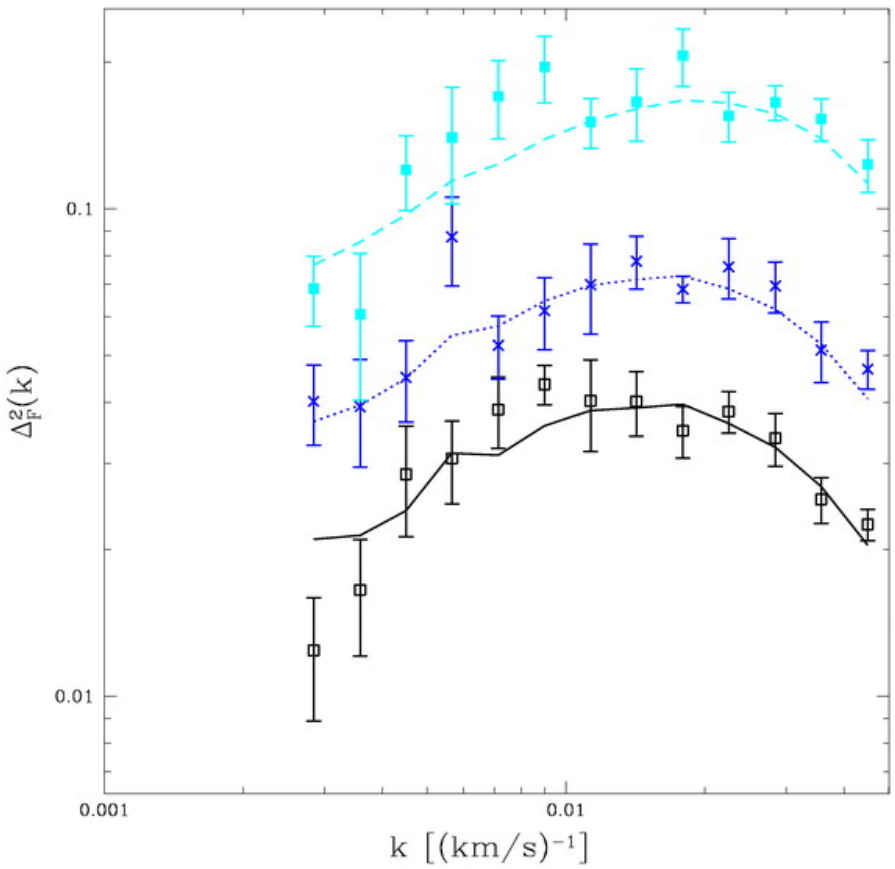

Deduced $P_L(k)$ (McDonald et al 2005)

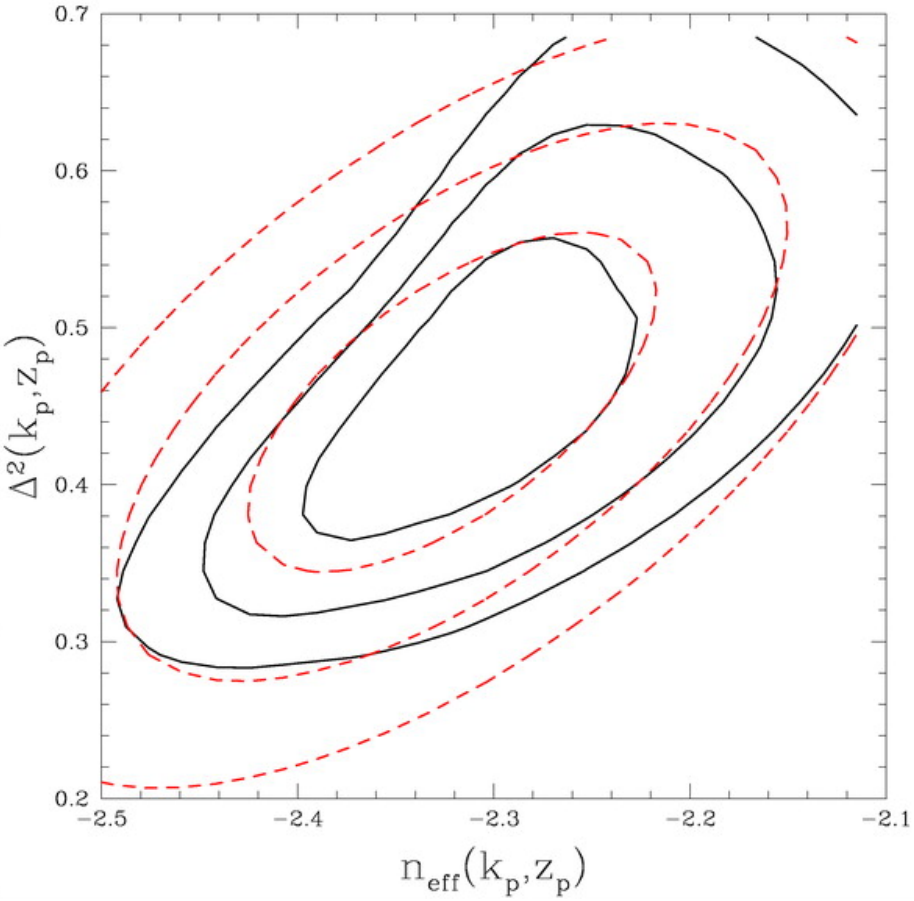

Deduced mean transmission

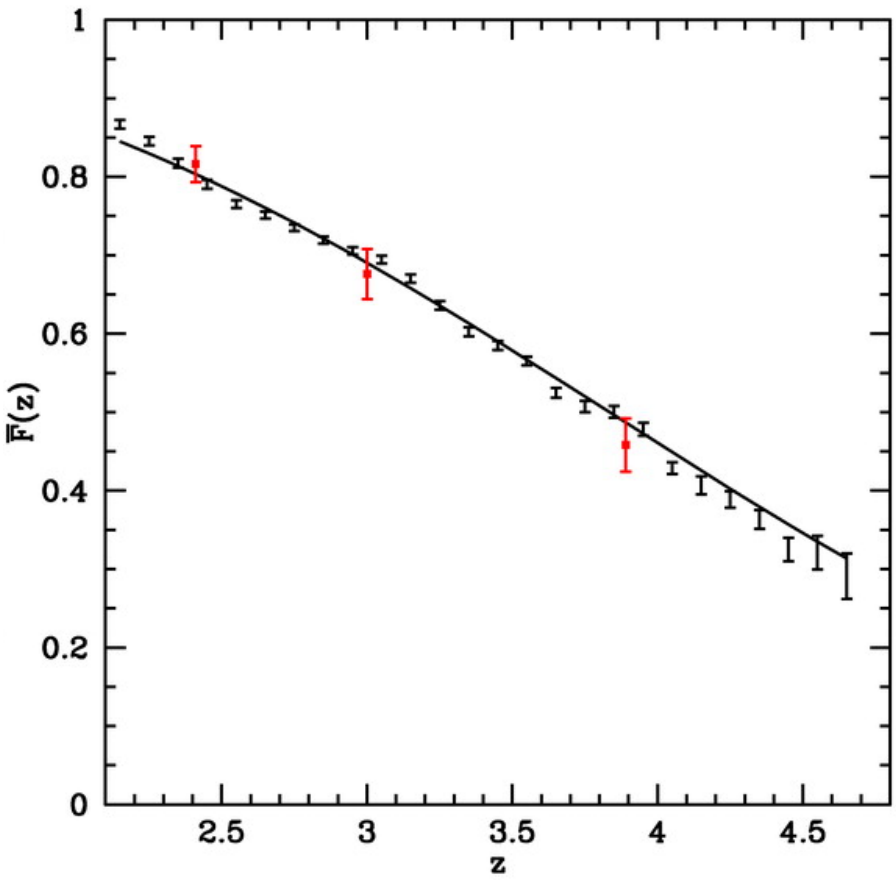

Deduced $P_L(k)$ (Seljak, Slosar, McDo 0604335)

Add measurement of $\bar{F}(z)$ from high-resolution spectra.

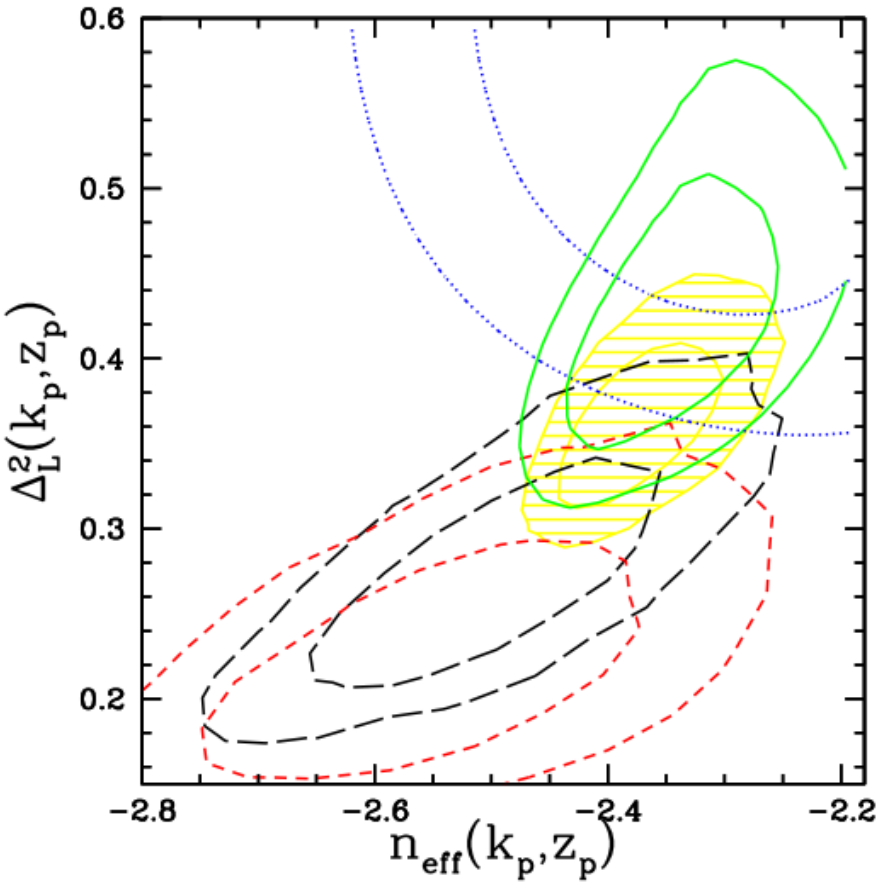

Lyα with $\bar{F}(z)$ measurement
WMAP3, running n
WMAP3 + galaxies + SN, running n
Combined

Deduced $P_L(k)$ (Palanque-Delabrouille et al 1410.7244)

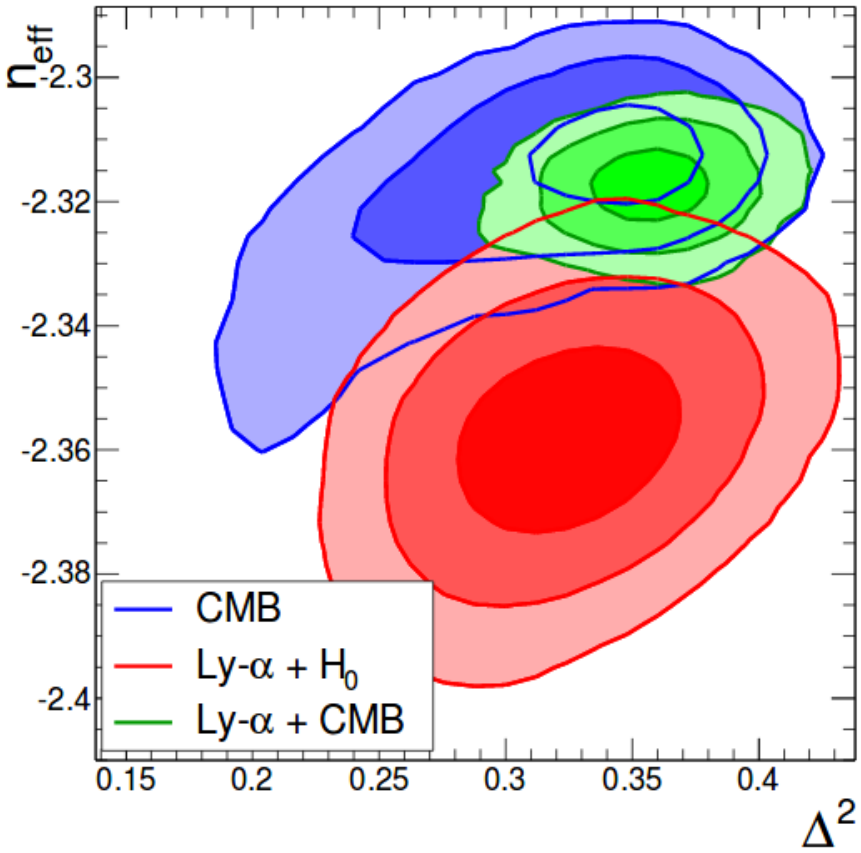

$$k_p = 0.009(km/sec)^{-1}$$
$$z_p = 3$$

Combination with CMB

Need to put CMB and Lyα inhomogenities on same comoving distance (r) or wavenumber (k) scale.

- CMB: $r = \Delta\theta \times D_M(z \sim 1070$
  $D_M(1070)$ known (r_d and CMB peak positions)
- Lyα: $r = \Delta z / H(z)$
  $H(z)^2 = H_0^2 + \Omega_k H_0^2[(1+z)^2 - 1] + \Omega_M H_0^2[(1+z)^3 - 1]$

Need $(\Omega_M h^2, \Omega_k h^2, h)$ to compare CMB and Lyα.
$\Omega_M h^2$ determined by CMB peak heights.
Further input or hypotheses needed for $(h, \Omega_k h^2)$

Effect of $m_\nu = 0.1$eV on CMB

Recombination:

- $z \sim 1000 \;\Rightarrow\; kT_\gamma \sim 0.2$eV
- $kT_\nu \sim 0.15\text{eV} \Rightarrow \langle p_\nu \rangle \sim 3\,T_\nu >> m_\nu$

$\Rightarrow m_\nu \sim 0.1$eV has little effect on shape of CMB spectrum.

$H(z < 100)$ is modified $\Rightarrow$ modified distance to LSS.

$\Rightarrow$ peak positions slightly modified.

(For fixed $\Omega_c h^2$: determined by CMB peak heights.)

Effect of $m_\nu = 0.1$eV on late-time $P_L(k, z)$

First, what is $P_L(k, z)$?

$$\rho(\vec{r}, z) = \bar{\rho}(z)\left[1 + \delta_{\vec{k}}(z)\exp(i\vec{k}\cdot\vec{r})\right] \qquad P(k) \propto \langle \delta_{\vec{k}}^2 \rangle$$

Power spectrum, $P(k)$, is Fourier trans. of correlation function, $\xi(r)$.

At early times, $|\delta(k, z)| \ll 1$ and obeys linear ordinary differential equations (modes independent).

$P_L(k, z)$ is late time extrapolation of early-time $P(k, z)$ using linear ordinary differential equations (modes independent.)

Effect of $m_\nu = 0.1$eV on late-time $P_L(k)$

Free streaming while $T_\nu > m_\nu$ suppresses power on small scales:

$$k_{fs} \sim 0.0017 \left[\frac{\Omega_c \sum m_\nu}{0.3 \times 0.1 eV} \right]^{1/2} (h^{-1}\mathrm{Mpc})^{-1}$$

$$\lambda_{fs} \sim 3600 \left[\frac{\Omega_c \sum m_\nu}{0.3 \times 0.1 eV} \right]^{-1/2} (h^{-1}\mathrm{Mpc})$$

Suppression factor (fixed $\Omega_c h^2$):

$$\frac{\Delta P_L}{P_L}(k \gg k_{fs}) \sim 8 \frac{\Omega_{\nu 0}}{\Omega_c} \sim 0.06 \frac{\sum m_\nu}{0.1 eV}$$

$\Delta P_L / P_L$ observable if P_L can be deduced from observed P_{NL} and then compared with prediction of CMB (function of m_ν).

Suppression of power by massive neutrinos.

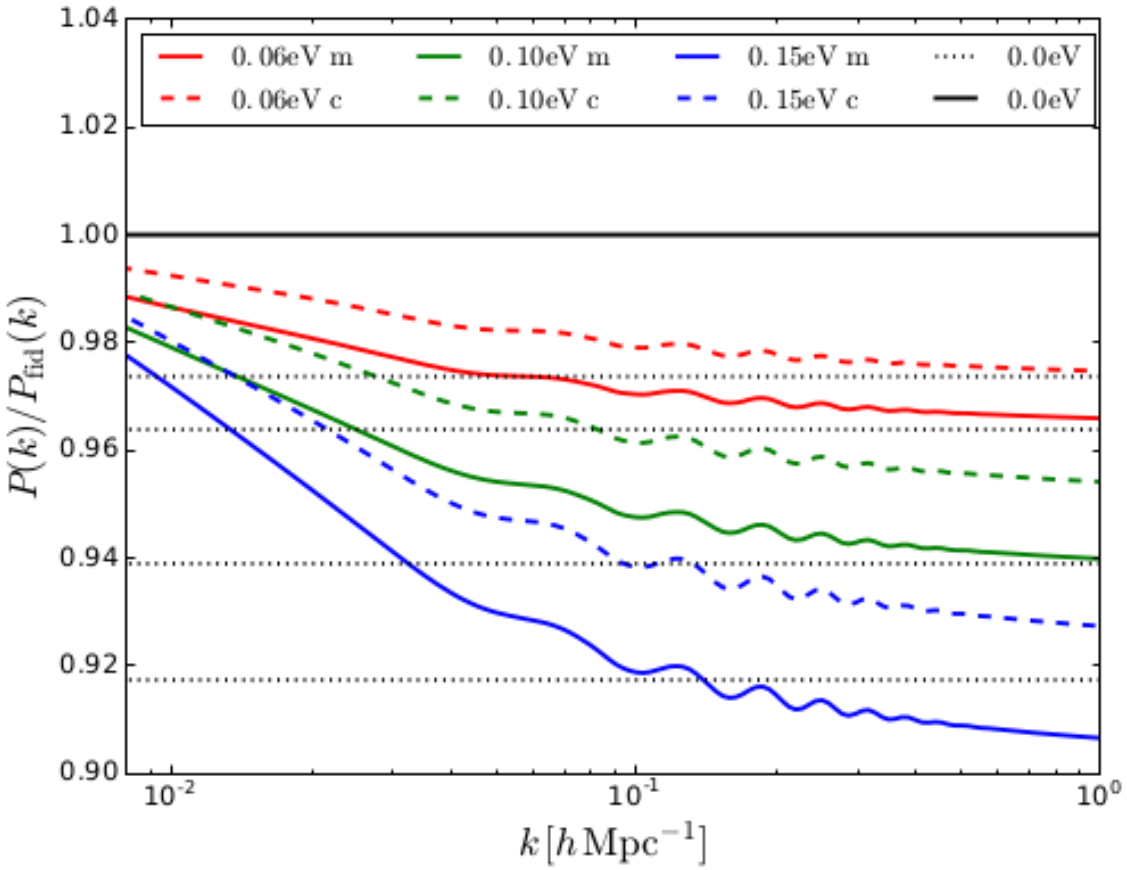

Figure 1. We carry out our analysis using simulations for different cosmologies with massive and massless neutrinos. In the plot we show the linear power spectrum of each model, normalized by the power spectrum of the fiducial cosmology (solid black line), at $z = 0$. The dotted black lines show the models with massless neutrinos and lower value of σ_8 than the fiducial model. The solid/dashed colored lines show the matter/CDM+baryons power spectrum of the models with massive neutrinos.

Villaescusa et al.
arXiv:1708.01154

Lyα $P_{1d}(k_{\|})$
$0.2 < k_{\|} < 4$

$P_{galaxy}(k)$
$0.01 < k < 1$

m_ν from CMB and Lyα (simplified)

$$P_L(k > k_{fs}) \sim P_L(k, A_s, n_s, \Omega_c h^2, \Sigma m_\nu \sim 0) \left[1 - 0.06 \frac{\Sigma m_\nu}{0.1 eV}\right]$$

- Simulate IGM to establish relation between $P_L(k)$ and $P_{NL}(k)$.
- Deduce l.h.s. from Lyα forest measurement of $P_{NL}(k)$
- Deduce $(A_s, n_s, \Omega_c h^2)$ from CMB anisotropy $\Rightarrow P_L(k, m_\nu \sim 0)$
- Use $(h, \Omega_c h^2)$ to put CMB anisotropies and Lyα inhomogeneities on the same distance scale (same k scale).
- Deduce $\sum m_\nu$

  Precision of 0.12 on $\Delta P_L / P_L \Rightarrow m_\nu < 0.2$eV
- mass limit depends on assumed form of primordial spectrum.

  Generally assume non-running n_s

Limits on m_ν

- Seljac et al. (2005) $m_\nu < 0.42$ eV
  $P_L(k_p)$ from McDonald et al (2005)
  CMB from WMAP 1yr
- Seljac, Slosar & McDonald (2006) $m_\nu < 0.17$ eV
  $P_L(k_p)$ from McDonald et al (2005)
  $\bar{F}(z)$ measurement with high-resolution spectra
  CMB from WMAP 3yr
- Palanque-Delabrouille et al. (2015) $m_\nu < 0.15$ eV
  New (better) simulations.
  fit directly for $(m_\nu, \sigma_8) + (\Omega_c, h, n_s)$
  CMB from Planck 1yr

All assume n_s not running.
Different fit parameters for Lyα fit, different simulations, and different CMB data makes comparison difficult.
Next generation experiments aim for $m_\nu \sim 0.06$eV (normal mass-ordering)